

Response for Referee #1

We thank Referee #1 for the support given to this paper and for the comments to improve it. His comments and remarks are carefully taken into account in the revised version of this manuscript.

General Comments

RC1:

The aim of this paper is to provide a database of dust optical properties, however only the aerosol extinction is discussed. Authors should include some discussions on the single scattering albedo and size distribution which are also key parameters for dust impact and life cycle. As dust optical efficiency strongly depend on the wavelength, the wavelength dependence of these two optical parameters should be analysed.

AC1:

Indeed, in this manuscript, only the optical thickness and the extinction coefficients are discussed and analyzed. We chose these two parameters to validate the optical properties simulated by ALADIN for three reasons: the first reason is the availability of observational data over a fairly long timescale for these two products, covering the total period of simulations, which highly facilitates a comparison. The second reason is the quality of these two products in the data, especially for optical thicknesses. The last reason is that only the extinction climatology is used in the radiative scheme of atmospheric models.

We agree that analyzing the SSA or g distribution and evolution would reinforce the paper particularly to see how these parameters are depending on size distribution (Mallet et al., 2009).

But in addition to that, we analyzed the dust source and deposition areas and the surface concentrations and we have given inter-comparisons with other previous studies.

The ALADIN model does simulate the single scattering albedo (SSA) and particle size distribution. But comparable observational products are not available for the period of simulation. The validation of these two products can be treated for specified case studies such as done in Mallet et al., 2009 or in Crumeyrolle et al., 2008, 2011. These studies use the same aerosol scheme and the same method to retrieve the aerosol optical properties (SSA, g , extinction). These references have been added in the revised paper: (i) to show that the aerosol distribution is correctly modeled over West Africa with the ORILAM aerosol scheme, and (ii) to add comments about the evolution of the two other aerosol optical parameters (SSA and asymmetric factor) during their transport over West Africa.

According to the two last remarks, we propose to update the title of the article in order to clarify the subject:

“3D dust aerosol distribution and extinction climatology over North Africa simulated with the ALADIN numerical prediction model from 2006 to 2010.”

RC2:

Discussions are full of vague terms as « compares well », « in good agreement », « reproduces well ». Statistical comparisons between simulations and observations should be added in order to have a better view of the performance of ALADIN in simulating the dust life cycle.

AC2:

In the paper, a qualitative comparison is made for concentrations (Fig. 12), a statistical comparison for optical thicknesses in order to evaluate the representativeness of our

simulation (Fig. 11, and discussion on AOT correlation coefficient, section 4.2). Furthermore, we have used a Z_a factor for the case of extinction coefficients, which gives access to the average vertical profile of extinctions (Fig. 13 and 14). Another quantitative evaluation was for emissions, where we compared the estimated values with those given in previous studies. We have also introduced in the manuscript the correlation coefficient for the dust surface concentration (see Fig. 1).

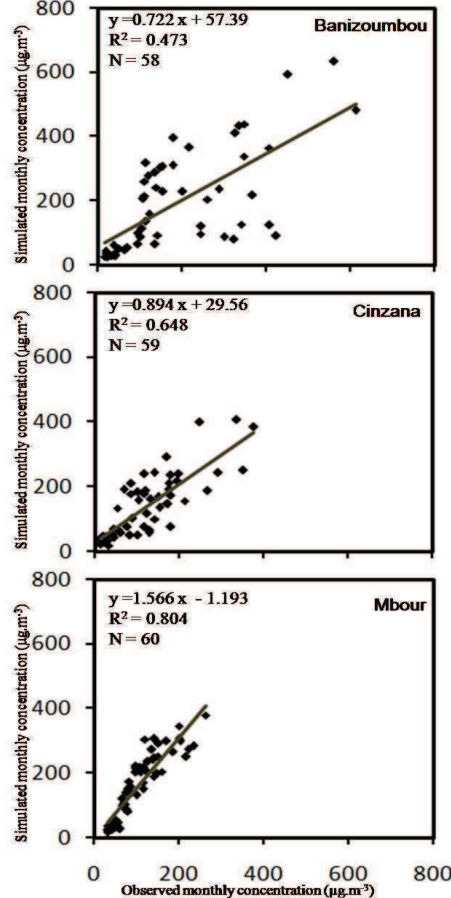


Fig.1: Scatter plot of monthly ALADIN dust surface concentration against observations over Banizoumbou, Cinzana and Mbour from 2006 to 2010. N is the number of averaged monthly surface concentration data available from 2006 to 2010. R is the correlation coefficient.

RC3:

It is stated in Section 3.3 that « we show that the use of a three dimensional NWP model such as ALADIN significantly improves the climatology of wet deposition of dust aerosols. » However, no comparisons with other models are made to support this statement. I suggest to compare the ALADIN statistical scores with the ones published for chemistry-transport models. Does a two-way meteorology-chemistry coupling give a better representation of dust life cycle than a state of the art chemistry- transport model off-line driven by meteorology?

AC3:

Indeed, in the first version of the paper, we have not made any comparison with other models in terms of dust wet deposition. We do believe, as noted in the paper, that the wet deposition simulated by ALADIN is realistic and can compare well with respect to other numerical models, since the ALADIN version used for our simulations is very close to an operational

version of the time of this study, therefore overall calibrated. As for the comparison with other CTM models, this would be difficult since values of wet deposition depend on the period of interest, and to our knowledge there are no wet deposition simulations covering this period.

We added in the revised manuscript the intercomparison with other models studies.

Page 5763 line 17: we add after dry deposition. The paragraph below:

“The inter-comparison of dust wet deposition simulated by ALADIN for the year 2006 with models used in the AEROCOM and SDS-WAS programs (BSC-DREAM8b, GOCART-v4Ed.A2 CTRL, GISS-modelE.A2 CTRL and TM5-V3.A2 CTRL, http://aerocom.met.no/cgi-bin/aerocom/surfobs_annualrs.pl) for the same period is given by the Table 1. The results show that the mean wet deposition estimated by ALADIN is much higher than those estimated by AEROCOM Model's. As discussed for the seasonal wet deposition, the major part of the wet deposition takes place during the wet season of the African Monsoon.

In terms of spatial distribution, the ALADIN model performs better for the estimation of the dust wet deposition associated with convective systems in the Sahelian regions. For example, the estimates of the BSC-DREAM8b model do not exceed $0.2 \text{ g.m}^{-2}.\text{year}^{-1}$ for the Sahel and the West African region. Those simulated by TM5-V3.A2 CTRL are less than $5 \text{ g.m}^{-2}.\text{year}^{-1}$ and those obtained by GOCART-v4Ed.A2 CTRL and GISS-modelE.A2 CTRL varied in the range $20-50 \text{ g.m}^{-2}.\text{year}^{-1}$. The fact that some part of the total precipitation of ALADIN is resolved can explain that the wet deposition processes in ALADIN are found to be more efficient than in some global models. “

Table 1: Mean dust wet deposition

Models	Wet deposition for 2006 in ($\text{g.m}^{-2}.\text{year}^{-1}$)
BSC-DREAM8b	0.46
GOCART-v4Ed.A2 CTRL	9.653
GISS-modelE.A2 CTRL	8.301
TM5-V3.A2 CTRL	4.673
This study	21,36

RC4:

Several aerosol climatologies are mentioned in the introduction and are considered by authors as not well adapted due to their coarse resolution. Does the climatology obtain in this study with a finer resolution (20x20 km) give a better estimation?

AC4:

In this paper, we have mentioned other global or regional climatologies for information:

- the one of Tegen et al., (1997) which is a simulated climatology
- the one obtained by combining a modelled and a satellite-derived climatology, from Nabet et al., (2013) and Kinne et al., (2013).

The Tegen climatology is now fairly old and it has low resolution ($5^\circ \times 4^\circ$). We further know that in desert regions, soil characteristics and local meteorological phenomena play an important role in the uprising of dust. Thus, it is very difficult to represent these phenomena and characteristics at this resolution. Therefore, the climatology presented in our paper for North Africa should be of superior quality compared with Tegen (which was used in the operational ALADIN version of that time (see Fig. 2)). Figure 2 shows that the climatology of Tegen is significantly underestimated over North Africa.

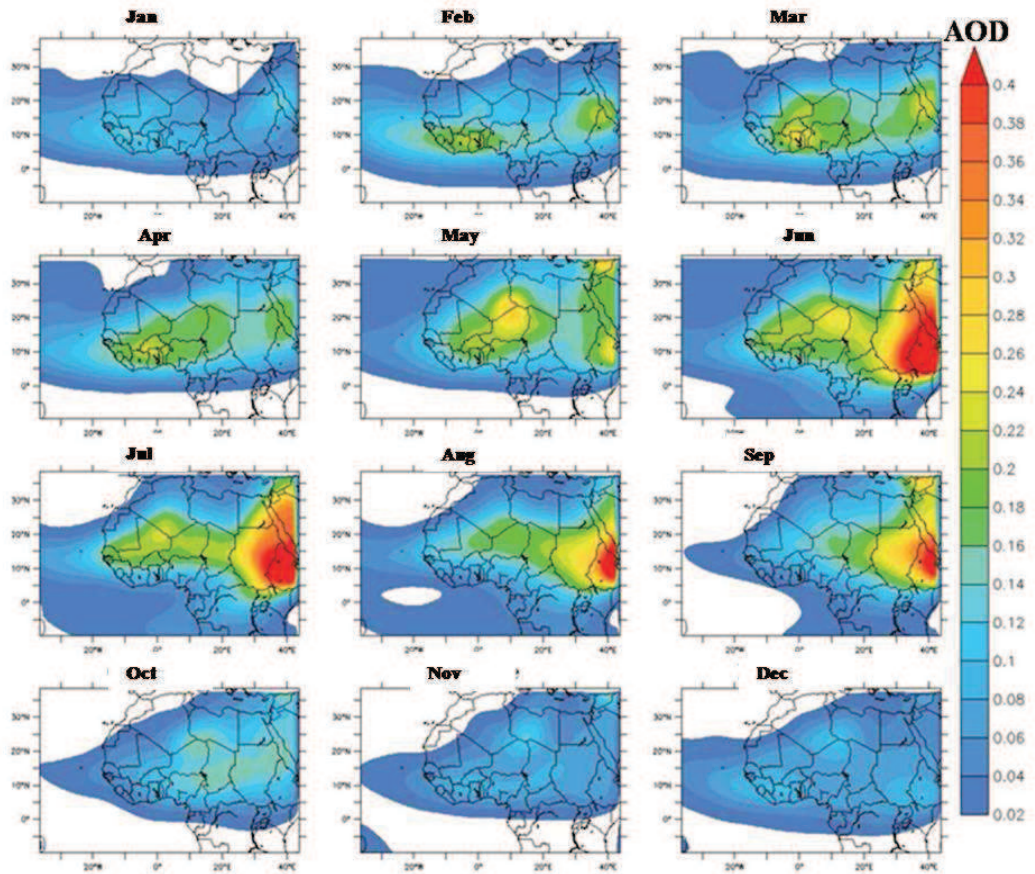


Fig. 2: Monthly climatology of aerosol optical Thickness derived from Tegen et al., (1997) for dust aerosol over North Africa.

We agree with the reviewer that a better resolution will necessary improve the dusts distribution for North Africa. Some sub-scales processes (emission, turbulence, and microphysics) will be resolved explicitly. However, in the end, a compromise between resolution and duration of the simulation is required which led in our case to choosing the resolution of 20 km. The rather long period of simulation of six years was chosen in order to better converge towards an average climate of the area of interest, at the expense of further increasing the horizontal or vertical resolution. The time step of the model and the resolution eventually are close to those of regional climate models.

Specific comments:

RC1:

Page 5753 L 2 : A new IPCC report has been published

AC1:

The reference is updated in the revised manuscript.

Page 5753 line 2-3: the sentence: “Dust aerosol....(IPCC,2007).” becomes:

“Mineral dust aerosol dominates the aerosol mass over some continental regions with relatively higher concentrations accounting for about 35% of the total aerosol mass (IPCC, 2013)”.

Ref:

Boucher, O., D. Randall, P. Artaxo, C. Bretherton, G. Feingold, P. Forster, V.-M. Kerminen, Y. Kondo, H. Liao, U. Lohmann, P. Rasch, S.K. Satheesh, S. Sherwood, B. Stevens and X.Y. Zhang: Clouds and Aerosols. In: Climate Change 2013: The Physical Science Basis. Contribution of Working Group I to the Fifth Assessment Report of the Intergovernmental Panel on Climate Change [Stocker, T.F., D. Qin, G.-K. Plattner, M. Tignor, S.K. Allen, J. Boschung, A. Nauels, Y. Xia, V. Bex and P.M. Midgley (eds.)]. Cambridge University Press, Cambridge, United Kingdom and New York, NY, USA, 1535 pp, doi:10.1017/CBO9781107415324, 2013.

RC2:

Page 5753 L 18 : To identify and quantify

AC2:

The sentence has been rectified in the revised manuscript.

Page 5753, line 17-19: sentence “Therefore, an accurate.....(RCMs)” will be:

“Therefore, an accurate database of aerosol content in this region is crucial to identify and quantify this impact, particularly in Regional Climate Models (RCMs).”

RC3:

Page 5753 L 20-23 : Could you explain this positive impact ?

AC3:

The positive impact of the switch from the Tanré et al. (1984) climatology to the Tegen et al. (1997) climatology was examined in Tompkins et al., (2005). In this study, Tompkins et al., (2005) have performed a couple of 5-day forecasts of the African Easterly Jet (AEJ) with the old and new climatology and the results are compared with high resolution dropsonde data from the JET2000 campaign. The results of these simulations show that the new aerosol climatology significantly improves some aspects of the AEJ structure and strength. In the same study, 4 months of 5-day forecasts was realized and compared using the contrasting aerosol distributions. The results show a clear improvement with the new climatology, with the jet strengthened, elongated to the east, and less zonal, in agreement with the analyses. The new climatology suppresses deep convection by stabilizing the atmosphere, preventing the ITCZ from progressively migrating north during the forecast. A strong reduction of mean equivalent potential temperature at the lowest model level is noted, with the southerly displacement of the ITCZ.

These explanations will be introduced in the final version of the manuscript.

Page 5753, line 20-23: the sentence “For example.....’Morcrette et al., 2009)’ will be:

“For example, various studies (Tompkins et al., 2005; Rodwell, 2005) have shown the positive impact of the switch from the Tanré et al. (1984) climatology to the Tegen et al. (1997) climatology for various aspects of the ECMWF model (Morcrette et al., 2009). Tompkins et al., (2005) have performed a couple of 5-day forecasts of the African Easterly Jet (AEJ) with the old and new climatology and the results are compared with high resolution dropsonde data from the JET2000 campaign. The results of these simulations show that the new aerosol climatology significantly improves some aspects of the AEJ structure and strength. In the same study, 4 months of 5-day forecasts was realized and compared using the contrasting aerosol distributions. The results show a clear improvement with the new climatology, with the jet strengthened, elongated to the east, and less zonal, in agreement with

the analyses. The new climatology suppresses deep convection by stabilizing the atmosphere, preventing the ITCZ from progressively migrating north during the forecast. A strong reduction of mean equivalent potential temperature at the lowest model level is noted, with the southerly displacement of the ITCZ.”

RC4:

Page 5755 L 17-23 : Could you add some details on these initiatives ?

AC4:

Some details have been added in the revised version of the manuscript and the paragraph will be:

Page 5755 line 17-23: The paragraph: “Initiatives havecapabilities” becomes: “Initiatives have already been taken to use operational Numerical Weather Prediction (NWP) and regional models at high resolution and short timescales. These efforts include the WMO Sand and Dust Storm Warning Advisory and Assessment (SDS-WAS, <http://sds-was.aemet.es>) program, whose mission is to achieve comprehensive, coordinated and sustained observations and modeling of sand and dust storms in order to improve the monitoring of such storms, increase understanding of the dust processes and enhance dust prediction capabilities. SDS-WAS is established as a federation of partners organized around regional nodes (Northern Africa-Middle East-Europe Node and Asian Node). About 16 dust prediction models have been used in SDS-WAS as BSC-DREAM8b, MACC-ECMWF, INCA-LMDZT, CHIMERE, SKIRON, ETA, NGAC, NAAPS....”

RC5:

Page 5757 L 11 : « are explicitly represented « Even at a 20x20 km resolution?

AC5 :

This text was corrected in the revised manuscript.

Page 5757, line 9-11: sentence “Microphysical processes (Lopez, 2002)” becomes:

“Microphysical processes such as auto-conversion, collection, evaporation, sublimation, melting and sedimentation are represented following the parametrization of Lopez (2002).”

RC6:

Page 5757 L 18-23 : The calculation of aerosol optical properties should be described in more details.

AC6:

The method of calculation of aerosol optical properties is described in more detail in Grini et al., (2006). The refraction indexes used have been calculated upon the AMMA data base (Tulet et al., 2008). These references have been added in the revised version of the manuscript.

In the description of ORILAM scheme:

Page 5757, line 20: after “.....(Binkowski and Roselle, 2003).” We add:

“The method of calculation of aerosol optical properties is described in Grini et al., (2006). The refraction indexes used in our work have been calculated following a table of interpolation proposed by Grini et al., (2006). The dust optical properties are calculated from these new indexes in function of lognormal parameter upon the AMMA size distribution (Tulet et al., 2008). ORILAM has been evaluated in several papers for the West Africa region. Crumeyrolle et al., (2008 and 2011) presented a thorough description of the size distribution

for the AMMA campaign. Mallet et al., (2009) studied the evolution of the asymmetry factor (g) and the single scattering albedo (SSA) for the dust storm event of March 2006 and studied the radiative balance over West Africa. Such specific studies however only can be carried out for particular situations.”

Ref:

Mallet, M., Tulet, P., Serc, D., Solmon, F., Dubovik, O., Pelon, J., Pont, V., and Thouron, O.: Impact of dust aerosols on the radiative budget, surface heat fluxes, heating rate profiles and convective activity over West Africa during March 2006, *Atmos. Chem. Phys.*, 9, 7143–7160, doi:10.5194/acp-9-7143-2009, 2009.

Crumeyrolle, S., Gomes, L., Tulet, P., Matsuki, A., Schwarzenboeck, A., and Crahan, K.: Increase of the aerosol hygroscopicity by cloud processing in a mesoscale convective system: a case study from the AMMA campaign, *Atmos. Chem. Phys.*, 8, 6907–6924, doi:10.5194/acp-8-6907-2008, 2008.

Tulet, P., Mallet, M., Pont, V., Pelon, J., and Boone, A.: The 7–13 March, 2006, dust storm over West Africa: generation, transport and vertical stratification, *J. Geophys. Res.*, 113, D00C08, doi:10.1029/2008JD009871, 2008.

RC7:

Page 5758 L 17-20 : This part should be rephrased

AC7:

The sentence becomes:

Page 5758, line 17-20: the sentence “Therefore, ECOCLIMAP.....ISBA.” Will be: “The ECOCLIMAP database is designed in compliance with the SURFEX “tile” approach: each grid box is composed of four adjacent surfaces for nature (ISBA vegetation classes), urban areas (TEB model), sea or ocean and lake.”

RC8:

Page 5766 L 11 : How this combination has been constructed ?

AC8:

We note that the Dark Target (DT) algorithm over land is not designed to retrieve aerosol over bright surfaces, including desert (eg, Levy et al., 2007). This leaves significant holes in global aerosol sampling. However, the Deep Blue (DB) algorithm can retrieve aerosol properties over brighter surfaces like desert and semi-desert areas (Hsu et al. (2004, 2006)). For this reason we used these two products to design a map of AOD over the whole of North Africa.

Over bright arid regions, only DB data are available and no choice is really offered (see Fig. 3a). Conversely, in areas with dense vegetation and ocean, only DT data are available (see Fig. 3b). Thus, we use this product for these areas. However, we have transition areas with low vegetation such as the Sahel (10°N-15°N). For these areas we have both the DB and DT products. These areas are shown in Figure 4 where we display the difference between the monthly aerosol optical thicknesses derived from DB and DT over North Africa for January over 2006-2010. We note that the DT product for the semi-arid region tends to be biased and underestimated. For example, the difference between DB and DT in some areas for this region exceeds 0.3. For this reason, we chose the DB product for the transition regions.

Recently, Levy et al., (2013) proposed another solution for the transition regions, namely to merge the two products and create an AOD product that combines DB and DT products. Levy et al., (2013) used the Normalized Difference Vegetation Index (NDVI) to identify these regions. Unfortunately, this solution has not yet been validated.

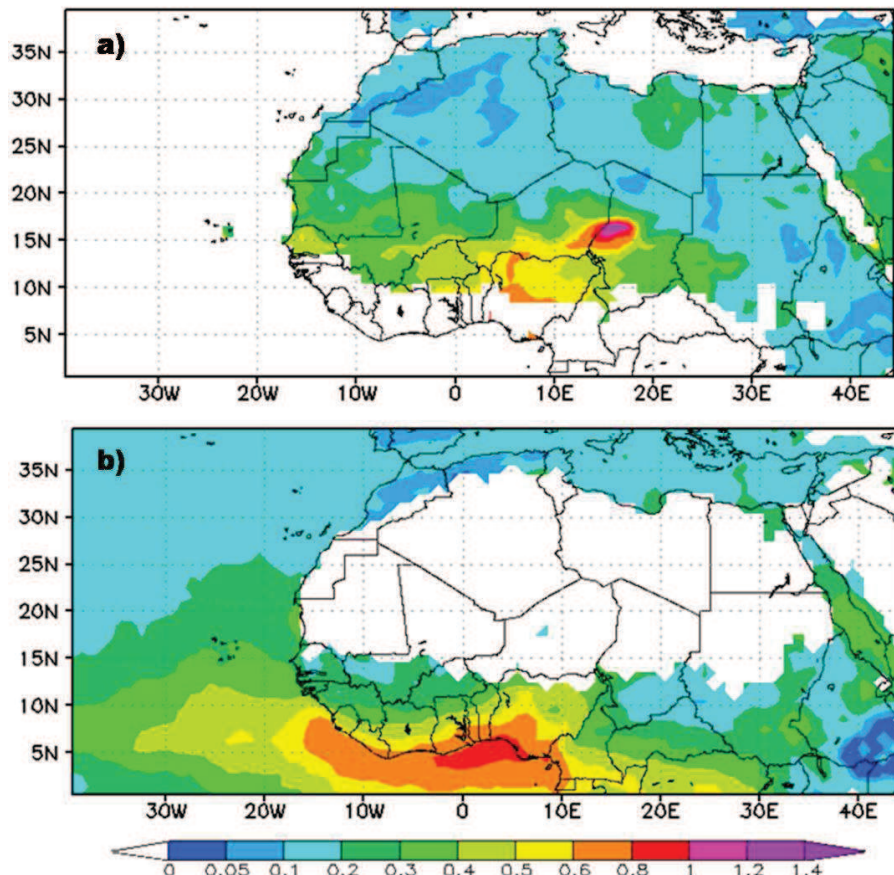


Fig. 3: Monthly aerosol optical thicknesses derived from a) DB and b) DT over North Africa for January over 2006-2010 periods.

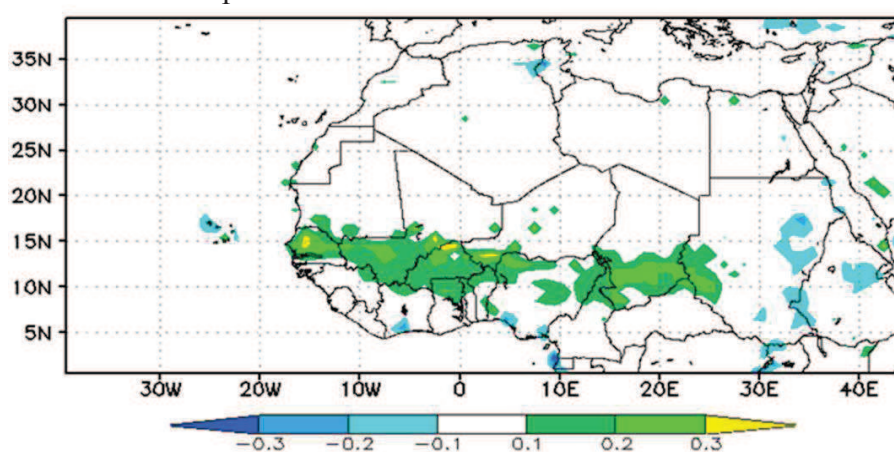


Fig 4: Difference between the monthly aerosol optical thicknesses derived from DB and DT over North Africa for January over 2006-2010 periods.

RC9:

Section 4.1 et 4.2 : Simulations take only into account mineral dust while AERONET and MODIS measurements take into account all possible aerosol species. This could induce a bias in the comparisons. Can you quantify it?

AC9:

We agree that the observations take into account all types of aerosol. In contrary, our simulations only show AOD due to desert aerosol. Then indeed, simulated AODs should be lower than the observed AODs and the bias might be quantified and attributed solely to the missing components. However, there also should be a missing contribution from the unresolved sub-mesh emission and there potentially also can be a systematic error due to the parameterization model controlling the modelled dust aerosol life cycle.

Thus, we do not have any simple way to separate the two sources of bias. In our case, the simulated AOD is overestimated and this is mentioned in the conclusion (page 5774 line 6-14), particularly during the period of biomass fires.

RC10:

Page 5767 : A figure showing the AERONET sites used in the study should be added.

AC10: We agree with the reviewer's proposal.

Page 5759, after sect. 2.3: we added the sub-section 2.4 which describes the observations used in this paper.

2.4 Dataset

2.4.1 Ground-based measurement

In this study we use the AERONET AOT product (level 2) and the PM10 measured dust mass concentration (Particulate Matter concentration, particles with diameter of 10 μm or less) in order to evaluate the model-simulated AOT and the surface dust concentration, respectively, from 2006 to 2010.

AERONET (<http://aeronet.gsfc.nasa.gov/>) is a federation of ground-based remote sensing instruments measuring aerosol and its characteristics (Holben et al., 1998). The AERONET sunphotometers directly measure aerosol optical thickness at seven wavelengths (approximately 0.340, 0.380, 0.440, 0.500, 0.675, 0.870, and 1.02 μm) with an estimated uncertainty of 0.01 – 0.02 (Holben et al., 2001). In the model, the AOT is simulated at 0.55 μm , and it is therefore compared to the AOT measured at the nearest wavelength, 0.440 μm or 0.675 μm . Following Schmechtig et al., (2011) the AOT measured over Banizoumbou, Cinzana and Mbour, at wavelength 0.44 μm and 0.675 μm , are significantly correlated ($r^2 = 0.99$) with slopes ranging from 1.04 in Cinzana to 1.06 in MBour. Thus, in our study, we used the AOT measured at 0.44 μm over the five AERONET sites located in West Africa at: Banizoumbou (Niger), Cinzana (Mali), DMN_Maine_Soroa (Niger), Mbour (Senegal) and Capo Verde (Fig. 5). We note that the AOT measurements only are possible during the day since they are based on measuring the solar radiation attenuation. This characteristic may be affecting the results of the intercomparison if a dust storm event occurred at night-time.

The three stations composing the “Sahelian Dust Transect” (SDT) (Marticorena et al., 2010) located in the Sahelian region at Banizoumbou, Cinzana and MBour are used to validate the surface dust concentration simulated by ALADIN. The SDT provides a continuous monitoring of the atmospheric concentrations PM10 with a 5 minute time step, using a Tapered Element Oscillating Microbalance (TEOM 1400A from Thermo Scientific) equipped with a PM10 inlet. PM10 measurements refer to particulate matter which passes through a

size-selective inlet with a 50% efficiency cutoff at 10 μm aerodynamic diameter (Marticorena et al., 2010). In terms of sensitivity, the detection limit of the instrument is about 0.06 $\mu\text{g.m}^{-3}$ for a one hour sampling time.

2.4.2 Satellite data

The Aqua-MODIS product (Tanré et al., 1997; Levy et al., 2007) was used to evaluate the AOTs simulated by ALADIN. This instrument is a multi-spectral radiometer, designed to retrieve aerosol microphysical and optical properties over ocean and land. Two products of Aqua-MODIS are considered in this study: the MODIS Dark Target (DT) and the MODIS Deep Blue (DB) algorithms (Hsu et al., 2004). The MODIS DT algorithm over land is not designed to retrieve aerosol over bright surfaces, such as the Saharan deserts due to the large values of surface reflectivity (Remer et al., 2005; Shi et al., 2013). This problem leads to large spatial gaps in the aerosol optical thickness recorded in desert regions, although these regions are affected by some of the largest aerosol loadings worldwide. However, the DB algorithm takes advantage of this surface phenomenology by performing aerosol retrievals in the visible blue spectrum (such as the 0.47 μm spectral channel in MODIS) and by utilizing the selected aerosol model in the inversion to generate the AOT (Hsu et al., 2004, 2006; Shi et al., 2013). Thus, a combination between these two products is made to complete the AOT database for the whole of North Africa (ocean and land).

Over bright arid region, only DB data are available, offering no alternative choice. Conversely, in the areas with dense vegetation and ocean, only DT data are available and are therefore used in our study, in these regions. In addition, we have transition areas with low vegetation such as the Sahel (10°N-15°N). For these areas, both the DB and DT products are available. The DT product for the semi-arid regions tends however to be biased and underestimated (Levy et al., 2010). For example, the difference between DB and DT estimated for the transition regions can exceed 0.3. For this reason we chose the DB product for the transition regions. Recently, Levy et al., (2013) proposed another solution for the transition regions, namely to merge the two products and create a combined AOD product. Levy et al., (2013) used the Normalized Difference Vegetation Index (NDVI) to identify these regions. Unfortunately, this solution has not yet been validated.

The CALIOP Level 2 Layer 5 km product was used to evaluate the mean particle vertical distributions simulated by ALADIN over North Africa. The CALIOP instrument (Winker et al., 2007) was launched in 2006 on the Cloud–Aerosol Lidar and Pathfinder Satellite Observations (CALIPSO) spacecraft, and has now provided over 8 years of nearly continuous global measurements of aerosols and clouds with high vertical and spatial resolution at two-wavelength (532 nm and 1064 nm) (Rogers et al., 2014). As part of the “A-train” multisatellite constellation, CALIPSO follows a 705 km sun-synchronous polar orbit, with an equator-crossing time of about 1:30 P.M., local solar time (Stephens et al., 2002). The orbit repeats the same ground track every 16 days. The vertical distribution of aerosols, provided by lidar, is important for radiative forcing (e.g., Satheesh, 2002), air quality studies (e.g., Al-Saadi et al., 2005; Engel-Cox et al., 2006), and model validation (Dirksen et al., 2009; Koffi et al., 2012). The CALIOP instrument and its initial performance assessment are described in Winker et al. (2007) and Hunt et al. (2009).



Fig. 5: Location of the five AERONET sites used in this study to evaluate the ALADIN simulated AOT over West Africa Banizoumbou (Niger), Cinzana (Mali), DMN_Maine_Soroa (Niger), M Bour (Senegal) and Capo verde.

Ref:

Levy, R. C., Remer, L. A., Kleidman, R. G., Mattoo, S., Ichoku, C., Kahn, R., and Eck, T. F.: Global evaluation of the Collection 5 MODIS dark-target aerosol products over land, *Atmos. Chem. Phys.*, 10, 10399–10420, doi:10.5194/acp-10-10399-2010, 2010.

Levy, R. C., Mattoo, S., Munchak, L. A., Remer, L. A., Sayer, A. M., Patadia, F., and Hsu N. C.: The Collection 6 MODIS aerosol products over land and ocean, *Atmos. Meas. Tech.*, 6, 2989–3034, doi:10.5194/amt-6-2989-2013, 2013

Winker, D. M., Hunt, W. H., and McGill, M. J.: Initial performance assessment of CALIOP, *Geophys. Res. Lett.*, 34, L19803, doi:10.1029/2007GL030135, 2007.

Hunt, W. H., Winker, D. M., Vaughan, M. A., Powell, K. A., Lucker, P. L., and Weimer, C.: CALIPSO lidar description and performance assessment, *J. Atmos. Ocean. Tech.*, 26, 1214–1228, doi:10.1175/2009jtecha1223.1, 2009.

Rogers, R. R., Vaughan, M. A., Hostetler, C. A., Burton, S. P., Ferrare, R. A., Young, S. A., Hair, J. W., Obland, M. D., Harper, D. B., Cook, A. L., and Winker, D. M.: Looking through the haze: evaluating the CALIPSO level 2 aerosol optical depth using airborne high spectral resolution lidar data, *Atmos. Meas. Tech.*, 7, 4317–4340, doi:10.5194/amt-7-4317-2014, 2014.

Holben, B. N., Tanre, D., Smirnov, A., Eck, T. F., Slutsker, I., Abuhassan, N., Newcomb, W. W., Schafer, J., Chatenet, B., Lavenue, F., Kaufman, Y., Van de Castle, J., Setzer, A., Markham, B., Clark, D., Frouin, R., Halthore, R., Karnieli, A., O'Neill, N. T., Pietras, C., Pinker, R. T., Voss, K., and Zibordi, G.: An emerging ground-based aerosol climatology: Aerosol Optical Depth from AERONET, *J. Geophys. Res.*, 106, 12067–12098, 2001.

Stephens, G. L., Vane, D. G., Boain, R. J., Mace, G. G., Sassen, K., Wang, Z., Illingworth, A. J., O'Connor, E. J., Rossow, W. B., Durden, S. L., Miller, S. D., Austin, R. T., Benedetti, A., and Mitrescu, C.: The cloudsat mission and the A-Train: a new dimension of space-based observations of clouds and precipitation, *B. Am. Meteorol. Soc.*, 83, 1771–1790+1742, 2002.

Al Saadi, J., Szykman, J., Pierce, R. B., Kittaka, C., Neil, D., Chu, D. A., Remer, L. A., Gumley, L., Prins, E., Weinstock, L., MacDonald, C., Wayland, R., Dimmick, F., and Fishman, J.: Improving national air quality forecasts with satellite aerosol observations, *Bull. Am. Meteorol. Soc.*, 86, 1249–1261, doi:10.1175/BAMS-86-9-1249, 2005.

Engel-Cox, J. A., Hoff, R. M., Rogers, R., Dimmick, F., Rush, A. C., Szykman, J. J., Al-Saadi, J., Chu, D. A., and Zell, E. R.: Integrating LIDAR and satellite optical depth with ambient monitoring for 3-D dimensional particulate characterization, *Atmos. Environ.*, 40, 8056–8067, 2006.

Dirksen, R. J., Boersma, K. F., de Laat, J., Stammes, P., van der Werf, G. R., Val Martin, M., and Kelder, H. M.: An aerosol boomerang: rapid around-the-world transport of smoke from the December 2006 Australian forest fires observed from space, *J. Geophys. Res.*, 114, D21201, doi:10.1029/2009JD012360, 2009.

Satheesh, S. K.: *Letter to the Editor* Aerosol radiative forcing over land: effect of surface and cloud reflection, *Ann. Geophys.*, 20, 2105–2109, doi:10.5194/angeo-20-2105-2002, 2002.

RC11:

Page 5769 L24-25 : Do you have an explanation ?

AC11:

The underestimation of the surface dust concentration from April to June over Banizoumbou is probably related to local dust uprisings that are not well simulated by the ALADIN model. This underestimation is strong in June, which marks the transition between the dry and the wet season monsoon in West Africa. Recently, a study realized by Kocha et al., (2013) shows the existence of two important processes responsible for dust uprising in West Africa, namely: (1) the diurnal variation of surface wind speed modulated by the low level jet occurring after sunrise due to turbulent mixing (Washington et al., 2006), especially in the Bodélé depression; (2) the gust wind associated with the density currents emanating from convective systems occurring in the afternoon.

We also noted a bias for the values of AOT in the same period but with a less pronounced intensity than for surface concentration.

Page 5769 line 22-25: Sentence “In summer,.....remains high” now reads:

“In summer, the simulated and observed surface concentrations are low for these two stations. In contrast, noticeable differences are seen from April to June at Banizoumbou. For this site, the simulated surface concentration decreases while the PM10 concentration remains high. The model underestimations observed during April to June are probably related to local dust uprisings that are not well simulated by ALADIN model. This underestimation is strong in June, which marks the transition between the dry and the wet season monsoon in West Africa. Recently, a study realized by Kocha et al., (2013) shows the existence of two important processes responsible for dust uprising in West Africa, namely: (1) the diurnal variation of surface wind speed modulated by the low level jet occurred after sunrise due to turbulent mixing (Washington et al., 2006), especially in Bodélé depression; (2) the gust wind associated with the density currents emanating from convective systems occurred at the

afternoon. This second phenomenon generate a strong gust winds can lead to the "dust wall" known "haboob" (Tulet et al., (2010) ; Knippertz et al. (2012)).

We also noted a bias for the values of AOT in the same period but with a less pronounced intensity than for surface concentration."

Ref:

Washington, R., Todd, M. C., Engelstaedter, S., Mbainayel, S., and Mitchell, F.: Dust and the low-level circulation over the Bodélé depression, Chad: Observations from BoDEx 2005, *J. Geophys. Res.*, 111, D03201, doi:10.1029/2005JD006502, 2006.

Knippertz P., and Todd, M. C., Mineral dust aerosols over the Sahara: Meteorological controls on emission and transport and implications for modeling, *Rev. Geophys.*, 50, RG1007, doi:10.1029/2011RG000362, 2012.

RC12:

Page 5770 L 10 : There is also a model overestimation during July.

AC12:

Thanks, it was a mistake. Rather, "there is also a model underestimation during July". This is corrected in the final version of the manuscript.

Page 5770 line 9-10: Sentence "Over Mbour.....in August." Will be "Over Mbour, the monthly simulated surface concentrations are larger than the observations over all months except in July and August."

Response for Referee #2

We thank Referee #2 for the support given to this paper and for the comments to improve it. His comments and remarks are carefully taken into account in the revised version of this manuscript.

General remarks

RC1:

The present manuscript search to quantify the dust emission and deposition over North Africa and establish a climatology of optical properties over the region using a 5-year simulation (2006-2010) of the ALADIN model which is coupled to the surface me SURFEX. The model results are compared against MODIS, CALIPSO and AERONET observations showing the ability of the model to reproduce the main dust patterns observed over North Africa.

While the results of the study are interesting to be published, their presentation and discussion are not yet sufficient enough to be published at Atmospheric Chemistry and Physics in the current form. The present manuscript is focusing on the model evaluation more than in the analysis of the processes associated to dust cycle or differences along the simulated period that can be affect the model results as changes in the land surface properties, for example. Therefore, I would suggest to the authors to resubmit the manuscript to Geoscientific Model Development (GMD).

AC1:

Our paper indeed includes a validation of the ALADIN model which could have been part of a publication material for GMD for instance. However, we believe that original parts of the modelling development work for ALADIN-DUST actually already have been published precisely in GMD, and we refer to the discussion of the numerical parameterization in Mokhtari et al., (2012). The main purpose of this paper is to produce a climatology of desert aerosols in North Africa. In this sense, we believe that the paper is closer to the ACP scopes. The relevance of this paper for ACP was already confirmed by the Scientific Editor for the article, upon submission time.

General Comments

RC1:

The manuscript demonstrates the ability of the ALADIN model to reproduce the main dust patterns observed over North Africa for the period 2006-2010. The authors include a set of observational datasets that focus to provide a database of dust optical properties, however only the aerosol extinction (AOT and extinction) is discussed.

In the current form, the present work is showing a model evaluation results and it would need to include to answer a particular question. Any sensitivity analysis to differences on the refractive index, single scattering albedo or size distribution is considered. Furthermore, an analysis of the processes associated to dust cycle or differences along the simulated period that can be affect the model results as changes in the land surface properties should be included in the manuscript. Also, if there is any new model development included in the present model configuration should be emphasized in the manuscript or a discussion that emphasize the improvement that represents to use a dust climatology based on a regional model instead to a global model.

AC1:

Indeed, in this manuscript, only the optical thickness and the extinction coefficients are discussed and analyzed. We chose these two parameters to validate the optical properties simulated by ALADIN for three reasons: the first reason is the availability of observational data over a fairly long timescale for these two products, covering the total period of simulations, which highly facilitates a comparison. The second reason is the quality of these two products in the data, especially for optical thicknesses. The last reason is that only the extinction climatology is used in the radiative scheme of atmospheric models.

We agree that analyzing the SSA or g distribution and evolution would reinforce the paper particularly to see how these parameters are depending on size distribution (Mallet et al., 2009).

But in addition to that, we analyzed the dust source and deposition areas and the surface concentrations and we have given inter-comparisons with other previous studies.

The ALADIN model does simulate the single scattering albedo (SSA) and particle size distribution. But comparable observational products are not available for the period of simulation. The validation of these two products can be treated for specified case studies such as done in Mallet et al., 2009 or in Crumeyrolle et al., 2008, 2011. These studies use the same aerosol scheme and the same method to retrieve the aerosol optical properties (SSA, g, extinction). These references have been added in the revised paper: (i) to show that the aerosol distribution is correctly modeled over West Africa with the ORILAM aerosol scheme, and (ii) to add comments about the evolution of the two other aerosol optical parameters (SSA and asymmetric factor) during their transport over West Africa.

According to the two last remarks, we propose to update the title of the article in order to clarify the subject:

“3D dust aerosol distribution and extinction climatology over North Africa simulated with the ALADIN numerical prediction model from 2006 to 2010.”

In the description of the ORILAM scheme:

Page 5757, line 20: after “.....(Binkowski and Roselle, 2003).” We add:

“The method of calculation of aerosol optical properties is described in Grini et al., (2006). The refraction indexes used in our work have been calculated following a table of interpolation proposed by Grini et al., (2006). The dust optical properties are calculated from these new indexes in function of lognormal parameter upon the AMMA size distribution (Tulet et al., 2008). ORILAM has been evaluated in several papers for the West Africa region. Crumeyrolle et al., (2008 and 2011) presented a thorough description of the size distribution for the AMMA campaign. Mallet et al., (2009) studied the evolution of the asymmetry factor (g) and the single scattering albedo (SSA) for the dust storm event of March 2006 and studied the radiative balance over West Africa. Such specific studies however only can be carried out for particular situations.”

Ref:

Mallet, M., Tulet, P., Serc, D., Solmon, F., Dubovik, O., Pelon, J., Pont, V., and Thouron, O.: Impact of dust aerosols on the radiative budget, surface heat fluxes, heating rate profiles and convective activity over West Africa during March 2006, *Atmos. Chem. Phys.*, 9, 7143–7160, doi:10.5194/acp-9-7143-2009, 2009.

Crumeyrolle, S., Gomes, L., Tulet, P., Matsuki, A., Schwarzenboeck, A., and Crahan, K.: Increase of the aerosol hygroscopicity by cloud processing in a mesoscale convective system:

a case study from the AMMA campaign, *Atmos. Chem. Phys.*, 8, 6907–6924, doi:10.5194/acp-8-6907-2008, 2008.

Tulet, P., Mallet, M., Pont, V., Pelon, J., and Boone, A.: The 7–13 March, 2006, dust storm over West Africa: generation, transport and vertical stratification, *J. Geophys. Res.*, 113, D00C08, doi:10.1029/2008JD009871, 2008.

In the sub-section (2.3) **2006-2010 simulations**:

Page 5759, Line 15: we add:

“In this paper, we restrict the analysis to the extinction coefficient and its vertical integration (AOT) for comparison with the observations available for the 2006-2010 period.”

RC2:

Discussions of the results would be easier to follow if some statistics were included in the AERONET and MODIS comparison. Also, I would suggest to include a new sub-section in Sect. 2 with the description of the different observational datasets used in the model comparison. This new section will include a description of the different AERONET sites and satellite aerosol products used and their limitations in the dust model comparison as other possible aerosol species that can affect the discussion of the results or the temporal and spatial resolution of these products.

AC2:

In the paper, a qualitative comparison is made for concentrations (Fig. 12), a statistical comparison for optical thicknesses in order to evaluate the representativeness of our simulation (Fig. 11, and discussion on AOT correlation coefficient, section 4.2). Furthermore, we have used a Z_a factor for the case of extinction coefficients, which gives access to the average vertical profile of extinctions (Fig. 13 and 14). Another quantitative evaluation was for emissions, where we compared the estimated values with those given in previous studies. We have also introduced in the manuscript the correlation coefficient for the dust surface concentration (see Fig. 1).

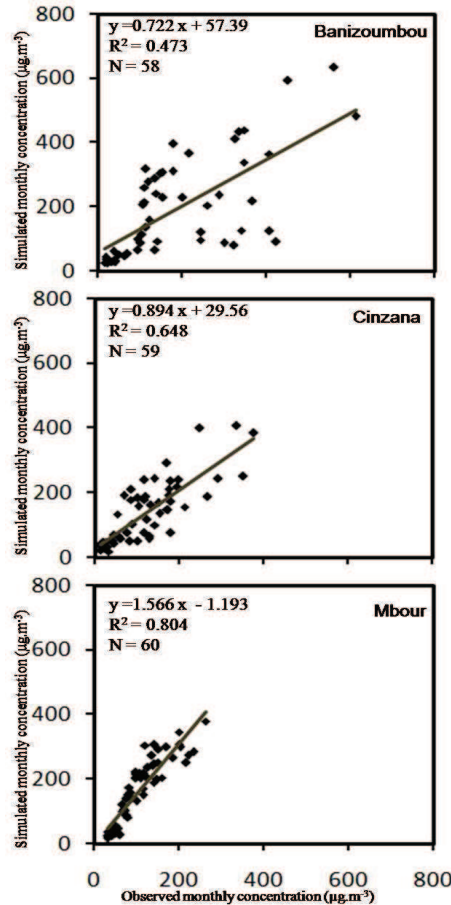


Fig.1: Scatter plot of monthly ALADIN dust surface concentration against observation over Banizoumbou, Cinzana and Mbour from 2006 to 2010. N is the number of averaged monthly surface concentration data available from 2006 to 2010. R is the correlation coefficient.

Concerning the integration of a subchapter describing different observational dataset used in the model, we have followed the recommendation of the Reviewer as this indeed clarifies the descriptions in our paper.

Page 5759, after sect. 2.3: we added the sub-section 2.4

2.4 Dataset

2.4.1 Ground-based measurement

In this study we use the AERONET AOT product (level 2) and the PM10 measured dust mass concentration (Particulate Matter concentration, particles with diameter of 10 μm or less) in order to evaluate the model-simulated AOT and the surface dust concentration, respectively, from 2006 to 2010.

AERONET (<http://aeronet.gsfc.nasa.gov/>) is a federation of ground-based remote sensing instruments measuring aerosol and its characteristics (Holben et al., 1998). The AERONET sunphotometers directly measure aerosol optical thickness at seven wavelengths (approximately 0.340, 0.380, 0.440, 0.500, 0.675, 0.870, and 1.02 μm) with an estimated uncertainty of 0.01 – 0.02 (Holben et al., 2001). In the model, the AOT is simulated at 0.55 μm , and it is therefore compared to the AOT measured at the nearest wavelength, 0.440 μm or 0.675 μm . Following Schmechtig et al., (2011) the AOT measured over Banizoumbou, Cinzana and Mbour, at wavelength 0.44 μm and 0.675 μm , are significantly correlated ($r^2 = 0.99$) with slopes ranging from 1.04 in Cinzana to 1.06 in MBour. Thus, in our study, we used the AOT measured at 0.44 μm over the five AERONET sites located in West Africa at:

Banizoumbou (Niger), Cinzana (Mali), DMN_Maine_Soroa (Niger), Mbour (Senegal) and Capo Verde (Fig. 2). We note that the AOT measurements only are possible during the day since they are based on measuring the solar radiation attenuation. This characteristic may be affecting the results of the intercomparison if a dust storm event occurred at nighttime.

The three stations composing the “Sahelian Dust Transect” (SDT) (Marticorena et al., 2010) located in the Sahelian region at Banizoumbou, Cinzana and Mbour are used to validate the surface dust concentration simulated by ALADIN. The SDT provides a continuous monitoring of the atmospheric concentrations PM10 with a 5 minute time step, using a Tapered Element Oscillating Microbalance (TEOM 1400A from Thermo Scientific) equipped with a PM10 inlet. PM10 measurements refer to particulate matter which passes through a size-selective inlet with a 50% efficiency cutoff at 10 μm aerodynamic diameter (Marticorena et al., 2010). In terms of sensitivity, the detection limit of the instrument is about 0.06 $\mu\text{g.m}^{-3}$ for a one hour sampling time.

2.4.2 Satellite data

The Aqua-MODIS product (Tanré et al., 1997; Levy et al., 2007) was used to evaluate the AOTs simulated by ALADIN. This instrument is a multi-spectral radiometer, designed to retrieve aerosol microphysical and optical properties over ocean and land. Two products of Aqua-MODIS are considered in this study: the MODIS Dark Target (DT) and the MODIS Deep Blue (DB) algorithms (Hsu et al., 2004). The MODIS DT algorithm over land is not designed to retrieve aerosol over bright surfaces, such as the Saharan deserts due to the large values of surface reflectivity (Remer et al., 2005; Shi et al., 2013). This problem leads to large spatial gaps in the aerosol optical thickness recorded in desert regions, although these regions are affected by some of the largest aerosol loadings worldwide. However, the DB algorithm takes advantage of this surface phenomenology by performing aerosol retrievals in the visible blue spectrum (such as the 0.47 μm spectral channel in MODIS) and by utilizing the selected aerosol model in the inversion to generate the AOT (Hsu et al., 2004, 2006; Shi et al., 2013). Thus, a combination between these two products is made to complete the AOT database for the whole of North Africa (ocean and land).

Over bright arid region, only DB data are available, offering no alternative choice. Conversely, in the areas with dense vegetation and ocean, only DT data are available and are therefore used in our study, in these regions. In addition, we have transition areas with low vegetation such as the Sahel (10°N-15°N). For these areas, both the DB and DT products are available. The DT product for the semi-arid regions tends however to be biased and underestimated (Levy et al., 2010). For example, the difference between DB and DT estimated for the transition regions can exceed 0.3. For this reason we chose the DB product for the transition regions. Recently, Levy et al., (2013) proposed another solution for the transition regions, namely to merge the two products and create a combined AOD product. Levy et al., (2013) used the Normalized Difference Vegetation Index (NDVI) to identify these regions. Unfortunately, this solution has not yet been validated.

The CALIOP Level 2 Layer 5 km product was used to evaluate the mean particle vertical distributions simulated by ALADIN over North Africa. The CALIOP instrument (Winker et al., 2007) was launched in 2006 on the Cloud–Aerosol Lidar and Pathfinder Satellite Observations (CALIPSO) spacecraft, and has now provided over 8 years of nearly continuous global measurements of aerosols and clouds with high vertical and spatial resolution at two-wavelength (532 nm and 1064 nm) (Rogers et al., 2014). As part of the “A-train” multisatellite constellation, CALIPSO follows a 705 km sun-synchronous polar orbit, with an equator-crossing time of about 1:30 P.M., local solar time (Stephens et al., 2002). The orbit

repeats the same ground track every 16 days. The vertical distribution of aerosols, provided by lidar, is important for radiative forcing (e.g., Satheesh, 2002), air quality studies (e.g., Al-Saadi et al., 2005; Engel-Cox et al., 2006), and model validation (Dirksen et al., 2009; Koffi et al., 2012). The CALIOP instrument and its initial performance assessment are described in Winker et al. (2007) and Hunt et al. (2009).



Fig. 2: Location of the five AERONET sites used in this study to evaluate the ALADIN simulated AOT over West Africa Banizoumbou (Niger), Cinzana (Mali), DMN_Maine_Soroa (Niger), MBour (Senegal) and Capo verde.

Ref:

Levy, R. C., Remer, L. A., Kleidman, R. G., Mattoo, S., Ichoku, C., Kahn, R., and Eck, T. F.: Global evaluation of the Collection 5 MODIS dark-target aerosol products over land, *Atmos. Chem. Phys.*, 10, 10399–10420, doi:10.5194/acp-10-10399-2010, 2010.

Levy, R. C., Mattoo, S., Munchak, L. A., Remer, L. A., Sayer, A. M., Patadia, F., and Hsu N. C.: The Collection 6 MODIS aerosol products over land and ocean, *Atmos. Meas. Tech.*, 6, 2989–3034, doi:10.5194/amt-6-2989-2013, 2013

Winker, D. M., Hunt, W. H., and McGill, M. J.: Initial performance assessment of CALIOP, *Geophys. Res. Lett.*, 34, L19803, doi:10.1029/2007GL030135, 2007.

Hunt, W. H., Winker, D. M., Vaughan, M. A., Powell, K. A., Lucker, P. L., and Weimer, C.: CALIPSO lidar description and performance assessment, *J. Atmos. Ocean. Tech.*, 26, 1214–1228, doi:10.1175/2009jtecha1223.1, 2009.

Rogers, R. R., Vaughan, M. A., Hostetler, C. A., Burton, S. P., Ferrare, R. A., Young, S. A., Hair, J. W., Oblad, M. D., Harper, D. B., Cook, A. L., and Winker, D. M.: Looking through the haze: evaluating the CALIPSO level 2 aerosol optical depth using airborne high spectral resolution lidar data, *Atmos. Meas. Tech.*, 7, 4317–4340, doi:10.5194/amt-7-4317-2014, 2014.

Holben, B. N., Tanre, D., Smirnov, A., Eck, T. F., Slutsker, I., Abuhassan, N., Newcomb, W. W., Schafer, J., Chatenet, B., Lavenu, F., Kaufman, Y., Van de Castle, J., Setzer, A., Markham, B., Clark, D., Frouin, R., Halthore, R., Karnieli, A., O'Neill, N. T., Pietras, C., Pinker, R. T., Voss, K., and Zibordi, G.: An emerging ground-based aerosol climatology: Aerosol Optical Depth from AERONET, *J. Geophys. Res.*, 106, 12067–12098, 2001.

Stephens, G. L., Vane, D. G., Boain, R. J., Mace, G. G., Sassen, K., Wang, Z., Illingworth, A. J., O'Connor, E. J., Rossow, W. B., Durden, S. L., Miller, S. D., Austin, R. T., Benedetti, A., and Mitrescu, C.: The cloudsat mission and the A-Train: a new dimension of space-based observations of clouds and precipitation, *B. Am. Meteorol. Soc.*, 83, 1771–1790+1742, 2002.

Al Saadi, J., Szykman, J., Pierce, R. B., Kittaka, C., Neil, D., Chu, D. A., Remer, L. A., Gumley, L., Prins, E., Weinstock, L., MacDonald, C., Wayland, R., Dimmick, F., and Fishman, J.: Improving national air quality forecasts with satellite aerosol observations, *Bull. Am. Meteorol. Soc.*, 1249–1261, doi:10.1175/BAMS-86-9-1249, 2005.

Engel-Cox, J. A., Hoff, R. M., Rogers, R., Dimmick, F., Rush, A. C., Szykman, J. J., Al-Saadi, J., Chu, D. A., and Zell, E. R.: Integrating LIDAR and satellite optical depth with ambient monitoring for 3-D dimensional particulate characterization, *Atmos. Environ.*, 40, 8056–8067, 2006.

Dirksen, R. J., Boersma, K. F., de Laat, J., Stammes, P., van der Werf, G. R., Val Martin, M., and Kelder, H. M.: An aerosol boomerang: rapid around-the-world transport of smoke from the December 2006 Australian forest fires observed from space, *J. Geophys. Res.*, 114, D21201, doi:10.1029/2009JD012360, 2009.

Satheesh, S. K.: *Letter to the Editor* Aerosol radiative forcing over land: effect of surface and cloud reflection, *Ann. Geophys.*, 20, 2105–2109, doi:10.5194/angeo-20-2105-2002, 2002.

Minor errors:

RC1:

Introduction Sect. should be updated with a more recent publications. For example, the latest IPCC report (IPCC, 2013) or the reference of the dust AEROCOM intercomparison (i.e. Huneeus et al., 2010) are missing.

AC1:

The reference is updated in the revised manuscript.

Page 5753 line 2-3: The sentence “Dust aerosol.....(IPCC,2007).” becomes:

“Mineral dust aerosol dominates the aerosol mass over some continental regions with relatively higher concentrations accounting for about 35% of the total aerosol mass (IPCC, 2013)”.

Ref:

Intergovernmental Panel on Climate Change (IPCC): Climate Change 2013: The Physical Science Basis in: Clouds and Aerosols, Contribution of Working Group I to the Fifth Assessment Report of the Intergovernmental Panel on Climate Change [Stocker, T.F., D. Qin, G.-K. Plattner, M. Tignor, S.K. Allen, J. Boschung, A. Nauels, Y. Xia, V. Bex and P.M. Midgley (eds.)], Boucher, O., D. Randall, P. Artaxo, C. Bretherton, G. Feingold, P. Forster, V.-M. Kerminen, Y. Kondo, H. Liao, U. Lohmann, P. Rasch, S.K. Satheesh, S. Sherwood, B. Stevens and X.Y. Zhang, Cambridge University Press, Cambridge, United Kingdom and New York, NY, USA, 1535 pp, doi:10.1017/CBO9781107415324, 2013.

RC2:

Page 5755 Line 18-19: The reference to the SDS-WAS is not well justify in the text.

AC2:

Some details have been added in the revised version of the manuscript and the paragraph now reads:

Page 5755 line 17-23: The paragraph: “Initiatives havecapabilities” becomes:

“Initiatives have already been taken to use operational Numerical Weather Prediction (NWP) and regional models at high resolution and short timescales. These efforts include the WMO Sand and Dust Storm Warning Advisory and Assessment (SDS-WAS, <http://sds-was.aemet.es>) program, whose mission is to achieve comprehensive, coordinated and sustained observations and modeling of sand and dust storms in order to improve the monitoring of such storms, increase understanding of the dust processes and enhance dust prediction capabilities. SDS-WAS is established as a federation of partners organized around regional nodes (Northern Africa-Middle East-Europe Node and Asian Node). About 16 dust prediction models have been used in SDS-WAS as BSC-DREAM8b, MACC-ECMWF, INCA-LMDZT, CHIMERE, SKIRON, ETA, NGAC, NAAPS....”

RC3

Page 5757 Line 18-23: The calculation of aerosol optical properties should be described in more details because the optical properties are the focus of the present study.

AC3:

The method of calculation of aerosol optical properties is described in more detail in Grini et al., (2006). The refraction indexes used in our work have been calculated following a table of interpolation proposed by Grini et al., (2006). The dust optical properties are calculated from these new indexes in function of lognormal parameter upon the AMMA size distribution (Tulet et al., 2008). These references have been added in the revised version of the manuscript. (See general comments, AC1)

RC4:

Page 5759 Sect. 2.3: The model simulation begins 1 January 2006, or is there a spin-up period for dust concentration?

AC4:

Thank you for this remark. Indeed, the model simulation do have a spin-up period. This is the reason why our numerical simulation period actually starts on 25 December 2005, in order to build up a more realistic initial state for the dust concentrations. This information was added in the revised version of the manuscript.

Page 5759 line 3-6: The sentence “To simulate next simulation.” becomes:

“To simulate the 2006–2010 period, successive forecasts of two consecutive days (48 h) are performed. The final term of each simulation is used as the initial condition for the dust concentration of the next simulation. The model simulation has a spin-up period and in order to start our study with a realistic initial state for dust concentrations, the start date of the numerical simulations is 25 December 2005. However, for the evaluations described in this article, only data from 1 January 2006 through 31 December 2010 are considered.”

RC5:

Page 5759 Line 14: Indicate the coordinate of the vertical layer (sigma?).

AC5:

Thank you for this remark, it is hybrid vertical coordinate.

Page 5759 line 13-14: The sentence: “The horizontal 67 km.” becomes in the revised manuscript:

“The horizontal resolution is 20 km x 20 km with 60 hybrid vertical levels; from the surface to 67 km.”

RC6:

Page 5760 Line 13: In the comparison of ALADIN with the rest of the model results (global and regional), ALADIN is the model that provides highest emissions between the regional models meanwhile it is lower with the global. This should be better discussed in the text.

AC6:

This is correct; the global models give large dust emission. This aspect is now discussed in the revised text.

Page 5760 line 5-13: the paragraph “Table 2 compares.....Zender et al. (2003)” becomes: “Table 2 compares the annual mean dust flux obtained in this work with other recent global and regional dust model studies. Important differences in the annual mean dust flux can be observed. The largest value of the annual mean dust flux is simulated by Ginoux et al. (2004) and is equal to $1430 \text{ Tg year}^{-1}$, which is twice as large as the value simulated by Marticorena and Bergametti (1996) ($665-586 \text{ Tg year}^{-1}$). Our estimation lies between those obtained by Ginoux et al. (2004) and by Marticorena and Bergametti (1996), and is in good agreement with the value obtained by d’Almeida (1986), Callot et al. (2000), Laurent et al. (2008) and Zender et al. (2003).

Dust emissions depend on both surface features and soil types, but they also depend on the meteorological conditions (wind and precipitation). These elements are defined differently from one model to another. Global models have a relatively low resolution, and thus misrepresent the surface characteristics (roughness) and the soil types (% of clay and % of sand). As a consequence, these models tend to overestimate the spread of dust emission areas. For example, at $1^\circ \times 1^\circ$ resolution (medium resolution of global models), an entire area can become a dust emission source when in reality it is not. Eventually, dust emission is overestimated as well. Regional models, due to their higher resolution, provide more details on the emission source areas compared with global models, which then in turn enables to diminish this positive bias.

It is also interesting to mention that the three values of dust emission estimated by Zender et al., (2003), Laurent et al., (2008), Marticorena et al., (1995) and the one of our study are all based on the same dust mobilization scheme of Marticorena et al. (1995). Therefore, a correlation between the estimates of these four studies can be expected.”

RC7:

Page 5761 Line 14: Again, the authors are compared the results of the regional ALADIN model with a global model results from Tanaka and Chiba (2005). I would be desirable to include a discussion about the possible improvement that represents to use a regional model at 20km x 20km in comparison with a global model.

AC7:

We have mentioned Tanaka and Chiba (2005) for the comparison of our results because this study shows the seasonal variation on dust emissions over North Africa. A discussion will be added in the text.

Page 5761 line 14-19: The paragraph: “This seasonality is consistentTanaka and Chiba (2005).” becomes:

“This seasonality reproduces the general pattern of the seasonality simulated by Tanaka and Chiba (2005) for the period 1979–2003 over North Africa with the global CTM model (MASINGAR) at a resolution of 1.8 x 1.8°. In contrast, in terms of intensity, the dust emission flux simulated by MASINGAR in spring accounts for almost half of the total emissions in North Africa (500 Tg). These estimates are higher than those simulated by ALADIN.

In summer, the dust emission flux simulated by MASINGAR is much underestimated compared with the flux estimated by ALADIN. Indeed, the summer season is characterized by significant dust uprising over the Sahel in connection with large convective systems. These systems generate strong gust winds at the leading edge of their cold pools which can lead to “walls of dust” known as “haboob”, a sometimes fast moving and extremely hazardous phenomenon (Knippertz et al. 2012). However, even regional models at resolution of about 10 km do not adequately represent these processes, neither in climatological terms nor for weather forecasting (Knippertz et al. 2012).”

Ref:

Knippertz P., and Todd, M. C., Mineral dust aerosols over the Sahara: Meteorological controls on emission and transport and implications for modeling, *Rev. Geophys.*, 50, RG1007, doi:10.1029/2011RG000362, 2012.

RC8:

Page 5762 Line 21-22: the authors indicates “we show that the use of a three dimensional NWP model such as ALADIN significantly improves the climatology of wet deposition of dust aerosols”. This sentence needs to be better justified with the comparison with other model studies.

AC8:

We added in the revised manuscript the intercomparison with other models studies.

Page 5763 line 17: we add after dry deposition. The paragraph below:

“The inter-comparison of dust wet deposition simulated by ALADIN for the year 2006 with models used in the AEROCOM and SDS-WAS programs (BSC-DREAM8b, GOCART-v4Ed.A2 CTRL, GISS-modelE.A2 CTRL and TM5-V3.A2 CTRL, http://aerocom.met.no/cgi-bin/aerocom/surfobs_annualrs.pl) for the same period is given by the Table 1. The results show that the mean wet deposition estimated by ALADIN is much higher than those estimated by AEROCOM Model's. As discussed for the seasonal wet deposition, the major part of the wet deposition takes place during the wet season of the African Monsoon.

In terms of spatial distribution, the ALADIN model performs better for the estimation of the dust wet deposition associated with convective systems in the Sahelian regions. For example, the estimates of the BSC-DREAM8b model do not exceed $0.2 \text{ g.m}^{-2}.\text{year}^{-1}$ for the Sahel and the West African region. Those simulated by TM5-V3.A2 CTRL are less than $5 \text{ g.m}^{-2}.\text{year}^{-1}$ and those obtained by GOCART-v4Ed.A2 CTRL and GISS-modelE.A2 CTRL varied in the range $20-50 \text{ g.m}^{-2}.\text{year}^{-1}$. The fact that some part of the total precipitation of ALADIN is resolved can explain that the wet deposition processes in ALADIN are found to be more efficient than in some global models.”

Table 1: Mean dust wet deposition

Models	Wet deposition for 2006 in (g.m ⁻² .year ⁻¹)
BSC-DREAM8b	0.46
GOCART-v4Ed.A2 CTRL	9.653
GISS-modelE.A2 CTRL	8.301
TM5-V3.A2 CTRL	4.673
This study	21,36

RC9:

Page 5762 Line 3: In Fig. 5, Bodélé is not the region with the maximum deposition, only in winter we find maximum deposition in this region. This is consequence to low level dust transport during this period. This should be emphasized in the text.

AC9:

Thank you for this remark.

The sentence: page 5762 line 5: “In winter200g/m⁻²” becomes :

“In winter, the maximum of the seasonal dust deposition flux is located in the Bodélé Depression, with a value reaching 200 g.m⁻². This maximum is a consequence of low level dust transport during this period.”

RC10:

Page 5764 Line 2: the climatology shown in Nabat et al. (2013), does it include the years analysed in the present study? It would be interesting that the authors would include it.

AC10:

The climatology of Nabat et al. (2013) covers the 1979-2009 period and has 50 km of resolution.

This information is included in the revised version of the manuscript.

Page 5755, line 14-16: The sentence “Based on bothSea” becomes

“Based on both satellite-derived monthly AOTs and a regional/chemistry model, Nabat et al. (2013) proposed a three-dimensional (3-D) monthly climatology of aerosol distribution over the Mediterranean Sea for the 1979-2009 period and at 50 km of resolution”

RC11:

Page 5767 Line 16: There isn't any Soroa AERONET site in the AERONET website (http://aeronet.gsfc.nasa.gov/cgi-bin/type_piece_of_map_opera_v2_new). Could the authors check it?

AC11:

Thank you for this remark, the Soroa AERONET site refers to the DMN_Maine_Soroa AERONET site. This is precision is added in the revised text

Page 5756 line 3: “Soroa” will be “DMN_Maine_Soroa (hereafter Soroa)”

RC12:

Page 5769 Line 22: The model underestimations observed during summer are associated to convective dust storms (haboobs) that the models are not capable to reproduce (see Knippertz and Todd, 2012).

AC12:

Thank you for this remark; this is corrected in the revised text.

Page 5769 line 22-25: Sentence "In summer,.....remains high" now reads:

"In summer, the simulated and observed surface concentrations are low for these two stations. In contrast, noticeable differences are seen from April to June at Banizoumbou. For this site, the simulated surface concentration decreases while the PM10 concentration remains high. The model underestimations observed during April to June are probably related to local dust uprisings that are not well simulated by ALADIN model. This underestimation is strong in June, which marks the transition between the dry and the wet season monsoon in West Africa. Recently, a study realized by Kocha et al., (2013) shows the existence of two important processes responsible for dust uprising in West Africa, namely: (1) the diurnal variation of surface wind speed modulated by the low level jet occurred after sunrise due to turbulent mixing (Washington et al., 2006), especially in Bodélé depression; (2) the gust wind associated with the density currents emanating from convective systems occurred at the afternoon. This second phenomenon generate a strong gust winds can lead to the "dust wall" known "haboob" (Tulet et al., (2010) ; Knippertz et al. (2012)).

We also noted a bias for the values of AOT in the same period but with a less pronounced intensity than for surface concentration."

RC13:

Page 5770 Line 6: "March" instead "Mars"

AC13:

Thanks, it will be been rectified in the revised manuscript.

Page 5770 line 5-7: Sentence "The maximum simulated.....for PM10). Will be:

"The maximum simulated surface concentration and observation is obtained in March (278 $\mu\text{g.m}^{-3}$ for ALADIN and 257 $\mu\text{g.m}^{-3}$ for PM10)."

RC14:

Page 5770 Line 10: There is also a model overestimation during July

AC14:

Thanks, it was a mistake. Rather, "there is also a model underestimation during July". This is corrected in the revised version of the manuscript.

Page 5770 line 9-10: Sentence "Over Mbour.....in August." now reads "Over Mbour, the monthly simulated surface concentrations are larger than the observations over all months except in July and August."

List of changes

- 1) **Title:** We suggest a new title to clarify the subject:
“3D dust aerosol distribution and extinction climatology over North Africa simulated with the ALADIN numerical prediction model from 2006 to 2010.”
- 2) **Page 5753 line 2-3:** The sentence “Dust aerosol.....(IPCC,2007).” becomes:
“Mineral dust aerosol dominates the aerosol mass over some continental regions with relatively higher concentrations accounting for about 35% of the total aerosol mass (IPCC, 2013)”.
Page 5753, line 17-19: sentence “Therefore, an accurate.....(RCMs)” will be:
“Therefore, an accurate database of aerosol content in this region is crucial to identify and quantify this impact, particularly in Regional Climate Models (RCMs).”
- 3) **Page 5753, line 20-23:** the sentence “For example.....’Morcrette et al., 2009)” will be:
“For example, various studies (Tompkins et al., 2005; Rodwell, 2005) have shown the positive impact of the switch from the Tanré et al. (1984) climatology to the Tegen et al. (1997) climatology for various aspects of the ECMWF model (Morcrette et al., 2009). Tompkins et al., (2005) have performed a couple of 5-day forecasts of the African Easterly Jet (AEJ) with the old and new climatology and the results are compared with high resolution dropsonde data from the JET2000 campaign. The results of these simulations show that the new aerosol climatology significantly improves some aspects of the AEJ structure and strength. In the same study, 4 months of 5-day forecasts was realized and compared using the contrasting aerosol distributions. The results show a clear improvement with the new climatology, with the jet strengthened, elongated to the east, and less zonal, in agreement with the analyses. The new climatology suppresses deep convection by stabilizing the atmosphere, preventing the ITCZ from progressively migrating north during the forecast. A strong reduction of mean equivalent potential temperature at the lowest model level is noted, with the southerly displacement of the ITCZ. More recently, Kocha et al. (2012) have shown the impact of dust storms on the cold extra-tropical outbreak and on the African Easterly Jet.”
- 5) **Page 5755, line 14-16:** The sentence “Based on bothSea” becomes
“Based on both satellite-derived monthly AOTs and a regional/chemistry model, Nabat et al. (2013) proposed a three-dimensional (3-D) monthly climatology of aerosol distribution over the Mediterranean Sea for the 1979-2009 periods and at 50 km of resolution”
- 6) **Page 5755 line 17-23:** The paragraph: “Initiatives havecapabilities” becomes:
“Initiatives have already been taken to use operational Numerical Weather Prediction (NWP) and regional models at high resolution and short timescales. These efforts include the WMO Sand and Dust Storm Warning Advisory and Assessment (SDS-WAS, <http://sds-was.aemet.es>) program, whose mission is to achieve comprehensive, coordinated and sustained observations and modeling of sand and dust storms in order to improve the monitoring of such storms, increase understanding of the dust processes and enhance dust prediction capabilities. SDS-WAS is established as a federation of partners organized around regional nodes (Northern Africa-Middle East-Europe Node and Asian Node). About 16 dust prediction models has been used in SDS-WAS as BSC-DREAM8b, MACC-ECMWF, INCA-LMDZT, CHIMERE, SKIRON, ETA, NGAC, NAAPS....”

7) **Page 5756 line 3:** “Soroa” will be “DMN_Maine_Soroa (hereafter cited Soroa)”

8) **Page 5757, line 9-11:** sentence “Microphysical processes (Lopez, 2002)” will be:
“Microphysical processes such as auto-conversion, collection, evaporation, sublimation, melting and sedimentation are represented following the parametrization of Lopez (2002).”

9) In the description of ORILAM scheme:

Page 5757, line 20: after “.....(Binkowski and Roselle, 2003).” We add:
“The method of calculation of aerosol optical properties is described in Grini et al., (2006). The refraction indexes used in our work have been calculated following a table of interpolation proposed by Grini et al., (2006). The dust optical properties are calculated from these new indexes in function of lognormal parameter upon the AMMA size distribution (Tulet et al., 2008). ORILAM has been evaluated in several papers for the West Africa region. Crumeyrolle et al., (2008 and 2011) presented a thorough description of the size distribution for the AMMA campaign. Mallet et al., (2009) studied the evolution of the asymmetry factor (g) and the single scattering albedo (SSA) for the dust storm event of March 2006 and studied the radiative balance over West Africa. Such specific studies however only can be carried out for particular situations.”

10) **Page 5758, line 17-20:** the sentence “Therefore, ECOCLIMAP.....ISBA.” Will be:
“The ECOCLIMAP database is designed in compliance with the SURFEX “tile” approach: each grid box is composed of four adjacent surfaces for nature (ISBA vegetation classes), urban areas (TEB model), sea or ocean and lake.”

11) **Page 5759 line 3-6:** The sentence “To simulate next simulation.” will be:
“To simulate the 2006–2010 period, successive simulations of two consecutive days (48 h) are simulated. The final term of each simulation is used as the initial condition for the dust concentration of the next simulation. The model simulation has a spin-up period in order to have a reasonably initial state for dust concentrations. So our simulations begin 25 December 2005 but only the results from 1 January 2006 through 31 December 2010 are considered.”

12) **Page 5759 line 13-14:** The sentence: “The horizontal 67 km.” becomes in the revised manuscript:
“The horizontal resolution is 20 km x 20 km with 60 hybrid vertical levels; from the surface to 67 km.”

13) In the sub-section (2.3) we add:
Page 5759, Line 15: “In this paper, we restrict the analysis to the extinction coefficient and its vertical integration (AOT) for comparison with the observations available for the 2006–2010 period.”

14) **We will introduce a new subchapter:**

Page 5759, after sect. 2.3: we add the sub-section 2.4

2.4 Dataset

2.4.1 Ground-based measurement

In this study we use the AERONET AOT product (level 2) and PM10 measured dust mass concentration (Particulate Matter concentration, particles with diameter of 10 μm or less) to evaluate the model-simulated AOT and surface dust concentration, respectively, from 2006 to 2010 period.

AERONET (<http://aeronet.gsfc.nasa.gov>) is a federation of ground-based remote sensing instruments measuring aerosol and its characteristics (Holben et al., 1998). The AERONET sunphotometers directly measure aerosol optical thickness at seven wavelengths (approximately 0.340, 0.380, 0.440, 0.500, 0.675, 0.870, and 1.02 μm) with an estimated uncertainty of 0.01 – 0.02 (Holben et al., 2001). In the model, the AOT is simulated at 0.55 μm , it is thus compared to the AOT measured at the closest wavelength, 0.440 or 0.675 μm . Following Schmechtig et al., (2011) the AOT measured over Banizoumbou, Cinzana and Mbour, at wavelength 0.44 and 0.675 μm are significantly correlated ($r^2 = 0.99$) with slopes ranging from 1.04 in Cinzana to 1.06 in MBour. So, in our study we used the AOT measured at 0.44 μm over the five AERONET sites located at the West Africa: Banizoumbou (Niger), Cinzana (Mali), DMN_Maine_Soroa (Niger), Mbour (Senegal) and Capo Verde (Fig. 1). We note that, the AOT measurements are only possible during the day as they are based on measuring the solar radiation attenuation. This may be affecting the intercomparison results if a dust storm event occurs at the night.

The three stations composing the “Sahelian Dust Transect” (SDT) (Marticorena et al., 2010) located in the Sahelian region: Banizoumbou, Cinzana and MBour are used to validate surface dust concentration simulated by ALADIN. The SDT provides a continuous monitoring of the atmospheric concentrations PM10 with a 5 minutes time step, using a Tapered Element Oscillating Microbalance (TEOM 1400A from Thermo Scientific) equipped with a PM10 inlet. PM10 measurements refer to particulate matter which passes through a size-selective inlet with a 50% efficiency cutoff at 10 μm aerodynamic diameter (Marticorena et al., 2010). In terms of sensitivity, the detection limit of the instrument is about 0.06 $\mu\text{g.m}^{-3}$ for a one hour sampling time.

2.4.2 Satellite data

The Aqua-MODIS product (Tanré et al., 1997; Levy et al., 2007) was used to evaluate the AOTs simulated by ALADIN. This instrument is a multi-spectral radiometer, designed to retrieve aerosol microphysical and optical properties over ocean and land. Two products of Aqua-MODIS are considered in this study: the MODIS Dark Target (DT) and the MODIS Deep Blue (DB) algorithms (Hsu et al., 2004). The MODIS DT algorithm over land is not designed to retrieve aerosol over bright surfaces, such as the Saharan deserts due to the large values of surface reflectivity (Remer et al., 2005; Shi et al., 2013). This problem leads to large spatial gaps in the aerosol optical thickness recorded in desert regions, although these regions are affected by some of the largest aerosol loadings worldwide. However, the DB algorithm takes advantage of this surface phenomenology by performing aerosol retrievals in the visible blue spectrum (such as the 0.47 μm spectral channel in MODIS) and by utilizing the selected aerosol model in the inversion to generate the AOT (Hsu et al., 2004, 2006; Shi et al., 2013). Thus, a combination between these two products is made to complete the AOT database for the whole of North Africa (ocean and land).

Over bright arid region, only DB data are available. Then there is no choice to be made in this case. Conversely, in the areas with densest vegetation and ocean, only DT data are available. Thus, we use this product for these areas. However, we have transition areas with low vegetation such as the Sahel (10°N-15°N). For these areas we have both the DB and DT products. Since DT product for the semi-arid region is tends to be biased and underestimated

(Levy et al., 2010). For example, the difference between DB and DT estimated for the transition region exceeds 0.3. For this reason we choice the DB product only for the transition regions. Recently, Levy et al., (2013) propose another solution for the case of these regions by merging the two products and creating a “best-of” AOD product that combines DB and DT products. Levy et al., (2013) used the Normalized Difference Vegetation Index (NDVI) to identify these regions. Unfortunately, this solution has not yet been validated.

The CALIOP Level 2 Layer 5 km product was used to evaluate the mean particle vertical distributions simulated by ALADIN over North Africa. The CALIOP instrument (Winker et al., 2007) was launched in 2006 on the Cloud–Aerosol Lidar and Pathfinder Satellite Observations (CALIPSO) spacecraft, and has now provided over 8 years of nearly continuous global measurements of aerosols and clouds with high vertical and spatial resolution at two-wavelength (532 and 1064 nm) (Rogers et al., 2014). As part of the “A-train” multisatellite constellation, CALIPSO follows a 705 km sun-synchronous polar orbit, with an equator-crossing time of about 1:30 P.M., local solar time (Stephens et al., 2002). The orbit repeats the same ground track every 16 days. The vertical distribution of aerosols, provided by lidar, is important for radiative forcing (e.g., Satheesh, 2002), air quality studies (e.g., Al-Saadi et al., 2005; Engel-Cox et al., 2006), and model validation (Dirksen et al., 2009; Koffi et al., 2012). The CALIOP instrument and its initial performance assessment are described in Winker et al. (2007) and Hunt et al. (2009).

15) Page 5759 line 19: change “Figure 1” by “Figure 2”

16) Page 5760 line 5-13: the paragraph “Table 2 compares.....Zender et al. (2003)” will be:

“Table 2 compares the annual mean dust flux obtained in this work with other recent global and regional dust model studies. Important differences in the annual mean dust flux can be observed. The largest value of the annual mean dust flux is simulated by Ginoux et al. (2004) and is equal to $1430 \text{ Tg year}^{-1}$, which is twice as large as the value simulated by Marticorena and Bergametti (1996) ($665\text{--}586 \text{ Tg year}^{-1}$). Our estimation lies between those obtained by Ginoux et al. (2004) and by Marticorena and Bergametti (1996), and is in good agreement with the value obtained by d’Almeida (1986), Callot et al. (2000), Laurent et al. (2008) and Zender et al. (2003).

Dust emissions depend on both surface features and soil types, but they also depend on the meteorological conditions (wind and precipitation). These elements are defined differently from one model to another. Global models have a relatively low resolution, and thus misrepresent the surface characteristics (roughness) and the soil types (% of clay and % of sand). As a consequence, these models tend to overestimate the spread of dust emission areas. For example, at $1^\circ \times 1^\circ$ resolution (medium resolution of global models), an entire area can become a dust emission source when in reality it is not. Eventually, dust emission is overestimated as well. Regional models, due to their higher resolution, provide more details on the emission source areas compared with global models, which then in turn enables to diminish this positive bias.

It is also interesting to mention that the three values of dust emission estimated by Zender et al., (2003), Laurent et al., (2008), Marticorena et al., (1995) and the one of our study are all based on the same dust mobilization scheme of Marticorena et al. (1995). Therefore, a correlation between the estimates of these four studies can be expected.”

17) Page 5760 line 20: change “Figure 2” by “Figure 3”

18) **Page 5760 line 25:** change “Figure 3” by “Figure 4”

19) **Page 5761 line 10:** change “Figure 4” by “Figure 5”

20) **Page 5761 line 14-19:** The paragraph: “This seasonality is consistentTanaka and Chiba (2005).” will be:
“This seasonality reproduces the general pattern of the seasonality simulated by Tanaka and Chiba (2005) for the period 1979–2003 over North Africa with the global CTM model (MASINGAR) at a resolution of $1.8 \times 1.8^\circ$. In contrast, in terms of intensity, the dust emission flux simulated by MASINGAR in spring accounts for almost half of the total emissions in North Africa (500 Tg). These estimates are higher than those simulated by ALADIN.
In summer, the dust emission flux simulated by MASINGAR is much underestimated compared with the flux estimated by ALADIN. Indeed, the summer season is characterized by significant dust uprising over the Sahel in connection with large convective systems. These systems generate strong gust winds at the leading edge of their cold pools which can lead to “walls of dust” known as “haboob”, a sometimes fast moving and extremely hazardous phenomenon (Knippertz et al. 2012). However, even regional models at resolution of about 10 km do not adequately represent these processes, neither in climatological terms nor for weather forecasting (Knippertz et al. 2012).”

21) **Page 5762 line 3:** change “Fig. 5” by “Fig. 6”

22) **Page 5762 line 5:** “In winter 200g.m^{-2} ” will be :
“In winter, the maximum of the seasonal dust deposition flux is located in the Bodélé Depression, with a value reaching 200 g.m^{-2} . This maximum is a consequence of low level dust transport during this period.”

23) **Page 5762 line 26:** change “Figure 6” by “Figure 7”

24) **Page 5763 line 17:** we add at the 3.3 section the paragraph below:
“The inter-comparison of dust wet deposition simulated by ALADIN for the year 2006 with models used in the AEROCOM and SDS-WAS programs (BSC-DREAM8b, GOCART-v4Ed.A2 CTRL, GISS-modelE.A2 CTRL and TM5-V3.A2 CTRL, http://aerocom.met.no/cgi-bin/aerocom/surfobs_annualrs.pl) for the same period is given by the Table 1. The results show that the mean wet deposition estimated by ALADIN is much higher than those estimated by AERCOM Model's. As discussed for the seasonal wet deposition, the major part of the wet deposition takes place during the wet season of the African Monsoon.
In terms of spatial distribution, the ALADIN model performs better for the estimation of the dust wet deposition associated with convective systems in the Sahelian regions. For example, the estimates of the BSC-DREAM8b model do not exceed $0.2 \text{ g.m}^{-2}.\text{year}^{-1}$ for the Sahel and the West African region. Those simulated by TM5-V3.A2 CTRL are less than $5 \text{ g.m}^{-2}.\text{year}^{-1}$ and those obtained by GOCART-v4Ed.A2 CTRL and GISS-modelE.A2 CTRL varied in the range $20-50 \text{ g.m}^{-2}.\text{year}^{-1}$. The fact that some part of the total precipitation of ALADIN is resolved can explain that the wet deposition processes in ALADIN are found to be more efficient than in some global models.”

25) **Page 5763 line 19:** change “Figure 7” by “Figure 8”

26) **Page 5764 line 22-25:** Sentence "Note that,.....in June" will be: "Note that, using both satellites and a regional chemistry model, Nabat et al. (2013) found, for the 1979-2009 periods, a value of 0.3 of AOT for these regions with a peak in June."

27) **Page 5765 line 3:** change "Fig. 8" by "Fig. 9"

28) **Page 5765 line 22-26 to Page 5766 line 1-10:** Remove "We use the (ocean and land)"

29) **Page 5766 line 11:** change "Figure 9" by "Figure 10"

30) **Page 5767 line 13-14:** change "Figures 10 and 11 show" by "Figures 11 and 12 show"

31) **Page 5767 line 20:** change "Fig. 10" by "Fig. 11"

32) **Page 5768 line 5:** change "Fig. 11" by "Fig. 12"

33) **Page 5769 line 17:** change "M'bour" by "Mbour"

34) **Page 5769 line 18:** change "Figure 12 showsM'bour" by "Figure 13 and 14 show, respectively, the monthly mean of the daily median value of measured and simulated surface concentrations and the scatter plot of monthly ALADIN dust surface concentration against observations over Banizoumbou, Cinzana and Mbour."

35) **Page 5769 line 22-25:** Sentence "In summer,.....remains high" will be: "In summer, the simulated and observed surface concentrations are low for these two stations. In contrast, noticeable differences are seen from April to June at Banizoumbou. For this site, the simulated surface concentration decreases while the PM10 concentration remains high. The model underestimations observed during April to June are probably related to local dust uprisings that are not well simulated by ALADIN model. This underestimation is strong in June, which marks the transition between the dry and the wet season monsoon in West Africa. Recently, a study realized by Kocha et al., (2013) shows the existence of two important processes responsible for dust uprising in West Africa, namely: (1) the diurnal variation of surface wind speed modulated by the low level jet occurred after sunrise due to turbulent mixing (Washington et al., 2006), especially in Bodélé depression; (2) the gust wind associated with the density currents emanating from convective systems occurred at the afternoon. This second phenomenon generate a strong gust winds can lead to the "dust wall" known "haboob" (Tulet et al., (2010) ; Knippertz et al. (2012)). We also noted a bias for the values of AOT in the same period but with a less pronounced intensity than for surface concentration."

36) **Page 5770 line 3:** we add after "....in August." The sentence: "The square of the correlation coefficient registered for Banizoumbou is equal 0.473 with a slop of the tendency curve equal 0.722."

37) **Page 5770 line 5-7:** Sentence "The maximum simulated.....for PM10). Will be: "The maximum simulated surface concentration and observation is obtained in March (278 $\mu\text{g.m}^{-3}$ for ALADIN and 257 $\mu\text{g.m}^{-3}$ for PM10)."

38) Page 5770 line 9: we add after “.....observed in August.” The sentence: “For this site, the correlation coefficient and the slope of the tendency curve are equal 0.648 and 0.894, respectively.

39) Page 5770 line 9-10: Sentence “Over Mbour.....in August.” Will be:
“Over Mbour, the monthly simulated surface concentrations are larger than the observations over all months except in July and August with a slope of tendency curve exceeds 1.566.”

40) Page 5770 line 13: add after “...in September” the sentence: “The correlation coefficient obtained over Mbour is equal 0.804.”

41) Page 5771 line 12: change “Figure 13” by “Figure 15”

42) Page 5771 line 20: change “Fig. 14” by “Fig. 16”

References:

Page 5775 line 20: add reference:

“Al Saadi, J., Szykman, J., Pierce, R. B., Kittaka, C., Neil, D., Chu, D. A., Remer, L. A., Gumley, L., Prins, E., Weinstock, L., MacDonald, C., Wayland, R., Dimmick, F., and Fishman, J.: Improving national air quality forecasts with satellite aerosol observations, Bull. Am. Meteorol. Soc., 1249–1261, doi:10.1175/BAMS-86-9-1249, 2005.”

Page 5776 line 22: add reference:

“Crumeyrolle, S., Gomes, L., Tulet, P., Matsuki, A., Schwarzenboeck, A., and Crahan, K.: Increase of the aerosol hygroscopicity by cloud processing in a mesoscale convective system: a case study from the AMMA campaign, Atmos. Chem. Phys., 8, 6907–6924, doi:10.5194/acp-8-6907-2008, 2008.”

Page 5776 line 30: add reference:

“Dirksen, R. J., Boersma, K. F., de Laat, J., Stammes, P., van der Werf, G. R., Val Martin, M., and Kelder, H. M.: An aerosol boomerang: rapid around-the-world transport of smoke from the December 2006 Australian forest fires observed from space, J. Geophys. Res., 114, D21201, doi:10.1029/2009JD012360, 2009.”

Page 5776 line 30: add reference:

“Engel-Cox, J. A., Hoff, R. M., Rogers, R., Dimmick, F., Rush, A. C., Szykman, J. J., Al-Saadi, J., Chu, D. A., and Zell, E. R.: Integrating LIDAR and satellite optical depth with ambient monitoring for 3-D dimensional particulate characterization, Atmos. Environ., 40, 8056–8067, 2006.”

Page 5777 line 18: add reference:

“Holben, B. N., Tanre, D., Smirnov, A., Eck, T. F., Slutsker, I., Abuhassan, N., Newcomb, W. W., Schafer, J., Chatenet, B., Lavenu, F., Kaufman, Y., Van de Castle, J., Setzer, A., Markham, B., Clark, D., Frouin, R., Halthore, R., Karnieli, A., O'Neill, N. T., Pietras, C., Pinker, R. T., Voss, K., and Zibordi, G.: An emerging ground-based aerosol climatology: Aerosol Optical Depth from AERONET, J. Geophys. Res., 106, 12067–12098, 2001.”

Page 5777 line 26: add reference:

“Hunt, W. H., Winker, D. M., Vaughan, M. A., Powell, K. A., Lucker, P. L., and Weimer, C.: CALIPSO lidar description and performance assessment, *J. Atmos. Ocean. Tech.*, 26, 1214–1228, doi:10.1175/2009jtecha1223.1, 2009.”

Page 5778 line 1: add reference:

“Intergovernmental Panel on Climate Change (IPCC): Climate Change 2013: The Physical Science Basis in: Clouds and Aerosols, Contribution of Working Group I to the Fifth Assessment Report of the Intergovernmental Panel on Climate Change [Stocker, T.F., D. Qin, G.-K. Plattner, M. Tignor, S.K. Allen, J. Boschung, A. Nauels, Y. Xia, V. Bex and P.M. Midgley (eds.)], Boucher, O., D. Randall, P. Artaxo, C. Bretherton, G. Feingold, P. Forster, V.-M. Kerminen, Y. Kondo, H. Liao, U. Lohmann, P. Rasch, S.K. Satheesh, S. Sherwood, B. Stevens and X.Y. Zhang, Cambridge University Press, Cambridge, United Kingdom and New York, NY, USA, 1535 pp, doi:10.1017/CBO9781107415324, 2013.”

Page 5778 line 15: add reference:

“Knippertz P., and Todd, M. C., Mineral dust aerosols over the Sahara: Meteorological controls on emission and transport and implications for modeling, *Rev. Geophys.*, 50, RG1007, doi:10.1029/2011RG000362, 2012.”

Page 5779 line 1: add reference:

“Levy, R. C., Remer, L. A., Kleidman, R. G., Mattoo, S., Ichoku, C., Kahn, R., and Eck, T. F.: Global evaluation of the Collection 5 MODIS dark-target aerosol products over land, *Atmos. Chem. Phys.*, 10, 10399–10420, doi:10.5194/acp-10-10399-2010, 2010.”

Page 5779 line 1: add reference:

“Levy, R. C., Mattoo, S., Munchak, L. A., Remer, L. A., Sayer, A. M., Patadia, F., and Hsu N. C.: The Collection 6 MODIS aerosol products over land and ocean, *Atmos. Meas. Tech.*, 6, 2989–3034, doi:10.5194/amt-6-2989-2013, 2013.”

Page 5779 line 9: add reference:

“Mallet, M., Tulet, P., Serc, D., Solmon, F., Dubovik, O., Pelon, J., Pont, V., and Thouron, O.: Impact of dust aerosols on the radiative budget, surface heat fluxes, heating rate profiles and convective activity over West Africa during March 2006, *Atmos. Chem. Phys.*, 9, 7143–7160, doi:10.5194/acp-9-7143-2009, 2009.”

Page 5781 line 2: add reference:

“Rogers, R. R., Vaughan, M. A., Hostetler, C. A., Burton, S. P., Ferrare, R. A., Young, S. A., Hair, J.W., Obland, M. D., Harper, D. B., Cook, A. L., and Winker, D. M.: Looking through the haze: evaluating the CALIPSO level 2 aerosol optical depth using airborne high spectral resolution lidar data, *Atmos. Meas. Tech.*, 7, 4317–4340, doi:10.5194/amt-7-4317-2014, 2014.”

Page 5781 line 4: add reference:

“Satheesh, S. K.: *Letter to the Editor* Aerosol radiative forcing over land: effect of surface and cloud reflection, *Ann. Geophys.*, 20, 2105–2109, doi:10.5194/angeo-20-2105-2002, 2002.”

Page 5781 line 21: add reference:

“Stephens, G. L., Vane, D. G., Boain, R. J., Mace, G. G., Sassen, K., Wang, Z., Illingworth, A. J., O’Connor, E. J., Rossow, W. B., Durden, S. L., Miller, S. D., Austin, R. T., Benedetti, A., and Mitrescu, C.: The cloudsat mission and the A-Train: a new dimension of space-based

observations of clouds and precipitation, B. Am. Meteorol. Soc., 83, 1771–1790+1742, 2002.”

Page 5782 line 16: add reference:

“Tulet, P., Mallet, M., Pont, V., Pelon, J., and Boone, A.: The 7–13 March, 2006, dust storm over West Africa: generation, transport and vertical stratification, J. Geophys. Res., 113, D00C08, doi:10.1029/2008JD009871, 2008.”

Page 5782 line 31: add reference:

“Washington, R., Todd, M. C., Engelstaedter, S., Mbainayel, S., and Mitchell, F.: Dust and the low-level circulation over the Bodélé depression, Chad: Observations from BoDEX 2005, J. Geophys. Res., 111, D03201, doi:10.1029/2005JD006502, 2006.”

Page 5783 line 3: add reference:

“Winker, D. M., Hunt, W. H., and McGill, M. J.: Initial performance assessment of CALIOP, Geophys. Res. Lett., 34, L19803, doi:10.1029/2007GL030135, 2007.”

43) After page 5785: add Table 3

Table 3: Mean dust wet deposition

Models	Wet deposition for 2006 in (g.m ⁻² .year ⁻¹)
BSC-DREAM8b	0.46
GOCART-v4Ed.A2 CTRL	9.653
GISS-modelE.A2 CTRL	8.301
TM5-V3.A2 CTRL	4.673
This study	21,36

44) After page 5785: add **Figure 1**



Figure 1: Location of the five AERONET sites used in this study to evaluate the ALADIN simulated AOT over West Africa Banizoumbou (Niger), Cinzana (Mali), DMN_Maine_Soroa (Niger), MBour (Senegal) and Capo verde.

- 45) **Page 5786:** change “Figure 1” by “Figure 2”
- 46) **Page 5787:** change “Figure 2” by “Figure 3”
- 47) **Page 5788:** change “Figure 3” by “Figure 4”
- 48) **Page 5789:** change “Figure 4” by “Figure 5”
- 49) **Page 5790:** change “Figure 5” by “Figure 6”
- 50) **Page 5791:** change “Figure 6” by “Figure 7”
- 51) **Page 5792:** change “Figure 7” by “Figure 8”
- 52) **Page 5793:** change “Figure 8” by “Figure 9”
- 53) **Page 5794:** change “Figure 9” by “Figure 10”
- 54) **Page 5795:** change “Figure 10” by “Figure 11”
- 55) **Page 5796:** change “Figure 11” by “Figure 12”
- 56) **Page 5797:** change “Figure 12” by “Figure 13”
- 57) Add after **Page 5797** Figure 14:

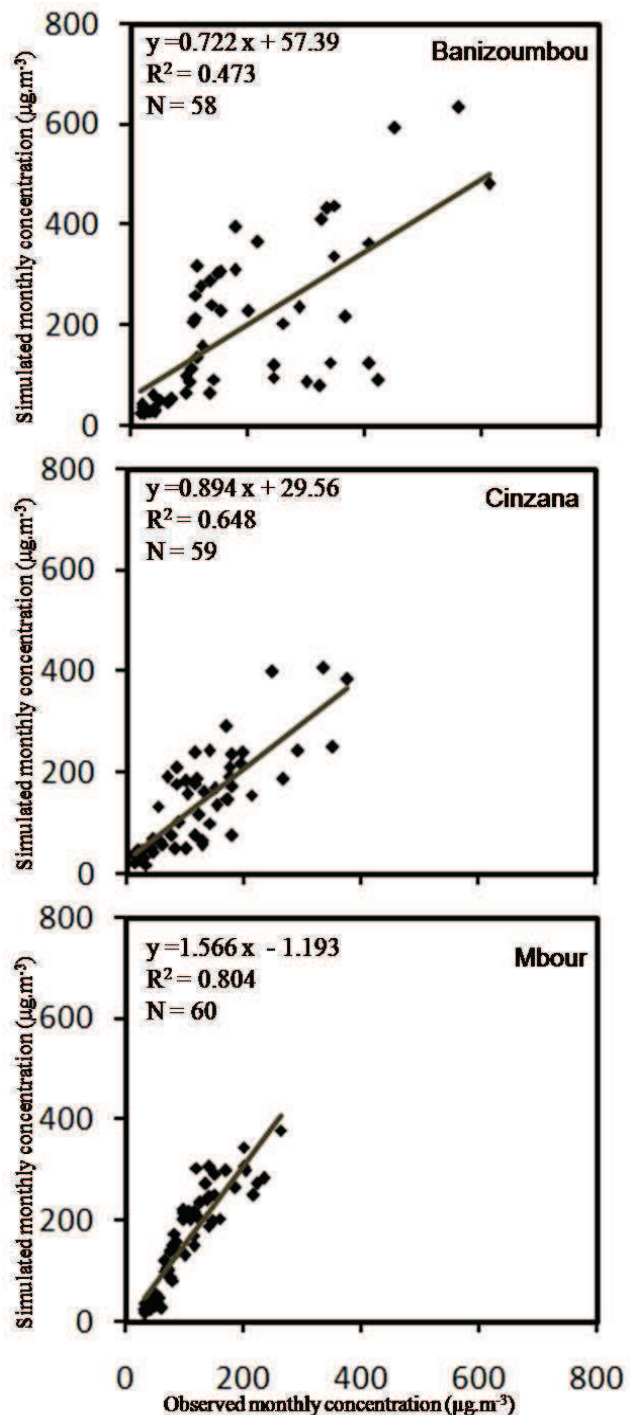


Figure 14: Scatter plot of monthly ALADIN dust surface concentration against observation over Banizoumbou, Cinzana and Mbour from 2006 to 2010. N is the number of averaged monthly surface concentration data available from 2006 to 2010. R is the correlation coefficient.

58) **Page 5798:** change “Figure 13” by “Figure 15”
 59) **Page 5799:** change “Figure 14” by “Figure 16”

1 **Dust aerosol and optical properties over North Africa**
2 **simulated with the ALADIN numerical prediction model**
3 **from 2006 to 2010 3D dust aerosol distribution and**
4 **extinction climatology over North Africa simulated with the**
5 **ALADIN numerical prediction model from 2006 to 2010**

6
7 **Mohamed Mokhtari^{1,2}, Pierre Tulet^{1,3}, Claude Fischer¹, Yves Bouteloup¹,**
8 **François Bouyssel¹, Omar Brachemi²**

9 [1] {CNRM/GAME, UMR3589 (Météo-France, CNRS), Toulouse, France}

10 [2] {Office National de la Météorologie (ONM), Algiers, Algeria}

11 [3] {LACy, UMR8105 (Université de La Réunion, Météo-France, CNRS), Saint-Denis de La
12 Réunion, France}

13 Correspondence to:

14 M. Mokhtari: m_morad06@yahoo.fr, P. Tulet pierre.tulet@univ-reunion.fr

15
16 **Abstract**

17 The seasonal cycle and optical properties of mineral dust aerosols in North Africa were
18 simulated for the period from 2006 to 2010 using the numerical atmospheric model ALADIN
19 coupled to the surface scheme SURFEX. The particularity of the simulations is that the major
20 physical processes responsible for dust emission and transport, as well as radiative effects, are
21 taken into account at short timescales and mesoscale resolution. The aim of these simulations
22 is to quantify the dust emission and deposition, locate the major areas of dust emission and
23 establish a climatology of aerosol optical properties in North Africa. The mean monthly
24 Aerosol Optical Thickness (AOT) simulated by ALADIN is compared with the AOTs
25 derived from the standard Dark Target (DT) and Deep Blue (DB) algorithms of the Aqua-

1 MODIS (MODerate resolution Imaging Spectroradiometer) products over North Africa, and
2 with a set of sun photometer measurements located at Banizoumbou, Cinzana, Soroa, Mbour
3 and Capo Verde. The vertical distribution of dust aerosol represented by extinction profiles is
4 also analysed using CALIOP (Cloud-Aerosol Lidar with Orthogonal Polarization)
5 observations.

6 The annual dust emission simulated by ALADIN over North Africa is 878 Tg.year^{-1} . The
7 Bodélé depression appears to be the main area of dust emission in North Africa, with an
8 average estimate of about $21.6 \text{ Tg.year}^{-1}$.

9 The simulated AOTs are in good agreement with satellite and sun photometer observations.
10 The positions of the maxima of the modelled AOTs over North Africa match the observed
11 positions, and the ALADIN simulations satisfactorily reproduce the various dust events over
12 the 2006-2010 period.

13 The AOT climatology proposed in this paper provides a solid database of optical properties
14 and consolidates the existing climatology over this region derived from satellites, the
15 AERONET network and Regional Climate Models. Moreover, the three-dimensional
16 distribution of the simulated AOTs also provides information about the vertical structure of
17 the dust aerosol extinction.

18

19 **1. Introduction**

20 ~~Dust aerosols emitted by wind erosion from arid and semi-arid regions of the globe represent~~
21 ~~more than 40% of annual tropospheric aerosols (IPCC, 2007). Mineral dust aerosol dominates~~
22 ~~the aerosol mass over some continental regions with relatively higher concentrations~~
23 ~~accounting for about 35% of the total aerosol mass (IPCC, 2013).~~ These terrigenous particles
24 transported by the atmosphere significantly alter the Earth's radiative budget by absorbing and
25 scattering incoming solar and outgoing terrestrial radiation (Haywood et al., 2001; Sokolik et

1 al., 2001, Houghton et al., 2001). They can affect cloud properties by modifying their
2 radiative properties and precipitation (IPCC, 2007; Twomey, 1959; Albrecht, 1989; Sandu et
3 al., 2008). They also play several roles in biogeochemical cycles (Martin, 1991; Swap et al.,
4 1992), atmospheric chemistry (Wang et al., 2002; Martin et al., 2003), visibility and human
5 health. Because of the important role that dust might play in future climate change and its
6 potential high impact on the Earth's ecosystems and natural and human environments, it is
7 important to know where the major dust sources are, how dust concentration varies in space
8 and time and what controls this variability. North Africa is the world's main source of dust
9 aerosol, with a relative contribution of about 50% of the total worldwide production (Zender
10 et al., 2003a). This region is well suited for studying the impact of aerosols on the radiation
11 budget and climate. Therefore, an accurate database of aerosol content in this region is crucial
12 to identifying identify and quantifying quantity this impact, particularly in Regional Climate
13 Models (RCMs). Changes to this database in numerical models have a sensitive impact on
14 model performance. ~~For example, various studies (Tompkins et al., 2005; Rodwell, 2005)~~
15 ~~have shown the positive impact of the switch from the Tanré et al. (1984) climatology to the~~
16 ~~Tegen et al. (1997) climatology for various aspects of the ECMWF model (Morcrette et al.,~~
17 ~~2009). For example, various studies (Tompkins et al., 2005; Rodwell, 2005) have shown the~~
18 ~~positive impact of the switch from the Tanré et al. (1984) climatology to the Tegen et al.~~
19 ~~(1997) climatology for various aspects of the ECMWF model (Morcrette et al., 2009).~~
20 Tompkins et al., (2005) have performed a couple of 5-day forecasts of the African Easterly Jet
21 (AEJ) with the old and new climatology and the results are compared with high resolution
22 dropsonde data from the JET2000 campaign. The results of these simulations show that the
23 new aerosol climatology significantly improves some aspects of the AEJ structure and
24 strength. In the same study, 4 months of 5-day forecasts was realized and compared using the
25 contrasting aerosol distributions. The results show a clear improvement with the new

1 climatology, with the jet strengthened, elongated to the east, and less zonal, in agreement with
2 the analyses. The new climatology suppresses deep convection by stabilizing the atmosphere,
3 preventing the ITCZ from progressively migrating north during the forecast. A strong
4 reduction of mean equivalent potential temperature at the lowest model level is noted, with
5 the southerly displacement of the ITCZ. More recently, Kocha et al. (2012) have shown the
6 impact of dust storms on the cold extra-tropical outbreak and on the African Easterly Jet.

7 Today, several datasets for aerosol parameters in North Africa are available. The Aerosol
8 Robotic Network (AERONET; <http://aeronet.gsfc.nasa.gov/>, Holben et al., 1998), with its
9 specifically designed geographical coverage, provides a robust database of aerosol optical
10 thickness, while the data itself describes local characteristics at station positions. Satellite
11 products allow the spatial and temporal variability of atmospheric dust aerosol concentrations
12 to be studied (Brooks and Legrand, 2000; Prospero et al., 2002; Washington et al., 2003).

13 These products provide a two dimensional (2D) horizontal representation of dust plumes and
14 offer maximum spatial coverage. Numerous studies have been conducted to reproduce the
15 dust aerosol contents in North Africa based on this type of data. For example, Engelstaedter et
16 al. (2006) used the TOMS (Total Ozone Mapping Spectrometer) AAI (Absorbing Aerosol
17 Index) product from 1980 to 1992 to identify Saharan dust source regions and create a
18 qualitative description of the annual dust cycle.

19 In the infrared spectrum, the Meteosat IDDI (Infrared Difference Dust Index) products are
20 also available. Brooks and Legrand (2000) used IDDI to localize the dust emission regions
21 over northern Africa for the period 1984-1993. In addition, very high resolution AOT data is
22 now available from satellites such as MODIS, MISR (Multi-angle Imaging
23 SpectroRadiometer) and SEAWIFS (Sea-viewing Wide Field-of-view Sensor) and inversion
24 codes such as Deep Blue (<http://gdata1.sci.gsfc.nasa.gov/daac->

1 bin/G3/gui.cgi?instance_id=aerosol_daily). Indeed, a recent comparative study (Bréon et al.,
2 2011) between AOTs derived from POLDER (Polarization and Directionality of Earth's
3 Reflectances), MODIS, MERIS (Medium Resolution Imaging Spectrometer), SEVIRI
4 (Spinning Enhanced Visible and Infrared Imager) and CALIOP (Cloud-Aerosol Lidar with
5 Orthogonal Polarization) shows that MODIS has the most reliable estimate of total AOT over
6 ocean and land. However, this data encompasses the collective contributions of maritime,
7 continental and desert dust aerosols. Furthermore, the quality of satellite dust products is
8 affected by a number of uncertainties related to the spatial/temporal resolution, atmospheric
9 conditions and range of wavelengths used by each satellite. These error sources are
10 thoroughly discussed in Schepanski et al. (2012). For example, Kocha et al. (2013) have
11 indicated that the specific transit time of MODIS over West Africa generates a bias in the
12 AOT dust retrieval due to the diurnal cycle of atmospheric processes such as convection and
13 the early morning low-level jet.

14 Numerical modelling provides a three-dimensional view of the atmosphere and can be used to
15 evaluate the individual role of each parameter involved in the optical thickness. The Tegen et
16 al. (1997) climatology gives an average distribution valid for one year (1990), obtained from a
17 combination of global distributions of aerosol data from different transport models for soil
18 dust (Tegen and Fung, 1995), sea salt (Tegen et al., 1997), sulfates (Chin et al., 1996) and
19 carbonaceous aerosols (Liousse et al., 1996). However, due to its low spatial resolution ($5^\circ \times$
20 4°), the content of dust aerosol over North Africa is not well represented. Recently, Kinne et
21 al. (2013) proposed a new monthly global climatology, MAC-v1 (Max-Planck-Institute
22 Aerosol Climatology version 1) with a $1^\circ \times 1^\circ$ resolution. This climatology addresses 3 aerosol
23 properties, namely the AOT, which provides information on the amount of aerosol, the SSA
24 (Single scattering albedo), which provides information on absorption and the Ap (Angstrøm
25 parameter), which provides information on size distribution.

1 Based on both satellite-derived monthly AOTs and a regional/chemistry model, Nabat et al.
2 (2013) proposed a three-dimensional (3D) monthly climatology of aerosol distribution over
3 the Mediterranean Sea. Based on both satellite-derived monthly AOTs and a
4 regional/chemistry model, Nabat et al. (2013) proposed a three-dimensional (3-D) monthly
5 climatology of aerosol distribution over the Mediterranean Sea for the 1979-2009 period and
6 at 50 km of resolution.

7 Initiatives have already been taken to use operational Numerical Weather Prediction (NWP)
8 and regional models at high resolution and short timescales. These efforts include the WMO
9 Sand and Dust Storm Warning Advisory and Assessment (SDS-WAS) programme, whose
10 mission is to achieve comprehensive, coordinated and sustained observations and modelling
11 of sand and dust storms in order to improve the monitoring of such storms, increase
12 understanding of the dust processes and enhance dust prediction capabilities. Initiatives have
13 already been taken to use operational Numerical Weather Prediction (NWP) and regional
14 models at high resolution and short timescales. These efforts include the WMO Sand and
15 Dust Storm Warning Advisory and Assessment (SDS-WAS, <http://sds-was.aemet.es>)
16 program, whose mission is to achieve comprehensive, coordinated and sustained observations
17 and modeling of sand and dust storms in order to improve the monitoring of such storms,
18 increase understanding of the dust processes and enhance dust prediction capabilities. SDS-
19 WAS is established as a federation of partners organized around regional nodes (Northern
20 Africa-Middle East-Europe Node and Asian Node). About 16 dust prediction models have
21 been used in SDS-WAS as BSC-DREAM8b, MACC-ECMWF, INCA-LMDZT, CHIMERE,
22 SKIRON, ETA, NGAC, NAAPS....

23 In this study, data and results from simulations using the ALADIN model over North Africa
24 from 2006 to 2010 are presented. This model takes into account the different physical
25 processes responsible for the emission, transport and deposition of dust. The aim of these

1 simulations is to quantify the annual and seasonal emissions, locate the main emission dust
2 sources and establish a climatology of dust aerosol optical properties in North Africa. The
3 mean monthly Aerosol Optical Thickness simulated by ALADIN is evaluated with the AOTs
4 derived from the standard Dark Target and Deep Blue algorithms of the Aqua-MODIS
5 products over North Africa and a set of sun photometer measurements located at
6 Banizoumbou, Cinzana, [Soroa](#)[DMN](#) [Maine](#) [Soroa](#) (hereafter [Soroa](#)), Mbour and Capo Verde.
7 In order to validate the ALADIN vertical distribution of aerosols, we use the mean extinction
8 profiles derived from CALIOP.

9 The paper is organised as follows. A brief description of the ALADIN model and the
10 methodology for analysing the data is given in Section 2. The numerical results of dust
11 emission, dry and wet deposition, AOT, and extinction coefficients are discussed in Section 3.
12 The comparison of the modelled data with Aqua-MODIS products, AERONET datasets,
13 surface concentration observation and CALIOP observation is presented in Section 4. Section
14 5 is devoted to the concluding discussion.

15 **2. Tools and methods**

16 **2.1 Model description and dust transport**

17 The spectral hydrostatic atmospheric numerical prediction model ALADIN is used in this
18 study. ALADIN is a primitive equations model using a two-time-level semi-Lagrangian semi-
19 implicit time integration scheme and a digital filter initialisation (Bubnová et al., 1995;
20 Radnóti, 1995). The atmospheric prognostic variables of the model comprise the wind
21 horizontal components, temperature, and specific humidity fields of water vapour and the
22 four types of hydrometeors (cloud droplets, ice crystals, rain and snow), as well as the
23 turbulent kinetic energy. The influence of subgrid physical processes (radiation,

1 microphysics, turbulence, convection, gravity waves, surface processes) on the evolution of
2 the model's prognostic variables is represented with physical parameterizations. The radiative
3 transfer in the atmosphere (gaseous, clouds, ozone, and aerosols) and with the surface is
4 described using the RRTM scheme (Rapid Radiative Transfer Model) for longwave radiation
5 (Mlawer et al., 1997) and the six-band Fouquart-Morcrette scheme for shortwave radiation
6 (Fouquart et al., 1980, Morcrette, 1991). Several phenomena linked to the subgrid orography,
7 such as gravity waves, their reflection and trapping, as well as upstream blocking, are taken
8 into account (Catry et al., 2008). The transport in the atmospheric boundary layer is
9 represented with a diffusion scheme based on prognostic turbulent kinetic energy (Cuxart et
10 al., 2000) using the Bougeault and Lacarrère (1989) mixing length, and on a mass flux
11 shallow convection scheme using a CAPE closure (Bechtold et al., 2001). Deep convection is
12 represented with a mass flux scheme based on a moisture convergence closure (Bougeault,
13 1985). A statistical cloud scheme (Smith, 1990; Bouteloup et al., 2005) is used for the
14 representation of stratiform clouds. ~~Microphysical processes linked to resolved precipitations
such as auto-conversion, collection, evaporation, sublimation, melting and sedimentation are
explicitly represented (Lopez, 2002).~~ Microphysical processes such as auto-conversion,
collection, evaporation, sublimation, melting and sedimentation are represented following the
parametrization of Lopez (2002).—Surface processes are calculated using the externalized
19 surface scheme SURFEX (SURFace EXternalisée) (Masson et al., 2013) which includes the
20 Interaction Soil Biosphere Atmosphere (ISBA) scheme (Noilhan and Planton, 1989). This
21 model configuration is very close to the operational configurations used at Météo-France-- in
22 ALADIN Overseas applications, for instance--and in about 16 National Weather Services
23 members of the ALADIN consortium.

24 Dust transport and optical properties are calculated using the three-moment Organic Inorganic
25 Log-normal Aerosol Model (ORILAM) (Tulet et al., 2005). ORILAM predicts the evolution

of the aerosol composition, along with the number, mean radius, and standard deviation of the aerosol distribution (Binkowski and Roselle, 2003). The method of calculation of aerosol optical properties is described in Grini et al., (2006). The refraction indexes used in our work have been calculated following a table of interpolation proposed by Grini et al., (2006). The dust optical properties are calculated from these new indexes in function of lognormal parameter upon the AMMA size distribution (Tulet et al., 2008). ORILAM has been evaluated in several papers for the West Africa region. Crumeyrolle et al., (2008 and 2011) presented a thorough description of the size distribution for the AMMA campaign. Mallet et al., (2009) studied the evolution of the asymmetry factor (g) and the single scattering albedo (SSA) for the dust storm event of March 2006 and studied the radiative balance over West Africa. Such specific studies however only can be carried out for particular situations. Dry deposition is calculated according to Seinfeld and Pandis (1997) using the resistance concept from Wesely (1989). Sedimentation of aerosols is driven by the gravitational velocity (Tulet et al., 2005).

The wet removal of dust aerosols is calculated using the SCAVenging submodel (Tost et al., 2006; Tulet et al., 2010). The dry deposition and sedimentation are driven by the Brownian diffusivity (Tulet et al., 2005).

2.2 Dust emission model

The dust fluxes are calculated using the Dust Entrainment And Deposition (DEAD) model (Zender et al., 2003a). The physical parameterizations in the DEAD scheme are based on the Marticorena and Bergametti (1995) scheme, in which dust is calculated as a function of saltation and sandblasting. The dust mobilization starts when the wind friction velocity over an erodible surface exceeds a threshold value (Bagnold, 1941; Chepil, 1951). This threshold

1 friction velocity is controlled primarily by surface and soil conditions (surface roughness, soil
2 size distribution ...).

3 DEAD was implemented in the ISBA scheme embedded in SURFEX (Grini et al., 2006).
4 Recently this emission parameterization has been improved by Mokhtari et al. (2012), in
5 order to better account for the soil aggregate distribution.

6 The erodible soil fraction is related to bare and rock soil. These surface types are derived from
7 the global dataset of land surface ECOCLIMAP at 1 km resolution which combines the global
8 land cover maps at 1/120° resolution and satellite information (Masson et al., 2003). Two
9 hundred and fifteen ecosystems were obtained by combining existing land cover and climate
10 maps, in addition to using Advanced Very High Resolution Radiometer (AVHRR) satellite
11 data. ~~Therefore, ECOCLIMAP is designed to satisfy both the tile approach of SURFEX—each~~
12 ~~grid box is made of four adjacent surfaces for nature, urban areas, sea or ocean and lake—and~~
13 ~~the vegetation types of ISBA. The ECOCLIMAP database is designed in compliance with the~~
14 ~~SURFEX “tile” approach: each grid box is composed of four adjacent surfaces for nature~~
15 ~~(ISBA vegetation classes), urban areas (TEB model), sea or ocean and lake.~~ The mass
16 fractions of clay, sand and silt are provided from the global 10 km FAO soil datasets. Soil
17 texture is classified following the USDA (1999) (United States Department of Agriculture)
18 textural classification with 12 basic textural definitions. Soil aggregate size distributions are
19 defined for each texture.

20 For the size distribution of the emitted dust, we adopted Crumevrolle et al.'s proposal (2011)
21 based on the measurements taken during the AMMA Special Observation Period (SOP) of
22 June 2006. The different parameters related to this distribution are shown in table I.

23 **2.3 2006-2010 simulations**

The ALADIN model is coupled to the ARPEGE global model, which provides the initial and boundary conditions every 3 hours. ~~To simulate the 2006–2010 period, successive simulations of two consecutive days (48 hours) are simulated, starting from 1 January 2006 through 31 December 2010. The final term of each simulation is used as the initial condition for the dust concentration of the next simulation.~~ To simulate the 2006–2010 period, successive forecasts of two consecutive days (48 h) are performed. The final term of each simulation is used as the initial condition for the dust concentration of the next simulation. The model simulation has a spin-up period and in order to start our study with a realistic initial state for dust concentrations, the start date of the numerical simulations is 25 December 2005. However, for the evaluations described in this article, only data from 1 January 2006 through 31 December 2010 are considered. The numerical integrations are performed over a fairly large domain (4°S–40°N, 40°W–50°E) including all dust emission sources in the Sahara and those of the Western part of the Arabian Desert. This choice minimizes the prediction errors in dust concentrations due to lateral coupling, as no dust modelling is included in the coupling global model. Here, care was taken to ensure that no dust emission zone was present outside and near the limited area domain. The post-processing domain was intentionally decreased in order to facilitate the exploitation of results; it extends from 2°N to 38°N and from 39°W to 45°E. ~~The horizontal resolution is 20 x 20 km with 60 vertical levels; from the surface to 67 km. The time step is 600 s. The horizontal resolution is 20 km x 20 km with 60 hybrid vertical levels; from the surface to 67 km. The time step is 600 s. In this paper, we restrict the analysis to the extinction coefficient and its vertical integration (AOT) for comparison with the observations available for the 2006–2010 period.~~

2.4 Dataset

2.4.1 Ground-based measurement

1 In this study we use the AERONET AOT product (level 2) and the PM10 measured dust mass
2 concentration (Particulate Matter concentration, particles with diameter of 10 μm or less) in
3 order to evaluate the model-simulated AOT and the surface dust concentration, respectively,
4 from 2006 to 2010.

5 AERONET (<http://aeronet.gsfc.nasa.gov/>) is a federation of ground-based remote sensing
6 instruments measuring aerosol and its characteristics (Holben et al., 1998). The AERONET
7 sunphotometers directly measure aerosol optical thickness at seven wavelengths
8 (approximately 0.340, 0.380, 0.440, 0.500, 0.675, 0.870, and 1.02 μm) with an estimated
9 uncertainty of 0.01 – 0.02 (Holben et al., 2001). In the model, the AOT is simulated at 0.55
10 μm , and it is therefore compared to the AOT measured at the nearest wavelength, 0.440 μm or
11 0.675 μm . Following Schmechtig et al., (2011) the AOT measured over Banizoumbou,
12 Cinzana and Mbour, at wavelength 0.44 μm and 0.675 μm , are significantly correlated (r^2
13 =0.99) with slopes ranging from 1.04 in Cinzana to 1.06 in MBour. Thus, in our study, we
14 used the AOT measured at 0.44 μm over the five AERONET sites located in West Africa at:
15 Banizoumbou (Niger), Cinzana (Mali), DMN Maine Soroa (Niger), Mbour (Senegal) and
16 Capo Verde (Fig. 1). We note that the AOT measurements only are possible during the day
17 since they are based on measuring the solar radiation attenuation. This characteristic may be
18 affecting the results of the intercomparison if a dust storm event occurred at night-time.

19 The three stations composing the “Sahelian Dust Transect” (SDT) (Marticorena et al., 2010)
20 located in the Sahelian region at Banizoumbou, Cinzana and MBour are used to validate the
21 surface dust concentration simulated by ALADIN. The SDT provides a continuous
22 monitoring of the atmospheric concentrations PM10 with a 5 minute time step, using a
23 Tapered Element Oscillating Microbalance (TEOM 1400A from Thermo Scientific) equipped
24 with a PM10 inlet. PM10 measurements refer to particulate matter which passes through a
25 size-selective inlet with a 50% efficiency cutoff at 10 μm aerodynamic diameter (Marticorena

1 et al., 2010). In terms of sensitivity, the detection limit of the instrument is about $0.06 \mu\text{g.m}^{-3}$
2 for a one hour sampling time.

3

4 **2.4.2 Satellite data**

5 The Aqua-MODIS product (Tanré et al., 1997; Levy et al., 2007) was used to evaluate the
6 AOTs simulated by ALADIN. This instrument is a multi-spectral radiometer, designed to
7 retrieve aerosol microphysical and optical properties over ocean and land. Two products of
8 Aqua-MODIS are considered in this study: the MODIS Dark Target (DT) and the MODIS
9 Deep Blue (DB) algorithms (Hsu et al., 2004). The MODIS DT algorithm over land is not
10 designed to retrieve aerosol over bright surfaces, such as the Saharan deserts due to the large
11 values of surface reflectivity (Remer et al., 2005; Shi et al., 2013). This problem leads to large
12 spatial gaps in the aerosol optical thickness recorded in desert regions, although these regions
13 are affected by some of the largest aerosol loadings worldwide. However, the DB algorithm
14 takes advantage of this surface phenomenology by performing aerosol retrievals in the visible
15 blue spectrum (such as the $0.47 \mu\text{m}$ spectral channel in MODIS) and by utilizing the selected
16 aerosol model in the inversion to generate the AOT (Hsu et al., 2004, 2006; Shi et al., 2013).
17 Thus, a combination between these two products is made to complete the AOT database for
18 the whole of North Africa (ocean and land).

19 Over bright arid region, only DB data are available, offering no alternative choice.
20 Conversely, in the areas with dense vegetation and ocean, only DT data are available and are
21 therefore used in our study, in these regions. In addition, we have transition areas with low
22 vegetation such as the Sahel (10°N - 15°N). For these areas, both the DB and DT products are
23 available. The DT product for the semi-arid regions tends however to be biased and
24 underestimated (Levy et al., 2010). For example, the difference between DB and DT
25 estimated for the transition regions can exceed 0.3. For this reason we chose the DB product

1 for the transition regions. Recently, Levy et al., (2013) proposed another solution for the
2 transition regions, namely to merge the two products and create a combined AOD product.
3 Levy et al., (2013) used the Normalized Difference Vegetation Index (NDVI) to identify these
4 regions. Unfortunately, this solution has not yet been validated.

5 The CALIOP Level 2 Layer 5 km product was used to evaluate the mean particle vertical
6 distributions simulated by ALADIN over North Africa. The CALIOP instrument (Winker et
7 al., 2007) was launched in 2006 on the Cloud–Aerosol Lidar and Pathfinder Satellite
8 Observations (CALIPSO) spacecraft, and has now provided over 8 years of nearly continuous
9 global measurements of aerosols and clouds with high vertical and spatial resolution at two-
10 wavelength (532 nm and 1064 nm) (Rogers et al., 2014). As part of the “A-train”
11 multisatellite constellation, CALIPSO follows a 705 km sun-synchronous polar orbit, with an
12 equator-crossing time of about 1:30 P.M., local solar time (Stephens et al., 2002). The orbit
13 repeats the same ground track every 16 days. The vertical distribution of aerosols, provided
14 by lidar, is important for radiative forcing (e.g., Satheesh, 2002), air quality studies (e.g., Al-
15 Saadi et al., 2005; Engel-Cox et al., 2006), and model validation (Dirksen et al., 2009; Koffi
16 et al., 2012). The CALIOP instrument and its initial performance assessment are described in
17 Winker et al. (2007) and Hunt et al. (2009).

18 3. Results

19 3.1 Dust emissions

20 3.1.1 Annual dust emissions and Interannual variability

21 [Figure 1](#) [Figure 2](#) shows the annual mean dust emissions over the Sahara averaged from 2006
22 to 2010 simulated by ALADIN coupled on-line with the ORILAM aerosol scheme and the
23 DEAD version of Mokhtari et al. 2012. The major dust sources are located over the Bodélé

1 Depression with an annual mean dust flux around $2 \text{ kg.m}^{-2}.\text{year}^{-1}$, the centre of Niger (400-
2 $600 \text{ g.m}^{-2}.\text{year}^{-1}$), the oriental and occidental great Erg in Algeria ($200-400 \text{ g.m}^{-2}.\text{year}^{-1}$), the
3 Western Sahara coast, the centre of Mauritania and Mali ($200-400 \text{ g.m}^{-2}.\text{year}^{-1}$), the
4 southeastern region of Libya and Sudan ($100-200 \text{ g.m}^{-2}.\text{year}^{-1}$), and along the border between
5 Egypt and Libya ($100-200 \text{ g.m}^{-2}.\text{year}^{-1}$).

6 The averaged annual dust emission over the whole Sahara and for the 5 years of simulation is

7 878 Tg.year^{-1} . Annual dust emissions vary from 843 Tg in 2010 to 924 Tg in 2008. [Table 2](#)

8 ~~compares the annual mean dust flux in this study and in other recent global and regional dust~~
9 ~~model studies. Important differences in the annual mean dust flux can be observed between~~
10 ~~these studies. The largest value of the annual mean dust flux is simulated by Ginoux et al.,~~

11 ~~(2004) and is equal to $1430 \text{ Tg.year}^{-1}$, which is twice as large as the value simulated by~~
12 ~~Marticorena and Bergametti, (1996) ($665-586 \text{ Tg.year}^{-1}$)~~. Our estimation lies between that

13 ~~obtained by Ginoux et al., (2004) and that of Marticorena and Bergametti, (1996), and is in~~
14 ~~good agreement with the value obtained by d'Almeida, (1986), Callot et al., (2000), Laurent et~~

15 ~~al., (2008) and Zender et al., (2003a)~~. [Table 2](#) compares the annual mean dust flux obtained in

16 ~~this work with other recent global and regional dust model studies. Important differences in~~
17 ~~the annual mean dust flux can be observed. The largest value of the annual mean dust flux is~~

18 ~~simulated by Ginoux et al. (2004) and is equal to $1430 \text{ Tg.year}^{-1}$, which is twice as large as the~~
19 ~~value simulated by Marticorena and Bergametti (1996) ($665-586 \text{ Tg.year}^{-1}$)~~. Our estimation

20 ~~lies between those obtained by Ginoux et al. (2004) and by Marticorena and Bergametti~~
21 ~~(1996), and is in good agreement with the value obtained by d'Almeida (1986), Callot et al.~~

22 ~~(2000), Laurent et al. (2008) and Zender et al. (2003)~~.

23 Dust emissions depend on both surface features and soil types, but they also depend on the
24 meteorological conditions (wind and precipitation). These elements are defined differently

25 from one model to another. Global models have a relatively low resolution, and thus

1 misrepresent the surface characteristics (roughness) and the soil types (% of
2 sand). As a consequence, these models tend to overestimate the spread of dust emission areas.
3 For example, at $1^{\circ} \times 1^{\circ}$ resolution (medium resolution of global models), an entire area can
4 become a dust emission source when in reality it is not. Eventually, dust emission is
5 overestimated as well. Regional models, due to their higher resolution, provide more details
6 on the emission source areas compared with global models, which then in turn enables to
7 diminish this positive bias.

8 It is also interesting to mention that the three values of dust emission estimated by Zender et
9 al., (2003), Laurent et al., (2008), Marticorena et al., (1995) and the one of our study are all
10 based on the same dust mobilization scheme of Marticorena et al. (1995). Therefore, a
11 correlation between the estimates of these four studies can be expected. Over the Bodélé
12 depression (10800 km^2), the annual mean dust emission is estimated at $21.4 \text{ Tg.year}^{-1}$.
13 Although this region represents only 0.13% of the Sahara, its contribution is around 2.4% of
14 the annual mean dust flux of the whole Sahara. This finding is in good agreement with
15 previous studies of this region (Zender et al., 2003a). Based on field observations, Todd et al.
16 (2007) suggest that the emission of aerosols minerals from the Bodélé Depression is $1.18 \pm$
17 0.45 Tg.day^{-1} during a substantial dust event.

18 [Figure 2](#) [Figure 3](#) presents the monthly emissions in Tg from January 2006 to December
19 2010. This figure shows that the largest monthly emissions are generally obtained in spring.
20 During the 5-year simulated period, a maximum (120 Tg per month) is simulated in March
21 2010 and the minimum (35 Tg per month) is obtained in December 2009.

22 3.1.2 Seasonality of the dust emissions

23 [Figure 3](#) [Figure 4](#) shows the seasonal mean dust emissions from 2006 to 2010. The seasonal
24 cycle is characterized by a maximum of dust emission in spring. All possible dust sources are

1 activated during this season. The minimum dust emissions are simulated in autumn, except
2 over the Bodélé region. In summer, dust emission remains strong in the Western Sahara,
3 while it decreases in the Eastern Sahara. In winter, dust emission sources are mainly located
4 in the Bodélé depression and the centre of Niger. These regions are indeed frequently exposed
5 to the Harmattan wind during the dry monsoon season, which is a favourable configuration
6 for dust emission. In spring and autumn, dust emission remains significant over the Bodélé
7 Depression, but the dust emission activity decreases in summer. This seasonality is in
8 agreement with the six-year simulation by Laurent et al. (2008) (1996-2001) and the
9 simulation by Schmechtig et al. (2011) for 2006.

10 ~~Figure 4~~Figure 5 presents the seasonal mean and interseasonal dust emissions over the Sahara
11 during the 5-year period. Our simulations estimate the seasonal mean dust emissions in spring
12 at around 296 Tg. In summer, the seasonal emissions remain significant, at about 233 Tg. In
13 winter and autumn, our estimations are 196 Tg and 150 Tg, respectively. ~~This seasonality is~~
14 ~~consistent with that obtained by Tanaka and Chiba (2005) for the period 1979–2003 over~~
15 ~~North Africa. Tanaka and Chiba (2005) estimate the largest emission in spring, which is~~
16 ~~similar to our results, but with a value greater than in our study using ALADIN (500 Tg). For~~
17 ~~the other seasons—winter, summer and autumn—our modelled estimations are very similar to~~
18 ~~those simulated by Tanaka and Chiba (2005). This seasonality reproduces the general pattern~~
19 ~~of the seasonality simulated by Tanaka and Chiba (2005) for the period 1979–2003 over~~
20 ~~North Africa with the global CTM model (MASINGAR) at a resolution of 1.8 x 1.8°. In~~
21 ~~contrast, in terms of intensity, the dust emission flux simulated by MASINGAR in spring~~
22 ~~accounts for almost half of the total emissions in North Africa (500 Tg). These estimates are~~
23 ~~higher than those simulated by ALADIN.~~

24 In summer, the dust emission flux simulated by MASINGAR is much underestimated
25 compared with the flux estimated by ALADIN. Indeed, the summer season is characterized

1 by significant dust uprising over the Sahel in connection with large convective systems. These
2 systems generate strong gust winds at the leading edge of their cold pools which can lead to
3 "walls of dust" known as "haboob", a sometimes fast moving and extremely hazardous
4 phenomenon (Knippertz et al. 2012). However, even regional models at resolution of about 10
5 km do not adequately represent these processes, neither in climatological terms nor for
6 weather forecasting (Knippertz et al. 2012).

7 3.2 Dry deposition

8 The annual dry deposition of mineral dust over North Africa is another estimated product of
9 the ALADIN integrations. Generally, regions of dry deposition are located near dust emission
10 regions, as most of the emitted dust mass is of the coarse type, which settles quickly. Thus, in
11 the Bodélé Depression, the dust mass subject to dry deposition is at its maximum (400-800
12 $\text{g.m}^{-2}.\text{year}^{-1}$), and corresponds to around half the annual dust emission. The Ergs located in the
13 centre of Mauritania, Mali, Niger, and the great Eastern and Western Erg in Algeria, Western
14 Sudan, South-West of Egypt and Libya come in second, with dry deposition values between
15 100-300 $\text{g.m}^{-2}.\text{year}^{-1}$. The mountainous and rocky deserts have a dry deposition ranging from
16 40-100 $\text{g.m}^{-2}.\text{year}^{-1}$.

17 The seasonal mean dry deposition flux is shown in [Figure 5](#) [Fig. 6](#). The southern boundary of
18 the dry deposition area is modulated by the position of the Inter Tropical Convergence Zone
19 (ITCZ). ~~In winter, the maximum of the seasonal dust deposition flux is located at the Bodélé~~
20 ~~Depression and Southern Niger, with a value reaching 200 g.m^{-2} .~~ [In winter, the maximum of](#)
21 [the seasonal dust deposition flux is located in the Bodélé Depression, with a value reaching](#)
22 [200 \$\text{g.m}^{-2}\$. This maximum is a consequence of low level dust transport during this period.](#) The
23 geographical extension of the dry deposition areas is very large, especially towards the south
24 and the west of the Sahara, which are the main areas of dust transport (Swap et al., 1992;

1 Kaufman et al., 2005). The area of dust deposition of more than 10 g.m^{-2} extends southward
2 to about 5°N and covers the subtropical Atlantic. In spring, the mean seasonal dust deposition
3 flux is high over the great Eastern and Western Erg in Algeria (150 g.m^{-2}), but decreases over
4 the Bodélé Depression and Niger. In this season, the southern limit of the extension of the
5 mean seasonal dry deposition area ($>10 \text{ g.m}^{-2}$) is at 10°N . In summer, this limit is located
6 around 15°N , in connection with the establishment of the West African monsoon and the
7 migration of the ITCZ towards the north. This season is characterized by high precipitation
8 over West Africa, which is very efficient at suppressing dust emission and generates
9 significant washout. In autumn, in conjunction with the decrease of the dust emission activity
10 over the Sahara, the mean seasonal dust deposition decreases, except in the Bodélé
11 Depression.

12 **3.3 Wet deposition**

13 In this section, we show that the use of a three-dimensional NWP model such as ALADIN
14 significantly improves the climatology of wet deposition of dust aerosols. Indeed, the model
15 provides a representation of large-scale and mesoscale precipitating processes, with a spatial
16 and temporal resolution and operational-like calibration of the schemes, which provides
17 insight into regional and seasonal aspects of wet deposition.

18 [Figure 6](#)[Figure 7](#) presents the mean seasonal wet deposition flux simulated by ALADIN over
19 North Africa, averaged for the 2006-2010 period. The localization of wet deposition areas
20 depends mainly on the distribution of large-scale and convective precipitations and the
21 direction of dust plume transport. In winter, during the dry West African monsoon season, the
22 mean wet deposition fluxes simulated by ALADIN do not exceed 10 g.m^{-2} in the Sahara and
23 Sahelian regions. In contrast, wet deposition is very active (20 to 60 g.m^{-2}) in the band from
24 0° to 10°N over the gulf of Guinea and the Atlantic Ocean. In spring, the highest mean wet

1 deposition flux is observed over the south of Niger, with values exceeding 40 g.m^{-2} . Summer
2 is the season of the wet African monsoon, characterized by large convective systems over the
3 Sahelian regions. These systems play a key role in the wet deposition of mineral dust
4 aerosols. Since these convective systems produce aerosols in the gust front, the associated
5 aerosols are to a large extent washed out by precipitation (Flamant et al., 2007; Tulet et al.,
6 2010). As a consequence, in our simulation, ALADIN simulates the maximum wet deposition
7 in the band from 15° N to 20° N . This band corresponds to western Chad, central Niger, Mali
8 and Mauritania, with average values of $60-140 \text{ g.m}^{-2}$. Autumn is characterized by the turning
9 of the African monsoon and the southward displacement of the ITCZ, in conjunction with a
10 decrease in precipitation and wet deposition over the Sahelian region. We note that, beyond
11 10°N , wet deposition processes are more efficient than dry deposition. The inter-comparison
12 of dust wet deposition simulated by ALADIN for the year 2006 with models used in the
13 AEROCOM and SDS-WAS programs (BSC-DREAM8b, GOCART-v4Ed.A2 CTRL, GISS-
14 modelE.A2 CTRL and TM5-V3.A2 CTRL, [http://aerocom.met.no/cgi-](http://aerocom.met.no/cgi-bin/aerocom/surfobs_annualrs.pl)
15 bin/aerocom/surfobs_annualrs.pl) for the same period is given by the Table 3. The results
16 show that the mean wet deposition estimated by ALADIN is much higher than those
17 estimated by AERCOM Model's. As discussed for the seasonal wet deposition, the major part
18 of the wet deposition takes place during the wet season of the African Monsoon.
19 In terms of spatial distribution, the ALADIN model performs better for the estimation of the
20 dust wet deposition associated with convective systems in the Sahelian regions. For example,
21 the estimates of the BSC-DREAM8b model do not exceed $0.2 \text{ g.m}^{-2} \text{ year}^{-1}$ for the Sahel and
22 the West African region. Those simulated by TM5-V3.A2 CTRL are less than $5 \text{ g.m}^{-2} \text{ year}^{-1}$
23 and those obtained by GOCART-v4Ed.A2 CTRL and GISS-modelE.A2 CTRL varied in the
24 range $20-50 \text{ g.m}^{-2} \text{ year}^{-1}$. The fact that some part of the total precipitation of ALADIN is

1 resolved can explain that the wet deposition processes in ALADIN are found to be more
2 efficient than in some global models.

3

4 **3.4 Monthly variation of Aerosol Optical Thickness**

5 Figure 7 Figure 8 shows the monthly aerosol optical thickness averaged from 2006 through
6 2010 over North Africa. The monthly variation is characterized by two maxima of AOT
7 exceeding 1.2. The first maximum is simulated in March and is located over the Sahelian
8 region in West Africa. This maximum is correlated with the high dust emissions observed in
9 the Bodélé depression and the centre of Niger. The second maximum is simulated in July and
10 is located over Mauritania and Mali. This maximum is related to the appearance of the heat
11 low in these regions and to the northward movement of the ITCZ in July. Low values of
12 AOTs are registered in autumn. This season is characterized by low dust emission activity,
13 and the simulated AOTs do not exceed 0.8. Over the southern part of the Mediterranean Sea
14 (Libyan and Egyptian coast), the AOTs due to dust are significant in spring and summer, with
15 a monthly peak of 0.5 in July. Note that, using both satellites and a regional chemistry model,
16 Nabat et al. (2013) found a value of 0.3 of AOT for these regions with a peak in June. Note
17 that, using both satellites and a regional chemistry model, Nabat et al. (2013) found, for the
18 1979-2009 period, a value of 0.3 of AOT for these regions with a peak in June.

19 In terms of extension, the spatial distribution of AOTs follows the preferred dust transport
20 direction in North Africa. The large values of AOT (0.6 to 1.2) are located in the south of the
21 domain, between 5°N and 20°N of latitude, from December to March. In contrast, beyond
22 20°N of latitude, the AOTs do not exceed 0.4 for this period. From April to August, the
23 regions with large AOTs (0.6 to 1.2) follow the northward displacement of the ITCZ.
24 Accordingly, in the ALADIN simulation, these regions extend fairly far north (> 10°N),
25 covering major parts of the Western Sahara and the Sahelian regions. In addition, a band of

1 high AOT (0.4 to 0.8), associated with the westward transport of dust aerosols towards the
2 Atlantic Ocean, is simulated between 10°N and 25°N. From September to November the dust
3 aerosol activity decreases and the regions of high AOT (0.6 to 0.8) are localised to only part
4 of the Sahelian region and the Bodélé Depression. The spatial distribution of AOT simulated
5 by ALADIN is well correlated with the monthly average of the AAI (Absorbing Aerosol
6 Index) derived from TOMS data, found by Engelstaedter et al. (2006) for the 1980-1992
7 period, especially for May, June, July and August. However, noticeable differences are
8 observed between AOT and AAI fields in winter, especially for the month of March, which
9 corresponds to a minimum of AAI and a maximum of AOT.

10 **3.5 Monthly variation of extinction coefficients**

11 The vertical distribution of aerosols in the troposphere is important for assessing their effects
12 on climate, and is a key parameter in the objective evaluation of radiative forcing (Li et al.,
13 2005; Kinne et al., 2006; Zhu et al., 2007). Meloni et al. (2005) found that the intensity of
14 shortwave radiative forcing at the top of the atmosphere is strongly dependent on the vertical
15 distribution of aerosols. In this paper, we show the monthly variation of the vertical
16 distribution of mineral dust from the surface to 10 km of altitude. In order to emphasize this
17 distribution for low altitudes, we chose the logarithmic scale for the vertical coordinate. The
18 vertical distribution is represented by the vertical cross section of the extinction coefficients
19 averaged longitudinally from 30°W to 40°E and from 2006 to 2010 ([Figure 8](#)) ([Fig. 9](#)). The
20 maximum of the extinction coefficient is simulated in January and February and reaches 0.36
21 km^{-1} . This maximum is located in the lowest layer (< 100 m) between 12°N and 17°N with a
22 vertical inclination toward the south. The southward inclination observed above 1.5 km of
23 altitude is due to the location of dust aerosols in the Saharan Atmospheric Layer (SAL) and
24 their transport by the Harmattan wind above the monsoon flux. This vertical structure is
25 mainly observed in winter during the dry West African monsoon. In this season, a strong

1 gradient of extinction coefficients can be observed at the surface around the ITCZ (5°N-
2 15°N), with values varying from 0.09 km^{-1} to 0.36 km^{-1} . In altitude, over the monsoon flux
3 (1.5 km to 3 km), the extinction coefficients are relatively large (0.09 km^{-1}). The annual
4 minimum of the maximum values of extinction are simulated in September and October and
5 do not exceed 0.12 km^{-1} , with a vertical extension limited to below 4 km. In summer, the
6 onset of the West African monsoon and the northward movement of the ITCZ confine the
7 transport of dust to the south. Instead, dust is mixed and transported vertically by convective
8 systems to high altitudes (6 km). At the surface, the limit of the southern extension of the
9 extinction coefficient ($> 0.06 \text{ km}^{-1}$) marks the position of the ITCZ. This limit varies between
10 2°N in winter and 15° N in summer.

11 **4. Comparison and evaluation**

12 **4.1 Comparison of simulation outputs to Aqua-MODIS observations**

13 ~~We use the Aqua-MODIS products (Tanré et al., 1997; Levy et al., 2007) to evaluate the~~
14 ~~AOTs simulated by ALADIN. This instrument is a multi-spectral radiometer, designed to~~
15 ~~retrieve aerosol microphysical and optical properties over ocean and land. Two products of~~
16 ~~Aqua-MODIS are considered in this study: the MODIS Dark Target (DT) and the MODIS~~
17 ~~Deep Blue (DB) algorithms (Hsu et al., 2004). The MODIS Dark Target products provide~~
18 ~~aerosol retrieval over global oceans and most land areas with almost daily coverage.~~
19 ~~However, the Dark Target retrievals fail over bright surfaces such as the Saharan deserts due~~
20 ~~to the large values of surface reflectivity (Remer et al., 2005; Shi et al., 2013). This problem~~
21 ~~leads to large spatial gaps in the aerosol optical thickness recorded in desert regions, although~~
22 ~~these regions are affected by some of the largest aerosol loadings worldwide. The Deep Blue~~
23 ~~algorithm takes advantage of this surface phenomenology by performing aerosol retrievals in~~
24 ~~the visible blue spectrum (such as the $0.47 \mu\text{m}$ spectral channel in MODIS) and by utilizing~~
25 ~~the selected aerosol model in the inversion to generate the AOT (Hsu et al., 2004; Hsu et al.,~~

1 ~~2006; Shi et al., 2013). Thus, using both two products enables complete coverage of North~~
2 ~~Africa (ocean and land).~~

3 Figure 9 Figure 10 shows the Level-3 monthly AOTs derived from the combination of the
4 Dark Target and Deep Blue products (MYD08_D3.051, MODIS-Aqua Ver. 5.1) at $1 \times 1^\circ$
5 resolution averaged from 2006 to 2010. The MODIS data shows important dust activity from
6 January to August. We observe high AOT values, in excess of 0.5, over large portions of
7 North Africa. The most important dust activity is observed in March. Two maxima exceeding
8 1 can be identified for this month. A primary maximum is located over the gulf of Guinea,
9 Nigeria, Benin and the region of Ouagadougou (south-west of Niger). This maximum is
10 associated with the southward dust transport, which is very significant in this season. The
11 secondary maximum is located in the Bodélé depression in Chad and is therefore collocated
12 with the main area of dust emission.

13 Compared with the simulated AOTs (Figure 7), ALADIN reproduces the monthly horizontal
14 distribution of AOT well. However, the model gives larger values of AOT than MODIS,
15 especially in the Sahelian region, central Mauritania and Mali, from March to July. Still, in
16 the Bodélé Depression, the maximum AOT (0.8 to 1) simulated by ALADIN in March is
17 underestimated compared with that given by MODIS (1.2 to 1.4) for the same month. Note
18 that for this region, Kocha et al. (2013) give an estimate of the AOT bias of MODIS of about
19 + 0.1. Indeed, AQUA and TERRA observe this region between 09:30 and 12:30 UTC and
20 capture the maximum of dust concentration. Therefore, Kocha et al (2013) conclude that the
21 overestimation of the AOT values in the MODIS monthly mean product due to the poor
22 representation of the diurnal cycle of dust is of the order of 0.1, i.e. 17%.

23 Over the gulf of Guinea, ALADIN underestimates the maximum AOT in March, with a value
24 around 0.7, while the observed value from MODIS exceeds 1. Over the Mediterranean Sea,

1 large values of AOT (around 0.5) observed by MODIS are obtained in April near the Libyan
2 coast, while the maxima of AOT (around 0.5) simulated by ALADIN are obtained in July and
3 August, with a localisation in the Eastern Mediterranean. Over the Atlantic Ocean, a good
4 agreement is obtained between ALADIN simulations and MODIS observations, in terms of
5 both horizontal distribution and maximum values of AOT.

6 **4.2 Comparison with AERONET measurements**

7 The AOTs simulated by ALADIN have also been compared with the AERONET observations
8 available in the AMMA database and the MODIS products. ~~Figures 10 and 11 show Figures~~
9 ~~11 and 12 show~~, respectively, the average and scatter plot of monthly optical thickness
10 observed by AERONET and MODIS and simulated by ALADIN from 2006 to 2010 over
11 Banizoumbou, Cinzana, Soroa, Mbour and Capo Verde.

12 The large values of AOT (> 0.6) measured by AERONET are observed from March to June at
13 the sites of Banizoumbou, Cinzana and Soroa, with a maximum exceeding 0.8 obtained in
14 March at Cinzana, in April at Banizoumbou and in May at Soroa (~~Figure 10 Fig. 11~~). Indeed,
15 these three stations are located at the same latitude (13° N) and they mark the southern
16 boundary of the sources of dust emission. They are affected by dust transport associated with
17 the Harmattan wind from March to June, which explains the large AOT values in this season.
18 The low AOTs are observed from November to January, with values around 0.35,
19 corresponding to the low dust emission activity. In August, the AOTs are also low at
20 Banizoumbou, Cinzana and Soroa. For this month, the West African monsoon is well
21 established and the air circulation is upturned, driving dust aerosol towards the north. A
22 comparison between MODIS and ALADIN shows that the variations in the averaged monthly
23 AOT are well correlated between the two datasets, but there are noticeable differences in
24 terms of quantification. For instance, over Banizoumbou, MODIS observations are slightly

1 larger than AERONET observations for all months, with a maximum of about 1 observed in
2 April. This overestimation is particularly perceptible in the wet monsoon season (July and
3 August). For this site, the MODIS data provides a good correlation coefficient (0.864) ([Figure](#)
4 [11](#) [Fig. 12](#)). For ALADIN, the maximum of AOT is given in March with a rather large value
5 of about 1.2. ALADIN overestimates the AOTs from November to March, and
6 underestimates them from April to September, except for July. For Banizoumbou, a lower
7 correlation coefficient (0.285) is obtained with ALADIN compared with MODIS. This weak
8 correlation is probably due to the resolution of the ALADIN model, which is believed to be
9 too small to provide an appropriate accurate representation of the surface parameters for this
10 region.

11 Over Cinzana, MODIS gives two maxima of AOT reaching 0.8. The first maximum is
12 obtained in April and the second in July. The MODIS AOTs are much larger than the
13 AERONET and ALADIN values, from May to August. The correlation coefficient obtained
14 for MODIS for Cinzana is about 0.549. In contrast, ALADIN simulates the maximum of AOT
15 in March (~1) with a correlation coefficient of about 0.418.

16 Over Soroa, the maximum AOT (~0.8) is observed by MODIS in July during the wet West
17 African monsoon. MODIS overestimates the AOTs from July to March and underestimates
18 them in May and June compared to AERONET. The correlation coefficient of MODIS is
19 around 0.128. For Soroa, the AOTs simulated by ALADIN are larger than 0.5 from January to
20 July, with a maximum of about 1.1 in March. The correlation coefficient obtained for
21 ALADIN is around 0.255.

22 At Mbour, the maximum AOT measured by AERONET is obtained in June and is around 0.7.
23 For this site, MODIS values of AOT are larger than AERONET values from January to
24 August. In July, the AOTs observed by MODIS (0.9) are twice as large as those measured by

1 AERONET. Like MODIS, ALADIN overestimates the AOTs from January to July, with a
2 maximum simulated in March (0.8). For Mbour, the correlation coefficients obtained for
3 MODIS and ALADIN with respect to AERONET are equal to 0.568 and 0.478, respectively.
4 Over Capo Verde, the averaged monthly AOTs observed by AERONET and MODIS, and
5 simulated by ALADIN, are in good agreement, except in July, where ALADIN overestimates
6 the AOTs. The maximum AOTs observed and simulated are obtained in July and are equal to
7 0.5 for AERONET and MODIS and 0.8 for ALADIN. For this site the correlation coefficients
8 observed for MODIS and ALADIN are 0.603 and 0.584, respectively.

9 **4.3 Comparison to surface dust concentration measurements**

10 ~~In this section we use the measured dust mass concentration PM10 (Particulate Matter~~
11 ~~concentration, particles with diameter of 10 μm or less) from the Sahelian Dust Transect~~
12 ~~(SDT) (Marticorena et al., 2010) to evaluate the simulated surface dust concentration from~~
13 ~~2006 to 2010. Note that PM10 measurements refer to particulate matter which passes through~~
14 ~~a size selective inlet with a 50% efficiency cutoff at 10 μm aerodynamic diameter~~
15 ~~(Marticorena et al., 2010). Therefore, for the simulated concentrations, we consider only the~~
16 ~~particles smaller than 10 μm in order to perform a consistent comparison with the~~
17 ~~observations. Note that the simulated mass concentration of particles of less than 10 μm in~~
18 ~~diameter represents 40.124% of the total mass.~~
19 In this section we use the measured dust mass
20 concentration PM10 from the SDT (Marticorena et al., 2010) to evaluate the simulated
21 surface dust concentration from 2006 to 2010. PM10 measurements refer to particulate matter
22 which passes through a size-selective inlet with a 50% efficiency cutoff at 10 μm
23 aerodynamic diameter. Therefore, for the simulated concentrations, we consider only the
particles smaller than 10 μm in order to perform a consistent comparison with the

1 observations. Note that the simulated mass concentration of particles of less than 10 μm in
2 diameter represents 40.124% of the total mass.

3 The SDT is composed of three stations, namely Banizoumbou, Cinzana and M'bour Mbour.
4 Figure 12 shows the monthly mean of the daily median value of measured and simulated
5 surface concentrations in Banizoumbou, Cinzana and M'bour Figure 13 and 14 show,
6 respectively, the monthly mean of the daily median value of measured and simulated surface
7 concentrations and the scatter plot of monthly ALADIN dust surface concentration against
8 observations over Banizoumbou, Cinzana and Mbour. The analysis of this figure shows that
9 the temporal pattern of simulated and observed concentrations is similar for the Cinzana and
10 Mbour sites, with high concentrations from November to May. In summer, the simulated and
11 observed surface concentrations are low for these two stations. In contrast, noticeable
12 differences are seen from April to June at Banizoumbou. For this site, the simulated surface
13 concentration decreases while the PM10 concentration remains high. In summer, the
14 simulated and observed surface concentrations are low for these two stations. In contrast,
15 noticeable differences are seen from April to June at Banizoumbou. For this site, the
16 simulated surface concentration decreases while the PM10 concentration remains high. The
17 model underestimations observed during April to June are probably related to local dust
18 uprisings that are not well simulated by ALADIN model. This underestimation is strong in
19 June, which marks the transition between the dry and the wet season monsoon in West Africa.
20 Recently, a study realized by Kocha et al., (2013) shows the existence of two important
21 processes responsible for dust uprising in West Africa, namely: (1) the diurnal variation of
22 surface wind speed modulated by the low level jet occurred after sunrise due to turbulent
23 mixing (Washington et al., 2006), especially in Bodélé depression; (2) the gust wind
24 associated with the density currents emanating from convective systems occurred at the
25 afternoon. This second phenomenon generate a strong gust winds can lead to the "dust wall"

1 known "haboob" (Tulet et al., (2010) ; Knippertz et al. (2012)). We also noted a bias for the
2 values of AOT in the same period but with a less pronounced intensity than for surface
3 concentration.

4 In terms of intensity, ALADIN overestimates the monthly surface concentration over
5 Banizoumbou from November to February. Nevertheless, it underestimates it from April to
6 July. ALADIN simulates the maximum concentration in March ($373 \mu\text{g.m}^{-3}$) which is in good
7 agreement with the maximum PM10 observation ($370 \mu\text{g.m}^{-3}$) registered during the same
8 period. The minimum simulated surface concentration ($31 \mu\text{g.m}^{-3}$) is obtained in September
9 but the minimum PM10 concentration ($21 \mu\text{g.m}^{-3}$) is observed in August. The square of the
10 correlation coefficient registered for Banizoumbou is equal 0.473 with a slop of the tendency
11 curve equal 0.722. Over Cinzana, a good correlation is obtained between the monthly
12 simulated surface concentration and the PM10 observation, especially from March to
13 October. The maximum simulated surface concentration and observation is obtained in
14 MarsMarch ($278 \mu\text{g.m}^{-3}$ for ALADIN and $257 \mu\text{g.m}^{-3}$ for PM10). The minimum surface
15 concentration ($25 \mu\text{g.m}^{-3}$) is simulated in September, and the minimum PM10 concentration
16 ($15 \mu\text{g.m}^{-3}$) is observed in August. For this site, the correlation coefficient and the slope of the
17 tendency curve are equal 0.648 and 0.894, respectively. Over Mbour, the monthly simulated
18 surface concentrations are larger than the observations over all months except in July and
19 August with a slope of tendency curve exceeds 1.566. ALADIN simulates the maximum
20 concentration in January ($299 \mu\text{g.m}^{-3}$) but the maximum PM10 is observed in March (202
21 $\mu\text{g.m}^{-3}$). The minimum surface concentration ($23 \mu\text{g.m}^{-3}$) is simulated in August and the
22 minimum PM10 concentration ($39 \mu\text{g.m}^{-1}$) is observed in September. The correlation
23 coefficient obtained over Mbour is equal 0.804.

1 It is worth mentioning that the dust surface concentration is strongly linked with the surface
2 dust emission activity. Thus, the largest values for surface concentrations are registered in
3 spring and winter, which correspond to the period of strong dust emission activity in the
4 Sahelian region.

5 **4.4 Comparison to CALIOP observations**

6 In this section we use the CALIOP Level 2 Layer version 3.01 product (Koffi et al., 2012)
7 over the 2007-2009 period to evaluate the ALADIN vertical distribution of dust aerosols.
8 This data was previously used in Koffi et al. 2012 to evaluate the 12 AeroCom-I (Aerosol
9 Comparison between observations and models, phase I) models over 13 sub-continental
10 regions. In this study, the ALADIN-CALIOP intercomparison was limited to the North Africa
11 (NAF) and Central Africa (CAF) regions. Note that the ALADIN model domain does not
12 completely cover these two regions. Therefore, in our case, these two regions are defined as
13 follows: [2°N-15°N ; 18°W-48°E] for CAF and [15°N-35°N ; 18°W-48°E] for NAF for
14 ALADIN. For CALIOP, the same regions as those defined by Koffi et al. (2012) are used:
15 [0°N-15°N ; 18°W-60°E] for CAF and [15°N-35°N ; 18°W-60°E] for NAF. The seasonal dust
16 aerosol mean extinction profiles from CALIOP observations (at 532) from January 2007 to
17 December 2009 over these two regions are available at
18 http://aerocom.met.no/download/CALIOP_BENCHMARK_KOFFI2012/.

19 Following Koffi et al. (2012), we calculate the mean extinction height Z_a over the lowest 10
20 km of the atmosphere in order to assess ALADIN's ability to reproduce the mean vertical
21 distribution of dust aerosols over CAF and NAF. The following formula is used for
22 computing Z_a :

$$1 \quad Z_a = \frac{\sum_{i=1}^n b_{ext,i} \cdot Z_i}{\sum_{i=1}^n b_{ext,i}} \quad (1)$$

2 With $b_{ext,i}$ the aerosol extinction coefficient (km^{-1}) at level i , and Z_i the altitude (km) of level i .

3 The sums apply to the first 10 km of the atmosphere.

4 [Figure 13](#) [Figure 15](#) shows the CALIOP and ALADIN mean seasonal extinction coefficient
5 profiles for NAF. The analysis of the CALIOP measurements allows the seasonal variability
6 of the dust aerosols profile over NAF to be assessed. In winter, large values for dust aerosol
7 extinction coefficients are observed between the ground and 2 km of height, which lead to
8 values of Z_a of about 1.23 km. In spring and summer, the vertical mixing and the activity of
9 sandstorms are at their maximum. Thus, in summer, Z_a (2.44 km) is twice as large as in
10 winter. In autumn, the decrease in dust activity is reflected by a value of Z_a equal to about
11 1.85 km.

12 This seasonality also exists for the CAF region ([Figure 14](#) [Fig. 16](#)). The maximum of Z_a is
13 obtained in June-July-August (2.39 km), with a bimodal vertical distribution. The second
14 peak is located at around 3.5 km of height. Koffi et al. (2012) explain this feature by the long-
15 range transport of mineral dust from the Sahara and Sahel regions and the cross-hemispheric
16 transport of biomass burning products from South Africa, which contribute to the aerosol load
17 in the free troposphere.

18 Over the NAF region, the ALADIN model reproduces both the shape and the seasonality of
19 the extinction coefficient profiles rather well. Note that in spring, ALADIN overestimates the
20 extinction coefficient in the first 2 km. At the surface, ALADIN simulates a peak of about
21 0.18 km^{-1} , while the value measured by CALIOP does not exceed 0.11 km^{-1} . Above 6 km of
22 altitude, ALADIN overestimates the extinction coefficient for all seasons. ALADIN

1 underestimates Z_a , over all seasons in the NAF region, with a maximum of Z_a (1.75 km)
2 simulated in summer, in accordance with the CALIOP data.

3 Over the CAF region, significant differences are observed in the shape of the CALIOP and
4 ALADIN extinction profiles. In winter, large extinction coefficient values ($>0.2 \text{ km}^{-1}$) are
5 simulated by ALADIN in the first 1 km. This is in connection with the overestimation of
6 surface dust concentration by ALADIN in this region. Note that the three measurement sites
7 of dust concentration investigated in section 4.3 (Banizoumbou, Cinzana and Mbour) are
8 located in this region. In summer and autumn, ALADIN greatly underestimates the extinction
9 coefficient in the first 5 km. The reason here is that, in addition to dust aerosol, the CALIOP
10 measurements are affected by other aerosols, such as biomass-burning products, which
11 contribute to an increase of the extinction coefficient. Note that the Z_a values simulated by
12 ALADIN are underestimated for all seasons over the CAF region.

13 **5. Conclusion**

14 This study focuses on the elaboration and interpretation of a dust aerosol climatology for
15 North Africa using an operational numerical weather prediction model. The use of a NWP
16 model for this type of study is novel and allows a better representation of the coupled
17 processes between the surface and the atmosphere (emission by density currents, topographic
18 forcing), and the mesoscale processes. The simulated climatology enables us to assess the
19 location of the main areas of dust emission, dry and wet deposition, and provides a three-
20 dimensional distribution of monthly dust aerosol optical properties over this region.

21 Results of five-year simulations for the 2006-2010 period are presented. The annual dust
22 emission in North Africa estimated by ALADIN is about 878 Tg.year^{-1} . The Bodélé
23 depression appears as the most important dust source region in North Africa with a total
24 annual emission of $21.4 \text{ Tg.year}^{-1}$. Dust emission over North Africa is characterized by strong

1 seasonal variability. The emission is important in spring (296 Tg) and summer (233 Tg), and
2 drops in winter and autumn to about 196 Tg and 150 Tg, respectively.

3 The principal dry deposition areas are located near dust source emissions. Thus, in the Bodélé
4 Depression, the mass of dry dust deposition corresponds to about half of the annual dust
5 emission ($400\text{-}800 \text{ g.m}^{-2}.\text{year}^{-1}$). The southern limit of the dry deposition area is modulated by
6 the position of the ITCZ. In winter, the extension of the dry deposition areas is very
7 significant, especially towards the south and west of Sahara. In summer, the southern limit of
8 the area of dust deposition is located around 15°N , in connection with the establishment of the
9 West African monsoon. The major wet deposition regions depend mainly on the distribution
10 of large scale and convective precipitation and the direction of dust plume transport. They are
11 located in the southern part of North Africa (Sahel, Gulf of Guinea, Central Africa and the
12 Atlantic Ocean). In winter, the wet deposition is very active (10 to 60 g.m^{-2}) in the band from
13 2° to 10°N over the Gulf of Guinea and the Atlantic Ocean. In spring, wet deposition does not
14 exceed 40 g.m^{-2} over all of North Africa. In summer, wet deposition is very active, with a
15 maximum simulated over the Bodélé depression and southern Niger (140 g.m^{-2}). These
16 findings are consistent with the existence of large convective systems over the Sahelian
17 regions in this season.

18 The simulated seasonal cycle of the AOT is in good agreement with MODIS observations.
19 ALADIN generates prominent features of geographical patterns and seasonal variations that
20 are in good agreement with the observations. The monthly climatology of AOT presented in
21 this paper is characterized by two maxima of AOT exceeding 1.2. The first is simulated over
22 the Sahel in March and the second in Mauritania and Mali in July. Low AOTs are simulated
23 in autumn, again in accordance with MODIS observations.

1 The vertical distribution of dust aerosol is characterized by a large concentration of dust
2 aerosol at low levels between 0 to 100 m. The maximum of the extinction coefficient is
3 simulated in March.

4 The comparison of the simulated AOTs with ground AERONET measurements generally
5 shows a good correlation at a remote site (Capo Verde). However, an overestimation of AOTs
6 is observed in winter at sites located in the vicinity of dust source regions (Banizoumbou,
7 Cinzana and Soroa). This overestimation suggests that the content of atmospheric dust is also
8 overestimated in these source areas in winter. There are two possible reasons here: either the
9 ALADIN model overestimates dust emission, or it underestimates the removal processes. In
10 the first case, a possibly overly large emission may be due to an overly low threshold friction
11 velocity simulated by the ALADIN model, so that the mobilization occurs at an overly low
12 wind speed.

13 ALADIN simulates the temporal pattern of monthly surface concentrations well, but
14 overestimates them from late autumn to late winter at all sites. As for the extinction
15 coefficients, ALADIN reproduces both the shape and the seasonal variability of extinction
16 coefficient profiles well, especially over the NAF region. In contrast, significant differences
17 between the CALIOP and ALADIN extinction profiles are obtained over the CAF region.
18 Indeed, this region is affected by salt and biomass-burning products which heavily influence
19 the extinction coefficients.

20 It is interesting to note that, despite the absence of any data assimilation process for dust
21 content in ALADIN, the simulations remain overall satisfactorily correlated with
22 observations. This result suggests that the model, whose initial and lateral boundary
23 conditions are regularly refreshed by the global model ARPEGE, does not generate any
24 significant drift of dust content over the whole five-year range of the simulations.

1 Furthermore, the model seems able to maintain a correct relative impact of emission and
2 deposition processes, which is reflected by the realistic characteristics of the predicted AOT
3 fields.

4 In future, ALADIN's ability to simulate the dust aerosol content over the Mediterranean Sea
5 will be investigated. For this purpose, the model will be tested within the framework of the
6 ChArMeX programme (<http://mistral.sedoo.fr/ChArMEx>) over the Mediterranean basin and
7 will be compared with regional climate models over this region.

8 **Acknowledgements**

9 This paper is dedicated to the memory of Laurent Gomes.

10 Based on a French initiative, AMMA was built by an international scientific group and is
11 currently funded by a large number of agencies, especially from France, United Kingdom,
12 USA and Africa. It has been the beneficiary of a major financial contribution from the
13 European Community's Sixth Framework Research Programme. Detailed information on
14 scientific co-ordination and funding is available on the AMMA International web site
15 <http://www.amma-international.org>. We also acknowledge the MODIS mission scientists and
16 associated NASA personnel for the production of the data used in this research effort. This
17 work was supported by the Algerian Met Office (ONM), Météo France, Centre National de
18 Recherches Météorologiques (CNRM) and the French Embassy in Algeria.

19 **References**

20 Albrecht, B. A.: Aerosols, cloud microphysics, and fractional cloudiness, *Science*, 245, 1227–
21 1230, 1989.

22 Bagnold, R. A.: *The Physics of Blown Sand and Desert Dunes*, 265 pp, Methuen, New York,
23 1941.

1 [Al Saadi, J., Szykman, J., Pierce, R. B., Kittaka, C., Neil, D., Chu, D. A., Remer, L. A.,](#)
2 [Gumley, L., Prins, E., Weinstock, L., MacDonald, C., Wayland, R., Dimmick, F., and](#)
3 [Fishman, J.: Improving national air quality forecasts with satellite aerosol observations, Bull.](#)
4 [Am. Meteorol. Soc., 1249–1261, doi:10.1175/BAMS-86-9-1249, 2005.](#)

5 Bechtold, P., Bazile, E., Guichard, F., Mascart, P., and Richard, E.: A Mass flux convection
6 scheme for regional and global models, *Q. J. R. Meteorol. Soc.* 127, 869-886, 2001.

7 Binkowski, F. S., and Roselle, S.: Models-3 community multiscale air quality (cmaq) model
8 aerosol component 1, model description, *J. Geophys. Res.* 108(D6), 4183, doi :
9 10.1029/2001JD001409, 2003.

10 Bougeault, P.: A simple parameterization of the large-scale effects of cumulus convection,
11 *MWR*, 113, 2108–2121, 1985.

12 Bougeault, P., and Lacarrère, P.: Parameterization of orography-induced turbulence in a
13 mesobeta-scale model, *Mon. Wea. Rev.* 117, 1872–1890, 1989.

14 Bouteloup, Y., Bouyssel, F., and Marquet, P. : Improvements of Lopez's prognostic large scale
15 cloud and precipitation scheme, *ALADIN Newsletter*. 28, p.66-73, 2005.

16 Bréon, F.M., Vermeulen, A., and Descloires, J.: An evaluation of satellite aerosol products
17 against sunphotometers measurements, *Remote Sens. Environ.* 115, 3102–3111,
18 doi:10.1016/j.rse.2011.06.017, 2011.

19 Brooks, N. P., and Legrand, M.: Dust variability over Northern Africa and rainfall in Sahel, in
20 linking the climate change to landsurface change, Kluwer Academic Publishers, 1–25 pp,
21 2000.

22 Bubnová, R., Hello, G., Bénard, P., and Geleyn, J. F.: Integration of the fully elastic equations
23 cast in the hydrostatic pressure terrain following coordinate in the framework of the ALADIN
24 NWP system, *Mon. Wea. Rev.* 123, 515–535, 1995.

1 Callot, Y., Marticorena, B., and Bergametti, G.: Geomorphologic approach for modelling the
2 surface features of arid environments in a model of dust emission: application to the Sahara
3 desert, *Geodinamica Acta* 13 245-270, 2000.

4 Catry, B., Geleyn, J.F., Bouyssel, F., Cedilnik, J., Brozkova, R., Derkova, M., Mladek, R.: A
5 new sub-grid scale lift formulation in a mountain drag parametrisation scheme,
6 *Meteorologische Zeitschrift*. 17, Issue 2, 193-208, 2008.

7 Chepil, W. S.: Properties of soil which influence wind erosion: IV. State or dry aggregate
8 structure, *Soil Sci.* 72, 387-401, 1951.

9 Chin, M., Jacob, D. J., Gardner, G. M., Foreman-Fowler, M.S., Spiro, P.A., and Savoie, D. L.:
10 A global three-dimensional model of tropospheric sulfate, *J. Geophys. Res.* 101, 18667–
11 18690, doi:10.1029/96JD01221, 1996.

12 [Crumeyrolle, S., Gomes, L., Tulet, P., Matsuki, A., Schwarzenboeck, A., and Crahan, K.:
13 Increase of the aerosol hygroscopicity by cloud processing in a mesoscale convective system:
14 a case study from the AMMA campaign, *Atmos. Chem. Phys.*, 8, 6907–6924,
15 doi:10.5194/acp-8-6907-2008, 2008.](#)

16 Crumeyrolle, S., Tulet, P., Gomes, L., Garcia-Carreras, L., Flamant, C., Parker, D. J.,
17 Matsuki, A., Formenti, P., and Schwarzenboeck, A.: Transport of dust particles from the
18 Bodélé region to the monsoon layer- AMMA case study of the 9-14 June 2006 period, *Atmos.*
19 *Chem. Phys.* 11, 479-494, doi:10.5194/acp-11-479-2011, 2011.

20 Cuxart, J., Bougeault, P., and Redelsperger, J.L.: A turbulence scheme allowing for mesoscale
21 and large-eddy simulations, *Q. J. R. Meteorol. Soc.* 126, p.1-30, 2000.

22 d'Almeida, G. A.: A model for Saharan dust transport, *J. Clim. Appl. Meteorol.* 25, 903-916,
23 1986.

24 [Dirksen, R. J., Boersma, K. F., de Laat, J., Stammes, P., van der Werf, G. R., Val Martin, M.,
25 and Kelder, H. M.: An aerosol boomerang: rapid around-the-world transport of smoke from](#)

1 [the December 2006 Australian forest fires observed from space, J. Geophys. Res., 114,](#)
2 [D21201, doi:10.1029/2009JD012360, 2009.](#)

3 [Engel-Cox, J. A., Hoff, R. M., Rogers, R., Dimmick, F., Rush, A. C., Szykman, J. J., Al-](#)
4 [Saadi, J., Chu, D. A., and Zell, E. R.: Integrating LIDAR and satellite optical depth with](#)
5 [ambient monitoring for 3-D dimensional particulate characterization, Atmos. Environ., 40,](#)
6 [8056–8067, 2006.](#)

7 Engelstaedter, S., Tegen, I., and Washington, R.: North African dust emissions and transport,
8 Earth-Sci. Rev. 79, 73-100, 2006.

9 Flamant, C., Chaboureau, J-P., Parker, D. J., Taylor, C. M., Cammas, J-P., Bock, O., Timouk,
10 P., and Pelon, J.: Airborne observations of the impact of a convective system on the planetary
11 boundary layer thermodynamics and aerosol distribution in the intertropical discontinuity
12 region of the West African monsoon, Q. J. R. Meteorol. Soc. 133, 1–28, 2007.

13 Fouquart, Y., and Bonnel, B.: Computations of solar heating of the earth's atmosphere: a new
14 parameterization, Beitr. Phys. Atmosph. 53, 35-62, 1980.

15 Ginoux, P., Prospero, J.M., Torres, O., and Chin, M.: Long-term simulation of global dust
16 distribution with the GOCART model: correlation with North Atlantic Oscillation, Environ.
17 Model. Software, 19, 113–128, 2004.

18 Grini, A., Tulet, P., and Gomes, L.: Dusty weather forecasts using the MesoNH mesoscale
19 atmospheric model, J. Geophys. Res. VOL. 111, D19205, doi:10.1029/2005JD007007, 2006.

20 Haywood, J.M., Francis, P.N., Glew, M.D., Taylor, J.P.: Optical properties and direct
21 radiative effect of Saharan dust: a case study of two Saharan dust outbreaks using aircraft
22 data. J. Geophys. Res. Atmospheres, 106 (D16), 18,417– 18,430, 2001.

23 Holben, B. N., Eck, T. F., Slutsker, I., Tanré, D., Buis, J. P., Setzer, A., Vermote, E., Reagan,
24 J. A., Kaufman, Y., Nakajima, T., Lavenu, F., Jankowiak, I., and Smirnov, A.: AERONET-A

1 Federated Instrument Network and Data Archive for Aerosol Characterization, Remote Sens.
2 Environ. 66, 1–16, doi:10.1016/S0034-4257(98)00031-5, 1998.

3 [Holben, B. N., Tanre, D., Smirnov, A., Eck, T. F., Slutsker, I., Abuhassan, N., Newcomb, W.](#)
4 [W., Schafer, J., Chatenet, B., Lavenu, F., Kaufman, Y., Van de Castle, J., Setzer, A.,](#)
5 [Markham, B., Clark, D., Frouin, R., Halthore, R., Karnieli, A., O'Neill, N. T., Pietras, C.,](#)
6 [Pinker, R. T., Voss, K., and Zibordi, G.: An emerging ground-based aerosol climatology:](#)
7 [Aerosol Optical Depth from AERONET, J. Geophys. Res., 106, 12067–12098, 2001.](#)

8 Houghton, J., Ding, Y., Griggs, D.J., Noguer, M., Vander Linden, P.J., Dai, X., Maskell, K.,
9 Johnson, C.A.: Climate Change 2001: The Scientific Basis. Cambridge University Press. New
10 York, 2001.

11 Hsu, N. C., Tsay, S.C., King, M., and Herman, J. R.: Aerosol properties over bright-reflecting
12 source regions, IEEE. T. Geosci. Remote, 42, 557–569, doi: 10.1109/TGRS.2004.824067,
13 2004.

14 Hsu, N. C., Tsay, S., King, M. D., and Herman, J. R.: Deep Blue Retrievals of Asian Aerosol
15 Properties During ACE-Asia, IEEE T. Geosci. Remote, 44, 3180–3195, 2006.

16 [Hunt, W. H., Winker, D. M., Vaughan, M. A., Powell, K. A., Lucker, P. L., and Weimer, C.:](#)
17 [CALIPSO lidar description and performance assessment, J. Atmos. Ocean. Tech., 26, 1214–](#)
18 [1228, doi:10.1175/2009jtech1223.1, 2009.](#)

19 Intergovernmental Panel on Climate Control (IPCC): Climate Change 2007: The Physical
20 Basis, in: Changes in Atmospheric Constituents and in Radiative Forcing, the Fourth,
21 Assessment Report of the IPCC, edited by: Forster, P., Ramaswamy, V., Artaxo, R., Berntsen,
22 T., Betts, R., Fahey, D. W., Haywood, J., Lean, J., Lowe, D. C., Myhre, G., Nganga, J., Prinn,
23 R., Raga, G., Schulz, M., and Van Dorland, R.: Cambridge University Press. Cambridge,
24 United Kingdom and New York, NY, USA, 2007.

1 [Intergovernmental Panel on Climate Change \(IPCC\): Climate Change 2013: The Physical](#)
2 [Science Basis in: Clouds and Aerosols, Contribution of Working Group I to the Fifth](#)
3 [Assessment Report of the Intergovernmental Panel on Climate Change \[Stocker, T.F., D.](#)
4 [Qin, G.-K. Plattner, M. Tignor, S.K. Allen, J. Boschung, A. Nauels, Y. Xia, V. Bex and P.M.](#)
5 [Midgley \(eds.\)\], Boucher, O., D. Randall, P. Artaxo, C. Bretherton, G. Feingold, P. Forster,](#)
6 [V.-M. Kerminen, Y. Kondo, H. Liao, U. Lohmann, P. Rasch, S.K. Satheesh, S. Sherwood, B.](#)
7 [Stevens and X.Y. Zhang, Cambridge University Press, Cambridge, United Kingdom and New](#)
8 [York, NY, USA, 1535 pp, doi:10.1017/CBO9781107415324, 2013.](#)

9 Kaufman, Y. J., Koren, I., Remer, L.A., Tanré, D., Ginoux, P., and Fan, S.: Dust transport and
10 deposition observed from the Terra-Moderate Resolution Imaging Spectroradiometer
11 (MODIS) spacecraft over the Atlantic Ocean, *J. Geophys. Res.* 110, D10S12,
12 doi:10.1029/2003JD004436, 2005.

13 Kinne, S., Schulz, M., Textor, C., Guibert, S., Balkanski, Y., Bauer, S. E., Berntsen, T.,
14 Berglen, T. F., Boucher, O., Chin, M., Collins, W., Dentener, F., Diehl, T., Easter, R.,
15 Feichter, J., Fillmore, D., Ghan, S., Ginoux, P., Gong, S., Grini, A., Hendricks, J., Herzog, M.,
16 Horowitz, L., Isaksen, I., Iversen, T., Kirkevåg, A., Kloster, S., Koch, D., Kristjansson, J. E.,
17 Krol, M., Lauer, A., Lamarque, J. F., Lesins, G., Liu, X., Lohmann, U., Montanaro, V.,
18 Myhre, G., Penner, J., Pitari, G., Reddy, S., Seland, O., Stier, P., Takemura, T., and Tie, X.:
19 An AeroCom initial assessment – optical properties in aerosol component modules of global
20 models, *Atmos. Chem. Phys.* 6, 1815–1834, doi:10.5194/acp-6-1815-2006, 2006.

21 Kinne, S., O'Donnell, D., Stier, P., Kloster, S., Zhang, K., Schmidt, H., Rast, S., Giorgi, M.,
22 Eck, T.F., and Stevens, B.: MAC-v1: A new global aerosol climatology for climate studies, *J.*
23 *Adv. Model. Earth Syst.* 5, 704–740, doi:10.1002/jame.20035, 2013.

1 [Knippertz P., and Todd, M. C., Mineral dust aerosols over the Sahara: Meteorological](#)
2 [controls on emission and transport and implications for modeling, Rev. Geophys., 50,](#)
3 [RG1007, doi:10.1029/2011RG000362, 2012.](#)

4 Kocha, C., Lafore, J.P., Tulet, P., and Seity, Y.: High resolution simulation of a major West
5 African dust storm: Comparison with observations and investigation of dust impact, Q. J. R.
6 Meteorol. Soc. 138, 455-470, doi:101002/qj.927, 2012.

7 Kocha, C., Tulet, P., Lafore, J.P., and Flamant, C.: The importance of the diurnal cycle of
8 Aerosol Optical Depth in West Africa, Geophys. Res. Lett. 40, doi:10.1002/grl.50143, 2013.

9 Koffi, B., Schulz, M., Bréon, F-M., Griesfeller, J., Winker, D.M.M., Balkanski, Y., Bauer, S.,
10 Berntsen, T., Chin, M., Collins, W.D., Dentener, F., Diehl, T., Easter, R.C., Ghan, S.J.,
11 Ginoux, P.A., Gong, S., Horowitz, L.W., Iversen, T., Kirkevag, A., Koch, D.M., Krol, M.,
12 Myhre, G., Stier, P., and Takemura, T.: Application of the CALIOP Layer Product to evaluate
13 the vertical distribution of aerosols estimated by global models: Part 1. AeroCom phase I
14 results, J. Geophys. Res. 117, no. D10, D10201, doi:10.1029/2011JD016858, 2012.

15 Laurent, B., Marticorena, B., Bergametti, G., Léon, J.F., and Mahowald, N.M.: Modeling
16 mineral dust emissions from the Sahara desert using new surface properties and soil database.
17 J. Geophys. Res. 113, D14218, doi:10.1029/2007JD009484, 2008.

18 Levy, R. C., Remer, L. A., Mattoo, S., Vermote, E. F., and Kaufman, Y. J.: Second-
19 generation operational algorithm: Retrieval of aerosol properties over land from inversion of
20 Moderate Resolution Imaging Spectroradiometer spectral reflectance, J. Geophys. Res., 112,
21 D13211, doi: 10.1029/2006JD007811, 2007.

22 [Levy, R. C., Remer, L. A., Kleidman, R. G., Mattoo, S., Ichoku, C., Kahn, R., and Eck, T. F.:](#)
23 [Global evaluation of the Collection 5 MODIS dark-target aerosol products over land, Atmos.](#)
24 [Chem. Phys., 10, 10399–10420, doi:10.5194/acp-10-10399-2010, 2010.](#)

1 [Levy, R. C., Mattoo, S., Munchak, L. A., Remer, L. A., Sayer, A. M., Patadia, F., and Hsu N.](#)
2 [C.: The Collection 6 MODIS aerosol products over land and ocean, Atmos. Meas. Tech., 6,](#)
3 [2989–3034, doi:10.5194/amt-6-2989-2013, 2013.](#)

4 Lioussse, C., Penner, J. E., Chuang, C., Walton, J. J., Eddleman, H., and Cachier, H.: A global
5 three-dimensional model study of carbonaceous aerosols, *J. Geophys. Res.* 101, 19411–
6 19432, doi:10.1029/95JD03426, 1996.

7 Lopez, P.: Implementation and validation of a new prognostic large-scale cloud and
8 precipitation scheme for climate and data-assimilation purposes, *Q. J. R. Meteorol. Soc.*, 128,
9 229–257, 2002.

10 Luo, C., Mahowald, N.M., and del Corral, J.: Sensitivity study of meteorological parameters
11 on mineral aerosol mobilization, transport, and distribution, *J. Geophys. Res.* 108, 4447,
12 doi:10.1029/2003JD003483, 2003.

13 [Mallet, M., Tulet, P., Serc, D., Solmon, F., Dubovik, O., Pelon, J., Pont, V., and Thouron, O.:](#)
14 [Impact of dust aerosols on the radiative budget, surface heat fluxes, heating rate profiles and](#)
15 [convective activity over West Africa during March 2006, Atmos. Chem. Phys., 9, 7143–7160,](#)
16 [doi:10.5194/acp-9-7143-2009, 2009.](#)

17 Marticorena, B., and Bergametti, G.: Modeling the atmospheric dust cycle: 1. Design of a
18 soil-derived dust emission scheme, *J. Geophys. Res.* 100, 16, 415–16, 430, 1995.

19 Marticorena, B., and Bergametti, G.: Two year simulations of seasonal and interannual
20 changes in Saharan dust emissions. *Geophys. Res. Lett.* 23, 1921–1924, 1996.

21 Marticorena, B., Chatenet, B., Rajot, J.L., Traoré, S., Coulibaly, M., Diallo, A., Koné, I.,
22 Maman, A., NDiaye, T., and Zakou, A.: Temporal variability of mineral dust concentrations
23 over West Africa: analyses of a pluriannual monitoring from the AMMA Sahelian Dust
24 Transect, *Atmos. Chem. Phys.* 10, 8899–8915, 2010.

25 Martin, J.H.: Iron still comes from above, *Nature* 353, 123–123, 1991.

1 Martin, R.V., Jacob, D.J., Yantosca, R.M., Chin, M., and Ginoux, P.: Global and regional de-
2 creases in tropospheric oxidants from photo-chemical effects of aerosols. *J. Geophys. Res.*
3 108 (D3), 4097, doi:10.1029/2002JD002622, 2003.

4 Masson, V., Champeaux, J., Chauvin, F., Meriguet, C., and Lacaze, R.: A global database of
5 land surface parameters at 1-km resolution in meteorological and climate models, *J. Clim.*
6 1261–1282, 2003.

7 Masson, V., Le Moigne, P., Martin, E., Faroux, S., Alias, A., Alkama, R., Belamari, S.,
8 Barbu, A., Boone, A., Bouyssel, F., Brousseau, P., Brun, E., Calvet, J.C., Carrer, D.,
9 Decharme, B., Delire, C., Donier, S., Essaouini, K., Gobelin, A.L., Giordani, H., Habets, F.,
10 Jidane, M., Kerdraon, G., Kourzeneva, E., Lafaysse, M., Lafont, S., Lebeaupin Brossier, C.,
11 Lemonsu, A., Mahfouf, J.F., Marguinaud, P., Mokhtari, M., Morin, S., Pigeon, G., Salgado,
12 R., Seity, Y., Taillefer, F., Tanguy, G., Tulet, P., Vincendon, B., Vionnet, V., and Volodire,
13 A.: The SURFEXv7.2 land and ocean surface platform for coupled or offline simulation of
14 earth surface variables and fluxes, *Geosci. Model Dev.* 6, 929–960, doi:10.5194/gmd-6-929-
15 2013, 2013.

16 Meloni, D., Sarra, A. D., Di Iorio, T., and Fiocco, G.: Influence of the vertical profile of
17 Saharan dust on the visible direct radiative forcing, *Journal of Quantitative Spectroscopy and*
18 *Radiative Transfer.* V. 93, issue 4, p. 397–413, 2005.

19 Mlawer, E. J., Taubman, S. J., Brown, P. D., Iacono, M.J., and Clough, S.A.: RRTM, a
20 validated correlated-k model for the longwave, *J. Geophys. Res.* 102, 16,663-16,682, 1997.

21 Mokhtari, M., Gomes, L., Tulet, P., and Rezoug, T.: Importance of the surface size
22 distribution of erodible material: an improvement on the Dust Entrainment And Deposition
23 (DEAD) Model. *Geosci. Model Dev.* 5, 581–598, doi:10.5194/gmd-5-581-2012, 2012.

24 Morcrette, J.J.: Radiation and cloud radiative properties in the ECMWF operational weather
25 forecast model. *J. Geophys. Res.* 96D, 9121-9132, 1991.

1 Morcrette, J.J., Boucher, O., Jones, L., Salmon, D., Bechtold, P., Beljaars, A., Benedetti, A.,
2 Bonet, A., Kaiser, J. W., Razinger, M., Schulz, M., Serrar, S., Simmons, A. J., Sofiev, M.,
3 Suttie, M., Tompkins, A. M., and Untch, A.: Aerosol analysis and forecast in the European
4 Centre for Medium-Range Weather Forecasts Integrated Forecast System: Forward modeling.
5 *J. Geophys. Res.* 114, D06206, doi:10.1029/2008JD011235, 2009.

6 Nabat, P., Somot, S., Mallet, M., Chiapello, I., Morcrette, J. J., Solmon, F., Szopa, S., Dulac,
7 F., Collins, W., Ghan, S., Horowitz, L. W., Lamarque, J. F., Lee, Y. H., Naik, V., Nagashima,
8 T., Shindell, D., and Skeie, R.: A 4-D climatology (1979–2009) of the monthly tropospheric
9 aerosol optical thickness distribution over the Mediterranean region from a comparative
10 evaluation and blending of remote sensing and model products, *Atmos. Meas. Tech.* 6, 1287–
11 1314, doi:10.5194/amt-6-1287, 2013.

12 Noilhan, J., And Planton, S.: A simple parameterization of land surface processes for
13 meteorological models. *Mon. Wea. Rev.* 117, 536–549, 1989.

14 Prospero, J.M., Ginoux, P., Torres, O., Nicholson, S.E., and Gill, T. E.: Environmental
15 characterization of global sources of atmospheric soil dust identified with the nimbus 7 total
16 ozone mapping spectrometer (toms) absorbing aerosol product. *Rev. Geophys.* 40,1002,
17 doi:10.1029/2000RG000095, 2002.

18 Radnóti, G.: Comments on “A spectral limited-area formulation with time-dependent
19 boundary conditions applied to the shallowwater equations”. *Mon. Wea. Rev.* 123, 3122–
20 3123, 1995.

21 Remer, L. A., Kaufman, Y. J., Tanré, D., Matoo, S., Chu, D. A., Martins, J. V., Li, R.R.,
22 Ichoku, C., Levy, R. C., Kiedman, R. G., Eck, T. F., Vermote, E., and Holben, B. N.: The
23 MODIS Aerosol Algorithm, Products, and Validation, *J. Atmos. Sci.* 62, 947–73, doi:
24 10.1175/JAS3385.1, 2005.

1 Rodwell, M.: The local and global impact of the recent change in model aerosol climatology.
2 ECMWF Newsl, 105, 17 – 23, 2005.

3 [Rogers, R. R., Vaughan, M. A., Hostetler, C. A., Burton, S. P., Ferrare, R. A., Young, S. A.,](#)
4 [Hair, J.W., Oblard, M. D., Harper, D. B., Cook, A. L., and Winker, D. M.: Looking through](#)
5 [the haze: evaluating the CALIPSO level 2 aerosol optical depth using airborne high spectral](#)
6 [resolution lidar data, Atmos. Meas. Tech., 7, 4317–4340, doi:10.5194/amt-7-4317-2014,](#)
7 [2014.](#)

8 Sandu, I., Brenguier, J., Geoffroy, O., Thouron, O., and Masson, V.: Aerosol impacts on the
9 diurnal cycle of marine stratocumulus. J. Atmos. Sci. 65, 2705–2718, 2008.

10 [Satheesh, S. K.: Letter to the Editor Aerosol radiative forcing over land: effect of surface and](#)
11 [cloud reflection, Ann. Geophys., 20, 2105–2109, doi:10.5194/angeo-20-2105-2002, 2002.](#)

12 Schepanski, K., Tegen, I., and Macke, A.: Comparison of satellite based observations of
13 Saharan dust source areas. Remote Sensing of Environment, V.123. 90-97, 2012.

14 Schmechtig, C., Marticorena, B., Chatenet, B., Bergametti, G., Rajot, J. L., and Coman, A.:
15 Simulation of the mineral dust content over Western Africa from the event to the annual scale
16 with the CHIMERE-DUST model. Atmos. Chem. Phys. 11, 7185–7207, doi:10.5194/acp-11-
17 7185-2011, 2011.

18 Seinfeld, J. H., and Pandis, S. N.: 1997. Atmospheric chemistry and physics, from Air
19 Pollution to Climate Change. Wiley, New York, 1997.

20 Shi, Y., Zhang, J., Reid, J. S., Hyer, E. J., and Hsu, N. C.: Critical evaluation of the MODIS
21 Deep Blue aerosol optical depth product for data assimilation over North Africa. Atmos.
22 Meas. Tech., 6, 949–969, doi:10.5194/amt-6-949, 2013.

23 Smith R.N.B.: A scheme for predicting layer clouds and their water content in a general
24 circulation model. Q. J .R. Meteorol. Soc. 116, 435-460, 1990.

1 Sokolik, I. N., Winker, D. M., Bergametti, G., Gillette, D. A., Carmichael, G., Kaufman, Y.
2 J., Gomes, L., Schuetz, L., and Penner, J. E.: Introduction to special section: Outstanding
3 prob-lems in quantifying the radiative impacts of mineral dust, *J. Geophys. Res.-Atmos.*
4 106(D16), 18015–18027, 2001.

5 Stephens, G. L., Vane, D. G., Boain, R. J., Mace, G. G., Sassen, K., Wang, Z., Illingworth, A.
6 J., O'Connor, E. J., Rossow, W. B., Durden, S. L., Miller, S. D., Austin, R. T., Benedetti, A.,
7 and Mitrescu, C.: The cloudsat mission and the A-Train: a new dimension of space-based
8 observations of clouds and precipitation, B. Am. Meteorol. Soc., 83, 1771–1790+1742, 2002.

9 Swap, R.M., Garstang, M., Greco, S., Talbot, R., Kallberg, P.: Saharan dust in the Amazon
10 basin. *Tellus B* 44, 133–149, 1992.

11 Tanaka, T.Y., and Chiba, M.: Global Simulation of Dust Aerosol with a Chemical Transport
12 Model, MASINGAR. *Journal of the Meteorological Society of Japan* Vol. 83A, pp. 255—
13 278, 2005.

14 Tanré, D., Geleyn, J.F., and Slingo, J. M.: First results of the introduction of an advanced
15 aerosol-radiation interaction in t he ECMWF low resolution global model, in *Aerosols and*
16 *Their Climatic Effects.* edited by H. E. Gerber, pp. 133 – 177, A. Deepak, Hampton, Va,
17 1984.

18 Tanré, D., Kaufman, Y. J., Herman, M., and Mattoo, S.: Remote sensing of aerosol properties
19 over oceans using the MODIS/EOS spectral radiances, *J. Geophys. Res.* 102, 16971–16988,
20 1997.

21 Tegen, I., and Fung, I.: Contribution to the atmospheric mineral aerosol load from land
22 surface modification, *J. Geophys. Res.*, 100, 18707–18726,doi:10.1029/95JD02051, 1995.

23 Tegen, I., Hollrig, P., Chin, M., Fung, I., Jacob, D., and Penner, J.: Contribution of different
24 aerosol species to the global aerosol ex-tinction optical thickness: Estimates from model
25 results, *J. Geo-phys. Res.* 102, 23895–23915, 1997.

1 Todd, M.C., Washington, R., Martins, J.V., Dubovik, O., Lizcano, G., M'Bainayel, S., and
2 Engelstaedter, S.: Mineral dust emission from the Bodélé Depression, northern Chad, during
3 BoDEX 2005. *J. Geophys. Res.* 112, D06207, doi:10.1029/2006JD007170, 2007.

4 Tompkins, A M., Cardinali, C., Morcrette, J.J., and Rodwell, M.: Influence of aerosol
5 climatology on forecasts of the African Easterly Jet, *Geophys. Res. Lett.* 32, L10801,
6 doi:10.1029/2004GL022189, 2005.

7 Tost, H., Jöckel, P., Kerkweg, A., Sander, R., and Leliveld, J.: Technical note: A new
8 comprehensive SCAVenging submodel for global atmospheric chemistry modelling, *Atmos.*
9 *Chem. Phys.*, 6, 565-574, 2006.

10 Tulet, P., Crassier, V., Cousin, F., Suhre, K., and Rosset, R.: ORILAM, a three-moment
11 lognormal aerosol scheme for mesoscale atmospheric model: Online coupling into the Meso-
12 NH-C model and validation on the Escompte campaign, *J. Geophys. Res.* VOL. 110, D18201,
13 doi:10.1029/2004JD005716, 2005.

14 Tulet, P., Mallet, M., Pont, V., Pelon, J., and Boone, A.: The 7–13 March, 2006, dust storm
15 over West Africa: generation, transport and vertical stratification, *J. Geophys. Res.*, 113,
16 D00C08, doi:10.1029/2008JD009871, 2008.

17 Tulet, P., Crahan-Kaku, K., Leriche, M., Aouizerats, B., and Crumeyrolle, S.: 2010. Mixing
18 of dust aerosols into mesoscale convective system : Generation, filtering and possible
19 feedbacks on ice anvils, *Atmospheric Research*, 96, 302–314,
20 doi:10.1016/j.atmosres.2009.09.011, 2010.

21 Twomey, S.: The nuclei of natural cloud formation. II: The supersaturation in natural clouds
22 and the variation of cloud droplet concentration, *Pure and Applied Geophysics* 43:243-249,
23 1959.

24 United States Department of Agriculture (USDA), Natural Resources Conservation Service
25 (NRCS).: Soil Taxonomy : A Basic System of Soil Classification for Making and Interpreting

1 Soil Surveys Agr. Handb. 436. U.S.Govt.Print.Office, Washington DC, 20402. Second
2 edition, 1999.

3 Wang, T., Cheung, T. F., Li, Y. S., Xu, X. M., and Blake, D. R.: Emission characteristics of
4 CO, NOx, SO2 and indications of biomass burning observed at a rural site in eastern China. J.
5 Geo-phys. Res. 107(D12), 4157, doi:10.1029/2001JD000724, 2002.

6 Washington, R., Todd, M., Middleton, N. J., and Goudie, A. S.: Dust-Storm source areas
7 determined by the total ozone monitoring spectrometer and surface observations, Annals of
8 the Association of American Geographers. 93 (2), 297, 2003.

9 Washington, R., Todd, M. C., Engelstaedter, S., Mbainayel, S., and Mitchell, F.: Dust and the
10 low-level circulation over the Bodélé depression, Chad: Observations from BoDEx 2005, J.
11 Geophys. Res., 111, D03201, doi:10.1029/2005JD006502, 2006.

12 Werner, M., Tegen, I., Harrison, S. P., Kohfeld, K. E., Prentice, I. C., Balkanski, Y., Rodh,
13 H., and Roelandt, C.: Seasonal and interannual variability of the mineral dust cycle under
14 present and glacial climate conditions, J. Geophys. Res. 107, 4744,
15 doi:10.1029/2002JD002365, 2002.

16 Winker, D. M., Hunt, W. H., and McGill, M. J.: Initial performance assessment of CALIOP,
17 Geophys. Res. Lett., 34, L19803, doi:10.1029/2007GL030135, 2007.

18 Zender, C. S., Bian, H., and Newman, D.: Mineral Dust Entrainment and deposition (DEAD)
19 model: Description and 1990s dust climatology, J. Geophys. Res. VOL. 108, NO. D14, 4416,
20 doi:10.1029/2002JD002775, 2003a.

21 Zhu, A., Ramanathan, V., Li, F., and Kim, D.: Dust plumes over the Pacific, Indian, and
22 Atlantic oceans: climatology and radiative impact, J. Geophys. Res. 112, D16208,
23 doi:10.1029/2007JD008427, 2007.

24
25

1 **Table 1:** Log-normal parameters of the AMMA size distribution used in DEAD coupled with
2 SURFEX.

	Mode 1	Mode 2	Mode 3
Number fraction (%)	97.52	1.95	0.52
Mass fraction (%)	0.08	0.92	99
Geometric standard deviation	1.75	1.76	1.7
Number median diameter (μm)	0.078	0.64	5.0
Mass median diameter (μm)	0.2	1.67	11.6

1 | **Table 2:** Comparison of regional annual mean dust flux between this study and other studies.

2 | The unit is Tg.year⁻¹.

3 |

References	Annual mean dust emission (Tg.year ⁻¹) in North Africa	
This study	878	period (2006-2010)
d'Almeida (1986)	630-710	period (1981-1982)
Luo et al.(2003)	1114	period (1979-2000)
Ginoux et al. (2004)	1430	period (1981-1996)
Marticorena et Bergametti (1996)	665-586	period (1991-1992)
Callot et al. (2000)	760	period (1990-1992)
Laurent et al. (2008)	580-760	period (1996-2001)
Tanaka and Chiba (2005)	1018	period (1979-2003)
Werner et al. (2002)	693	period (1979-1989)
Zender et al. (2003a)	980	period (1990-1999)

1 | **Table 3:** Mean dust wet deposition

<u>Models</u>	<u>Wet deposition for 2006 in (g.m⁻².year⁻¹)</u>
<u>BSC-DREAM8b</u>	<u>0.46</u>
<u>GOCART-v4Ed.A2 CTRL</u>	<u>9.653</u>
<u>GISS-modelE.A2 CTRL</u>	<u>8.301</u>
<u>TM5-V3.A2 CTRL</u>	<u>4.673</u>
<u>This study</u>	<u>21.36</u>

2
3



Figure 1: Location of the five AERONET sites used in this study to evaluate the ALADIN simulated AOT over West Africa Banizoumbou (Niger), Cinzana (Mali), DMN_Maine_Soroa (Niger), Mbour (Senegal) and Capo verde.

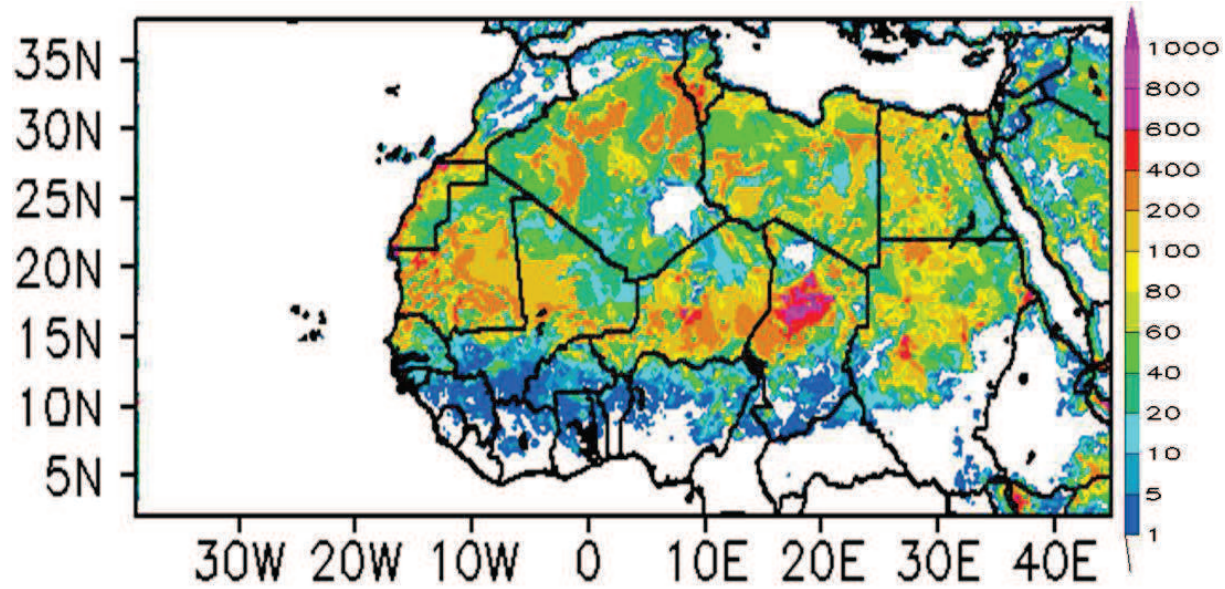
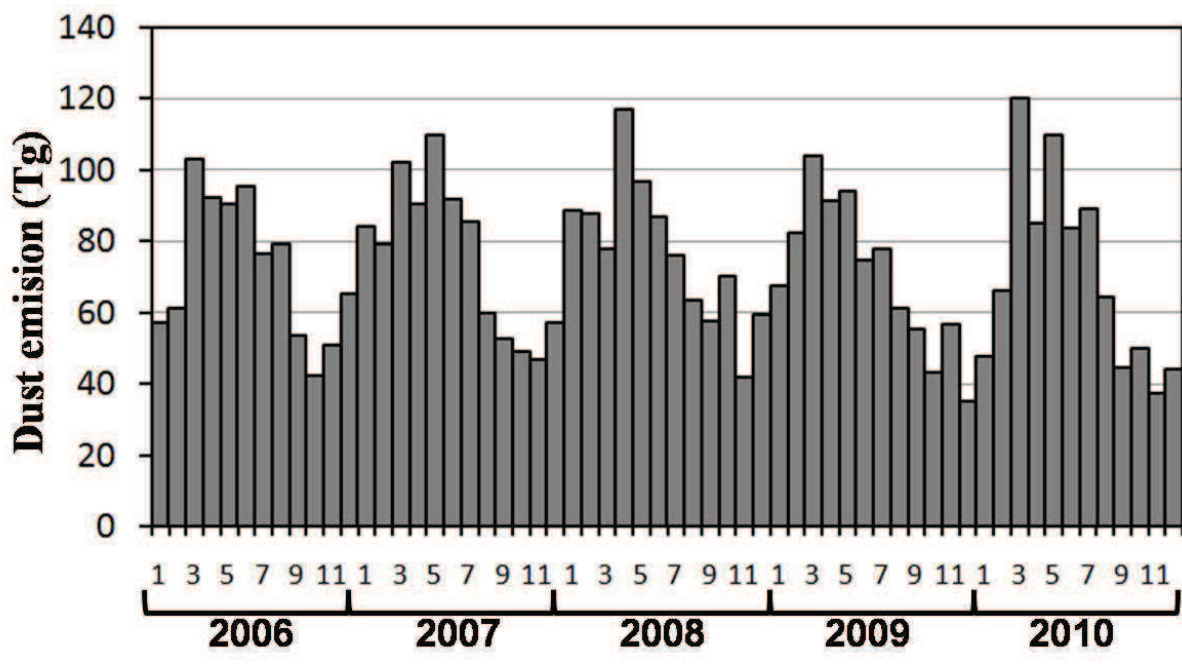
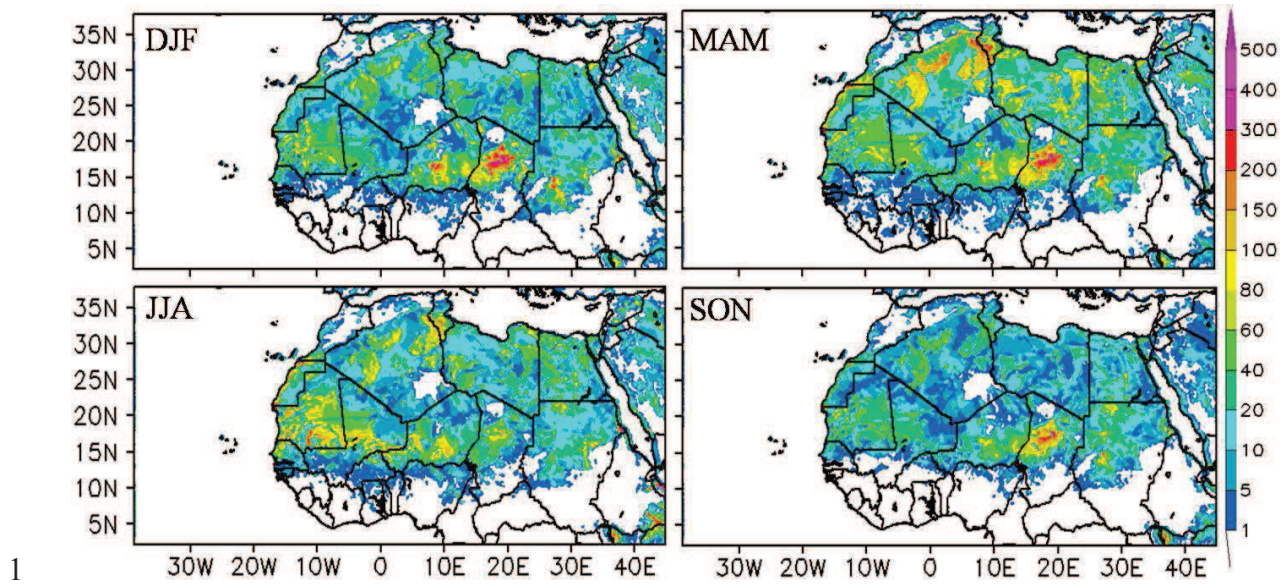


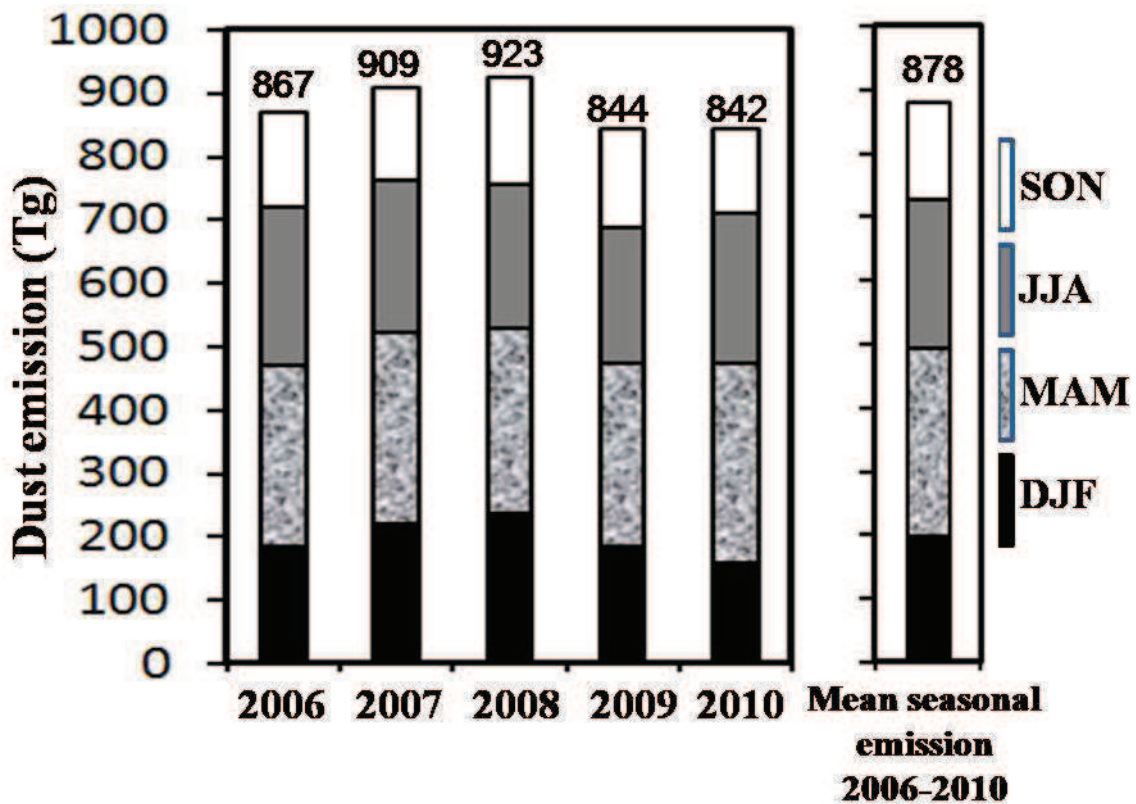
Figure 42: Annual mean dust emissions (in g.m^{-2}) over North Africa averaged for the 2006-2010 period simulated by ALADIN.



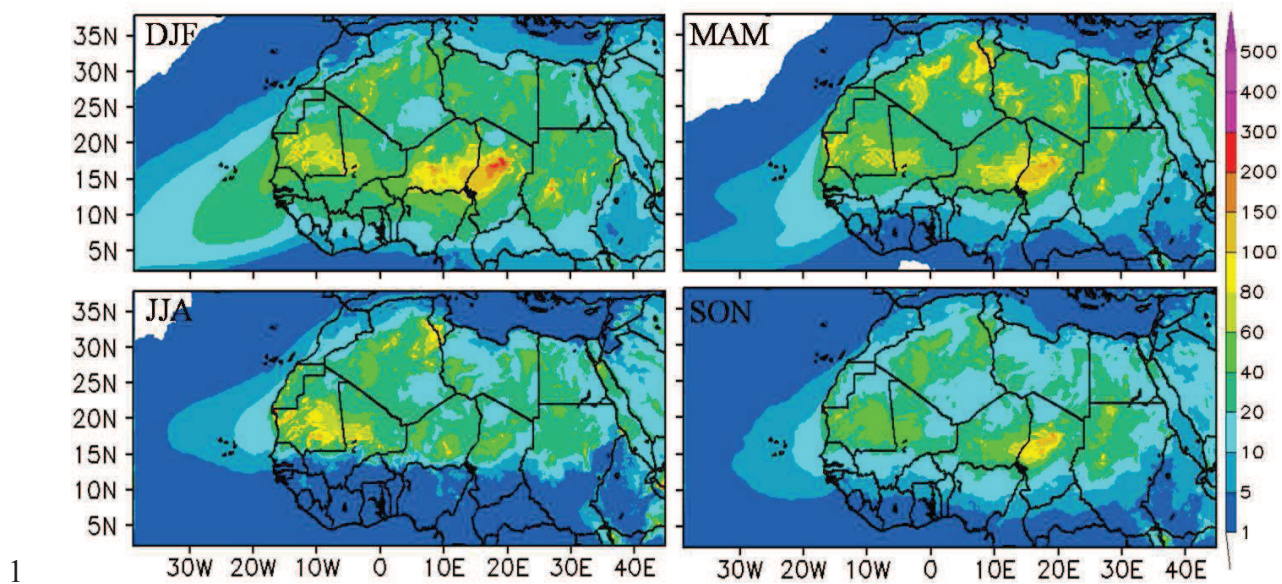
2 | **Figure 32:** Monthly dust emissions (in Tg) over North Africa from 2006 to 2010 period.



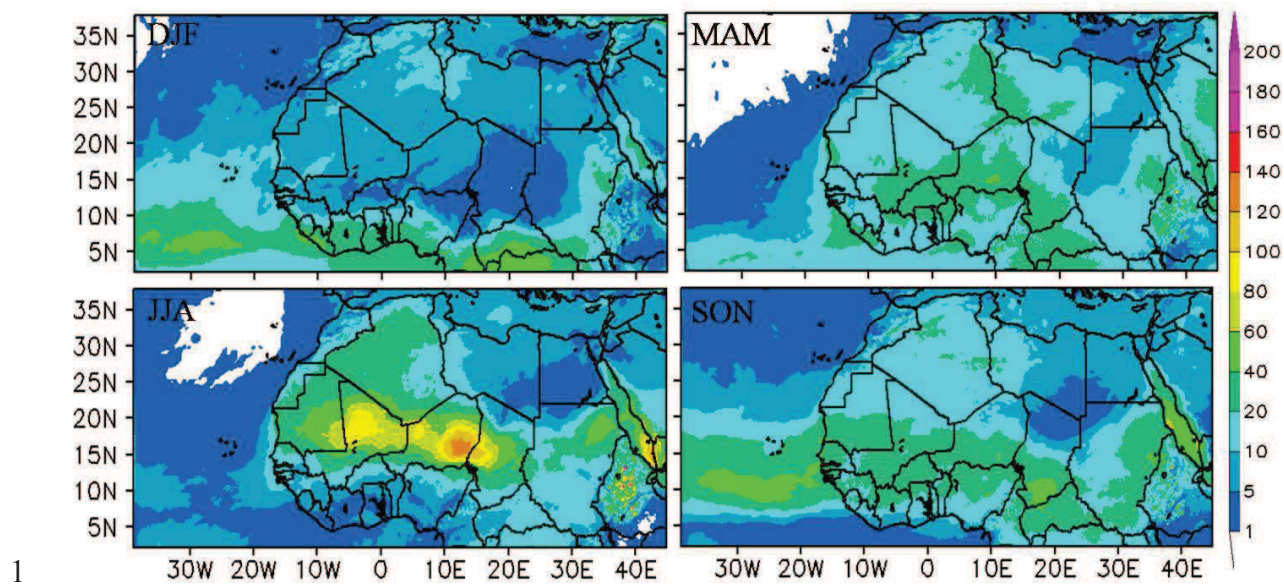
2 | **Figure 43:** Seasonal mean aerosol dust emissions simulated by ALADIN (in g.m^{-2}) over
3 North Africa averaged for the 2006-2010 period.



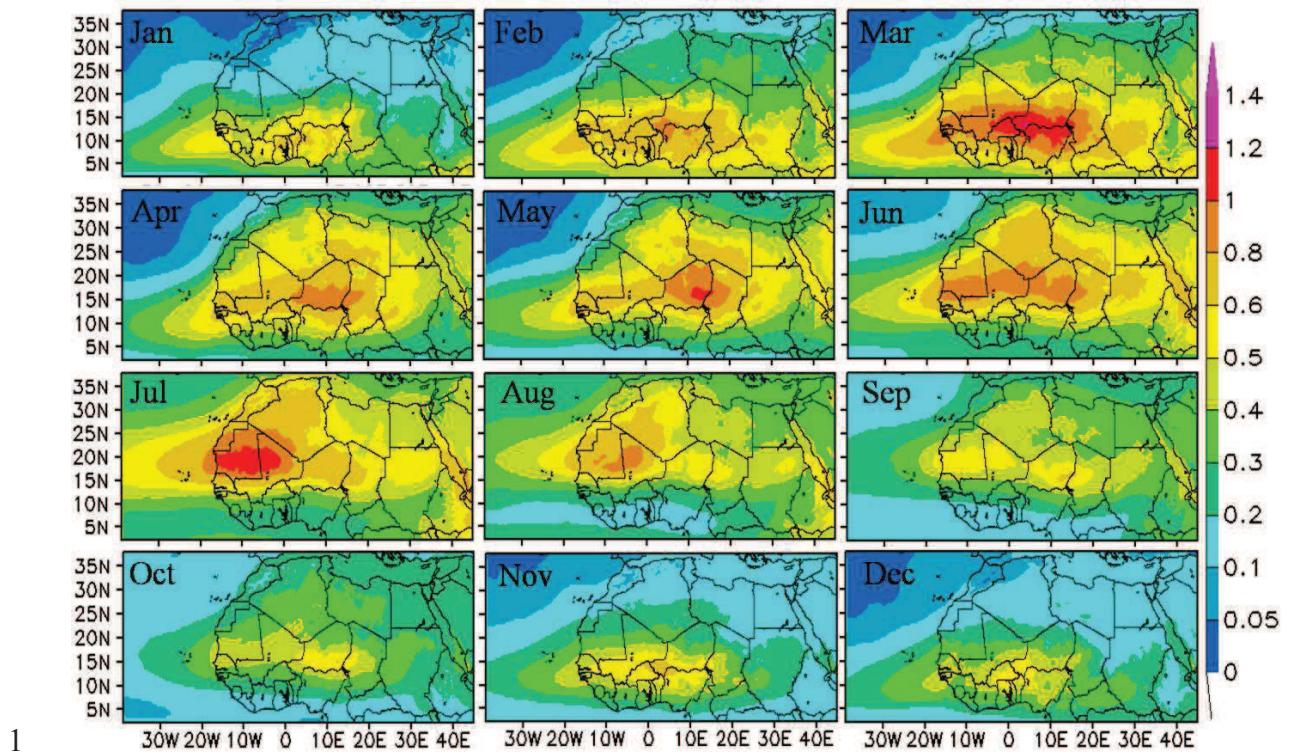
1
 2 | **Figure 54:** Seasonal mean and interseasonal dust emissions (in Tg) simulated by ALADIN
 3 | over North Africa from 2006 to 2010. The annual average emission is given at the top of each
 4 | bar.



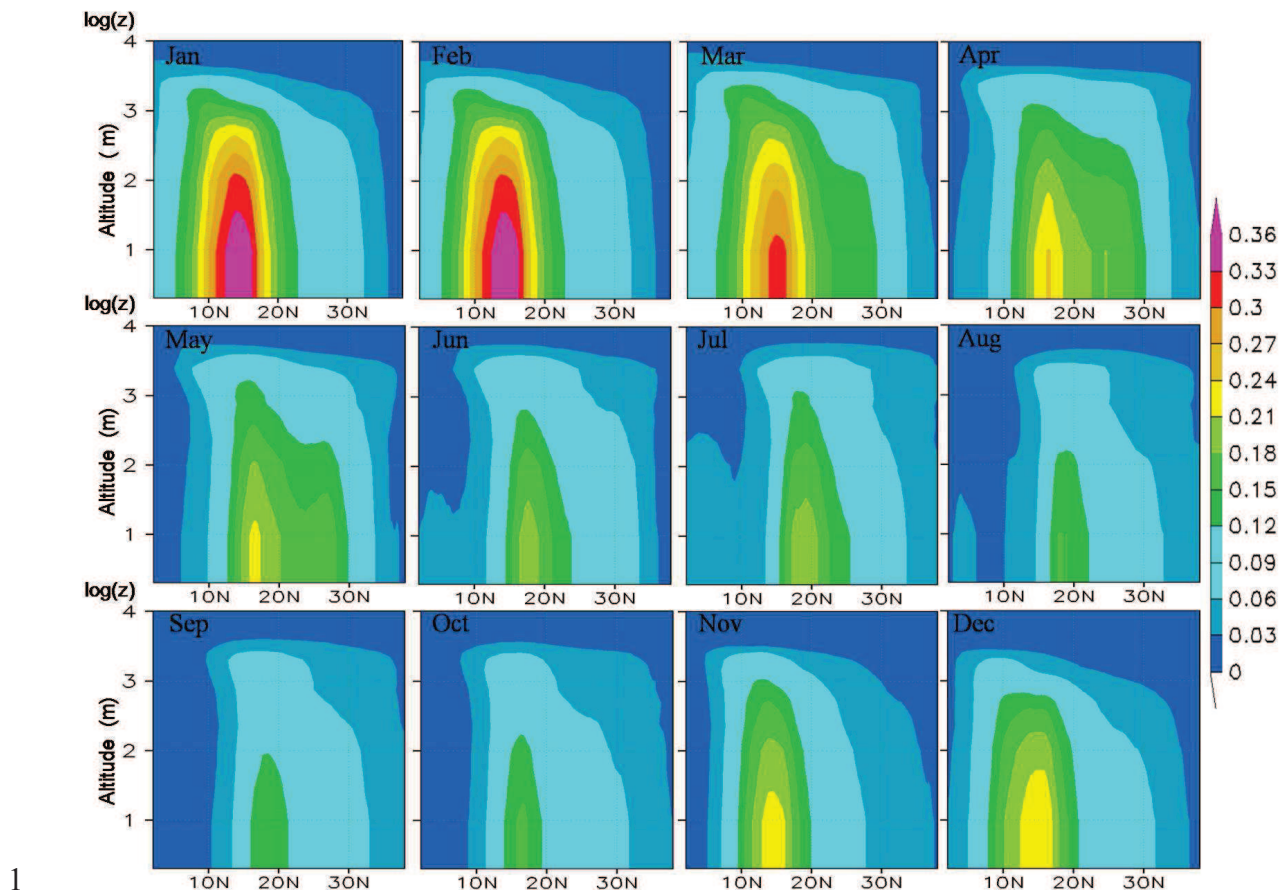
2 | **Figure 65:** Seasonal mean dry deposition flux simulated by ALADIN (in g.m^{-2}) over North
3 | Africa averaged for the 2006-2010 period.



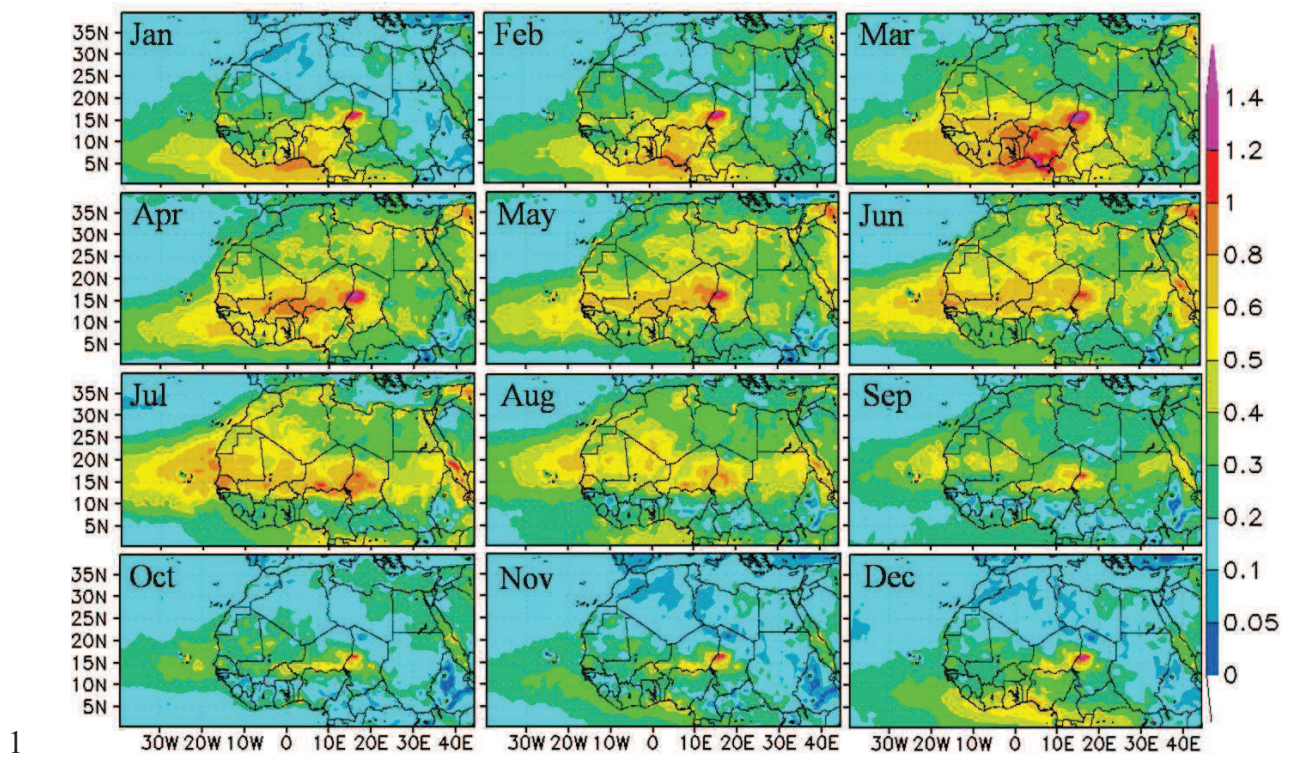
2 **Figure 76:** Seasonal mean wet deposition flux simulated by ALADIN (in g.m^{-2}) over North
3 Africa averaged for the 2006-2010 period.



2 **Figure 87:** Monthly Aerosol Optical Thickness (AOT) simulated by ALADIN averaged over
3 the 2006-2010 period.



2 **Figure 28:** Monthly vertical cross section (30° W - 40° E) of extinction coefficients (in km^{-1})
3 simulated by ALADIN averaged from 2006 to 2010 over North Africa.



2 **Figure 109:** Monthly aerosol optical thickness derived from the combination of the standard
 3 and Deep Blue products applied to AQUA/MODIS data over North Africa for the 2006-2010
 4 period.

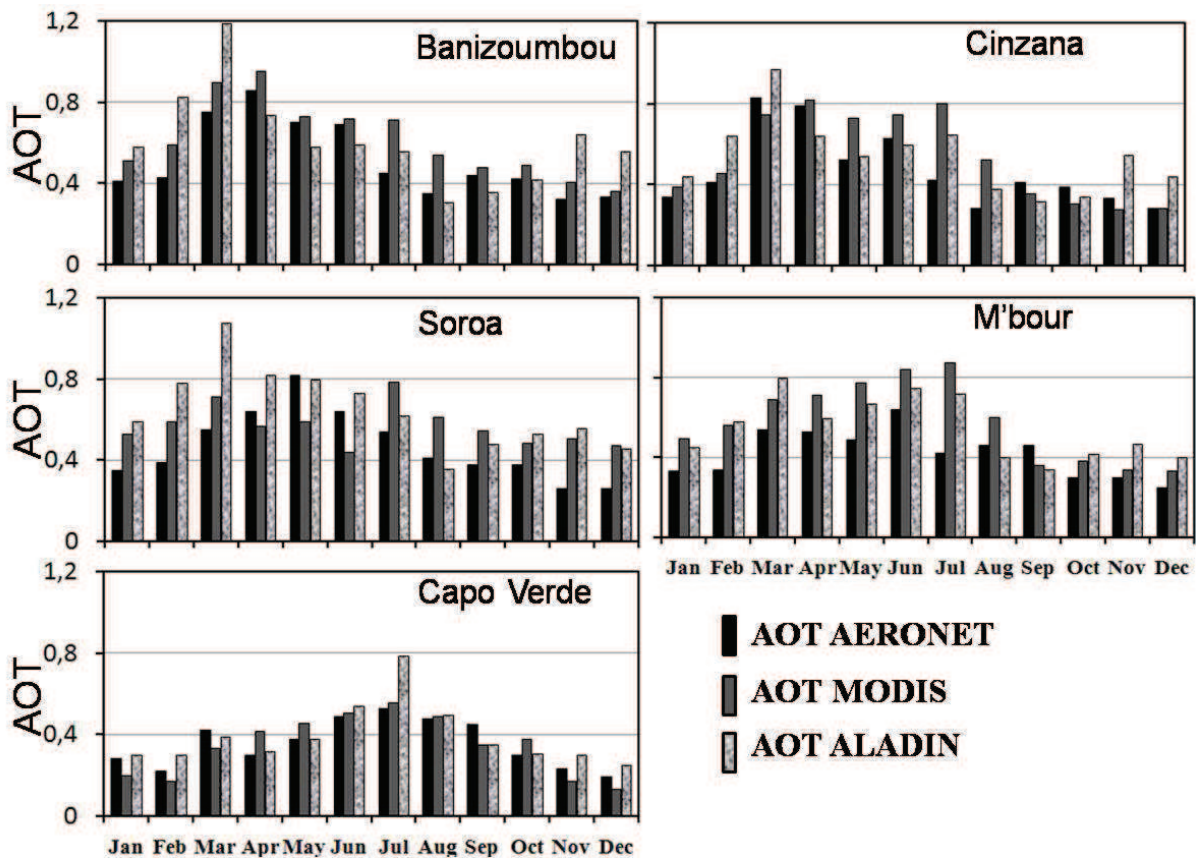


Figure 1140: Monthly aerosol optical thickness observed by sun photometer (black), MODIS (dark gray) and simulated by ALADIN (gray) averaged from 2006 to 2010 over Banizoumbou (13°32'2"N, 2°39'54"E), Cinzana (13°16'40"N, 5°56'2"W), Soroa (13°13'1"N, 12°1'22"E), Mbour (14°23'38"N, 16°57'32"W) and Capo Verde (16°43'58"N, 22°56'6"W).

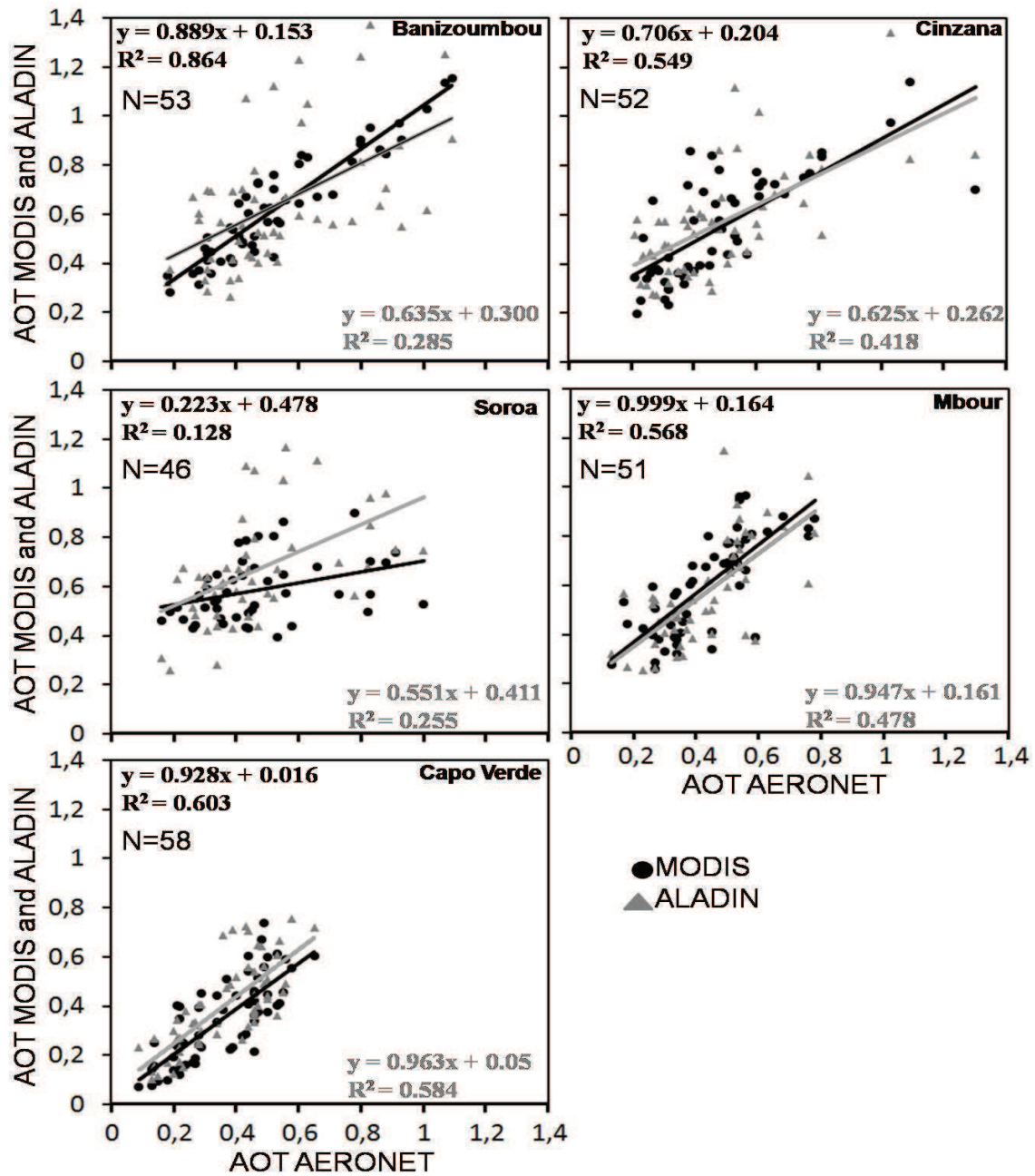


Figure 124: Scatter plot of monthly ALADIN (gray) and MODIS (black) aerosol optical thickness against AERONET measurements over Banizoumbou, Cinzana, Soroa, Mbour and Capo Verde from 2006 to 2010. In abscissa, AERONET measurements; in ordinate, ALADIN and MODIS AOTs. N is the number of averaged monthly data of AOT available from 2006 to 2010. Each marker represents the averaged monthly AOT from 2006 to 2010. R is the correlation coefficient.

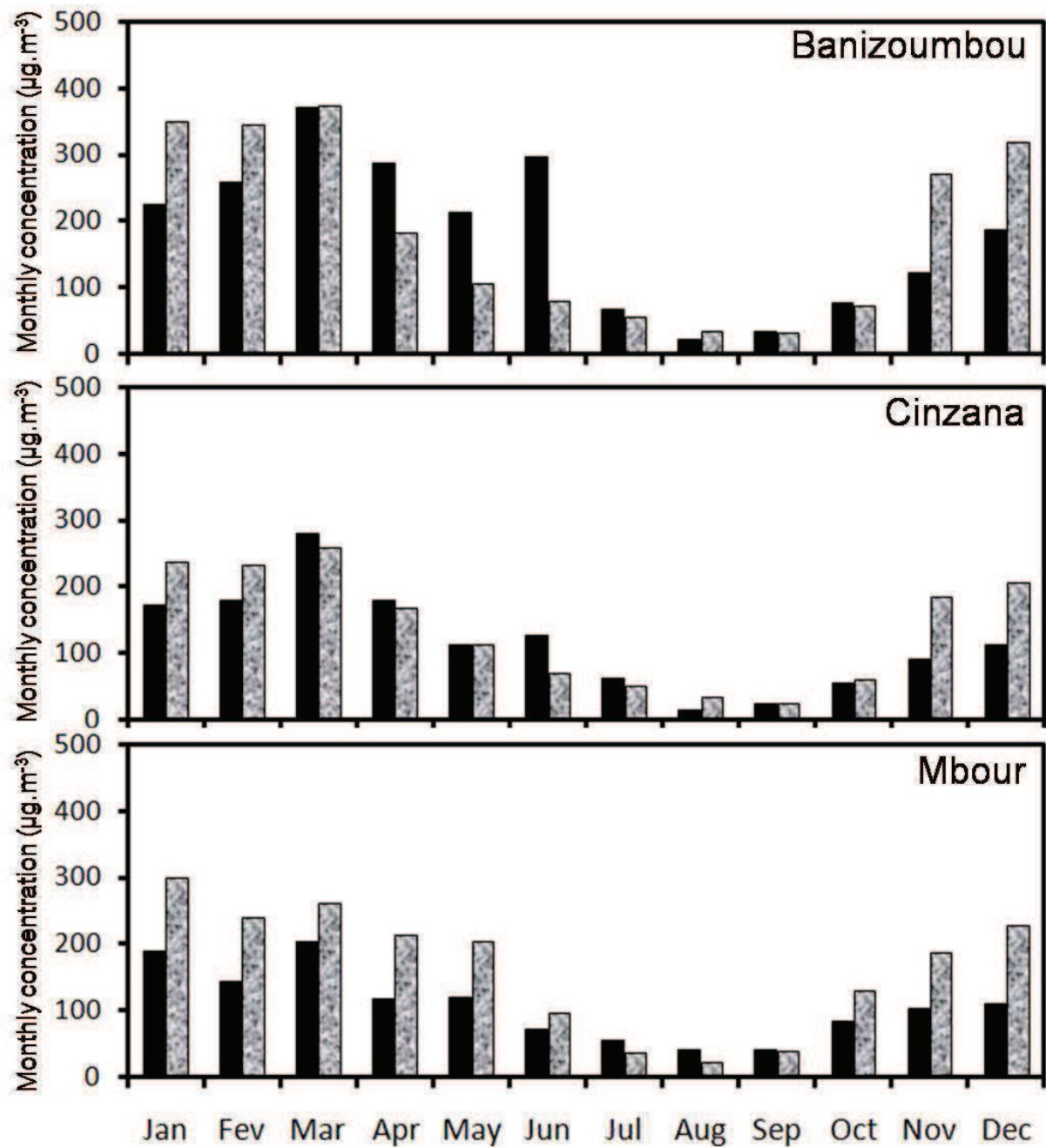


Figure 1342: Monthly mean of daily median measured (black) and simulated (grey) surface concentration (in $\mu\text{g.m}^{-3}$) in Banizoumbou, Cinzana and M'bour from 2006 to 2010.

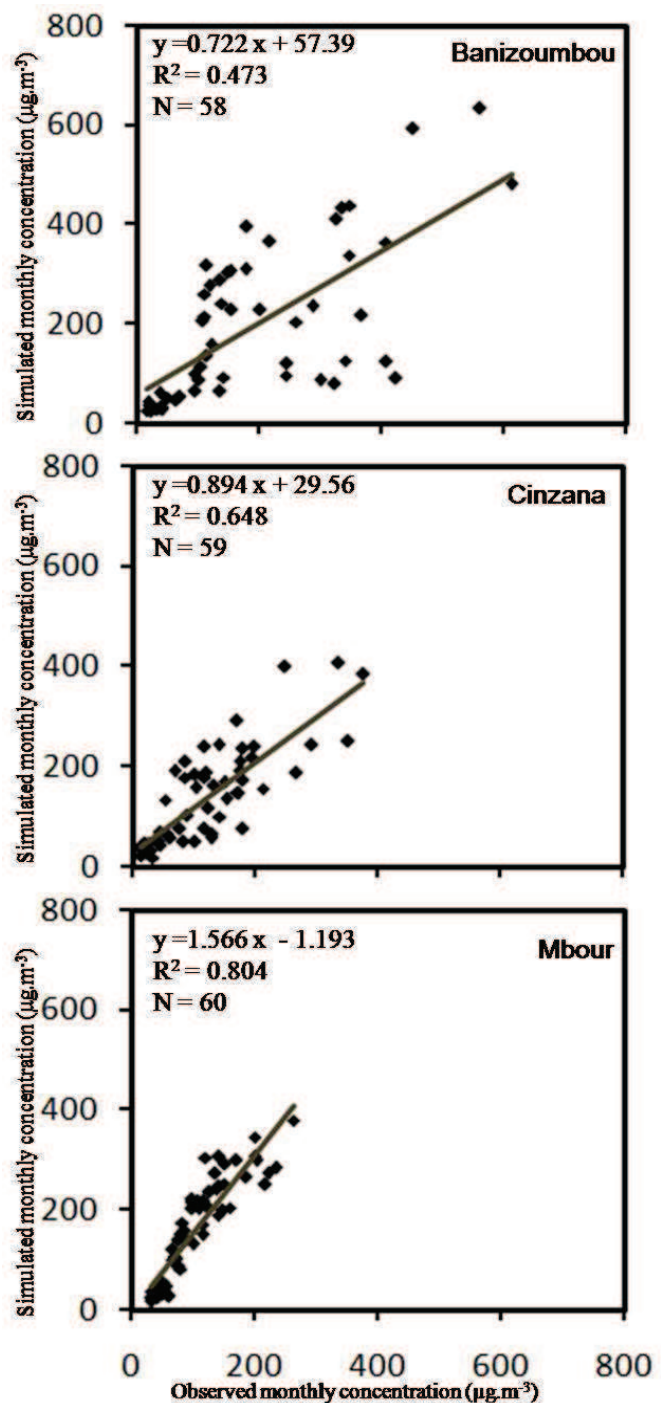


Figure14: Scatter plot of monthly ALADIN dust surface concentration against observation

over Banizoumbou, Cinzana and Mbour from 2006 to 2010. N is the number of averaged monthly surface concentration data available from 2006 to 2010. R is the correlation coefficient.

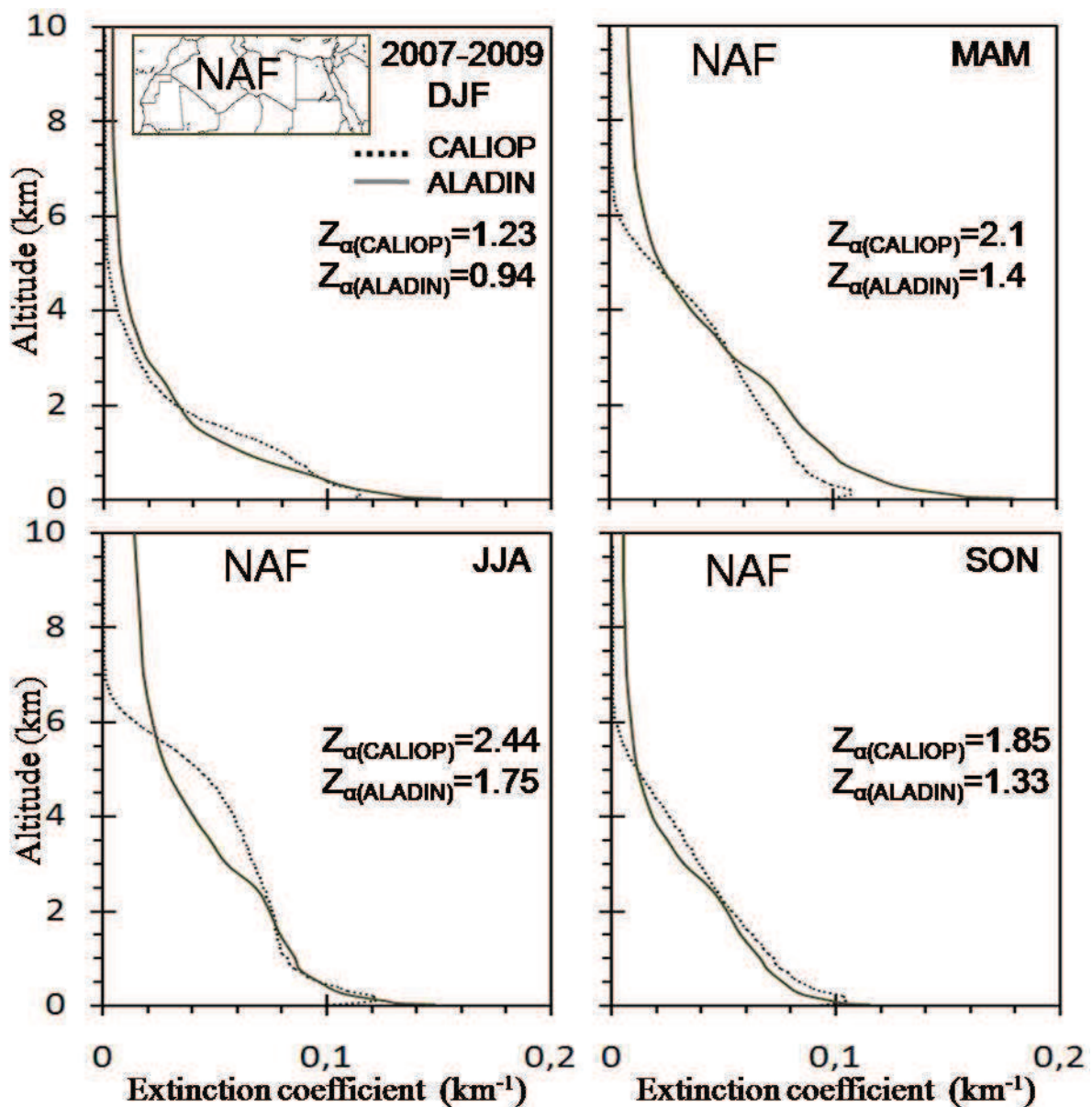


Figure 1513: CALIOP and ALADIN mean seasonal extinction coefficient (km^{-1}) profiles (at 532 and 550 nm, respectively) averaged from 2007 to 2009 over North Africa (NAF). CALIOP profiles are shown as dark dashed lines and ALADIN profiles are shown as continuous grey lines. For each season, we give the Z_α value for CALIOP and ALADIN.

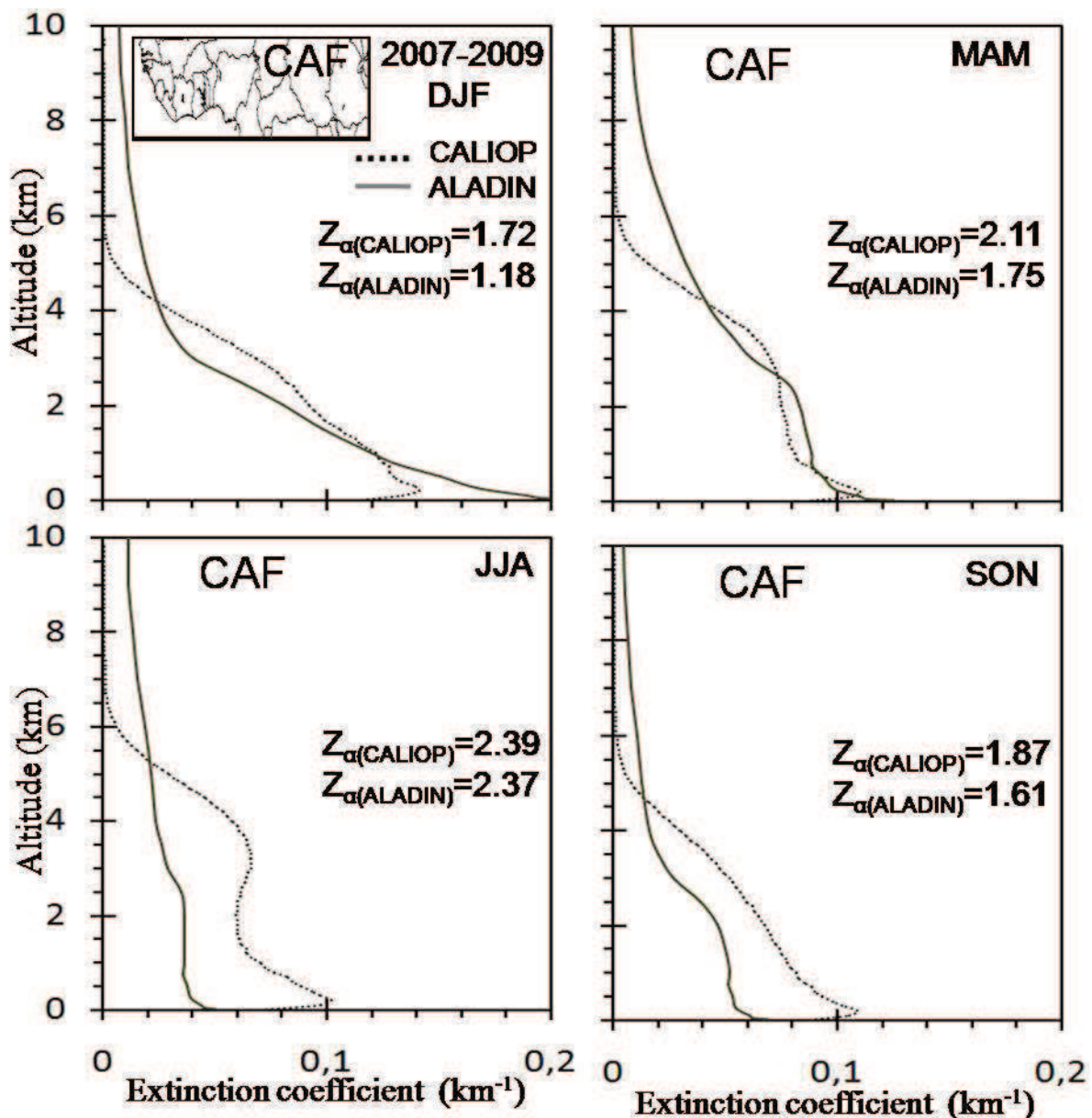


Figure 1644: CALIOP and ALADIN mean seasonal extinction coefficient (Km⁻¹) profiles (at 532 and 550 nm, respectively) averaged from 2007 to 2009 over North Africa (CAF). CALIOP profiles are shown as dark dashed lines and ALADIN profiles are shown as continuous grey lines. For each season, we give the Z_α value for CALIOP and ALADIN.